UNIVERSITÀ DEGLI STUDI DI MILANO

SCUOLA DI DOTTORATO
Scuola di Dottorato in Scienze Biochimiche, Nutrizionali e Metaboliche

DIPARTIMENTO
Dipartimento di Scienze Molecolari Agroalimentari

CORSO DI DOTTORATO
Dottorato di Ricerca in *Biochimica*

FRAMING THE ROLE OF RHODANESE-LIKE PROTEINS IN CELL REDOX BALANCE IN TWO BACTERIAL MODEL SYSTEMS

BIO/10

NOME DEL DOTTORANDO
William REMELLI

TUTOR
Francesco Bonomi

DOCENTE GUIDA
Fabio Forlani

COORDINATORE DEL DOTTORATO
Francesco Bonomi

A.A. 2010-2011

I want to dedicate this work to whoever helps me to grow as a scientist but first of all as a man, to whoever fed my knowledge appetite regarding the biochemical sciences and to the friends that welcomed me in their lab making easier the path I decided to take...

Index

CHAPTER 1:

Abstract

A key component of the host's ability to survive bacterial challenge consist in the innate ability of macrophages to ingest and destroy the invading organism *via* various mechanisms which the most thoroughly studied is oxidative burst (Hanna et al., 1994). In response pathogens have evolved different approaches to survive the severe oxidative stress generated by the host.

Genome analysis have clustered more than 14000 sequences coding for putative rhodanese-like proteins. These sequences contain domains structurally similar to those of the extensively studied bovine rhodanese, and were found in more than 2100 species homogeneously distributed in all life's phyla. Proteins belonging to the rhodanese-like superfamily (PFAM accession number: PF00581) are characterized by having more than 140 different architectures of the rhodanese domain, that can be present mostly alone or in tandem with another rhodanese domain, or fused to other functional domains. Although only few amino acid residues are conserved among rhodanese-like proteins, their most distinctive structural feature is the active site configuration, that contains an electronegative residue (generally cysteine) surrounded by positively charged residues. This particular architecture allows rhodanese-like proteins to bear a low pK_a catalytic residue that can be the clue to explain their biological activity (Bordo et al 2001).

Although the *in vitro* reported sulfurtransferase activity for the few characterized rhodanese-like proteins is the transfer of sulfur atom from a sulfur donor (e.g. thiosulfate) to a thiophilic acceptor (e.g. cyanide) (E.C. 2.8.1.x), in the last two decades the scientific community has started to indicate biological roles different from cyanide detoxification for rhodanese-like proteins. Proposed roles for rhodanese-like proteins can be summarized in two different but complementary fields. Rhodanese-like proteins can function as source of bioactive sulfur equivalents by the formation of a persulfide sulfur on a cysteine residue (R-SSH) (Cartini et al 2011), or can be involved in maintaining redox homeostasis acting as a direct or indirect scavengers of reactive oxygen species (ROS).

My PhD research project was devoted to unravel the biological roles of rhodanese-like proteins using two prokaryotic model systems: the *Azotobacter vinelandii* and the *Bacillus subtilis* system.

A. vinelandii is a Gram-negative bacterium of the Pseudomonadaceae family in which redox balance must be carefully controlled due to its ability to fix molecular nitrogen *via* the molybdenum-iron-sulfur cluster enzyme nitrogenase (Setubal et al., 2009). The *A. vinelandii* genome possesses 14 ORFs coding for rhodanese-like proteins with the tandem-domain rhodanese-like protein RhdA (Gene ID: 7759697) being responsible for more than 80% of the crude extract thiosulfate:cyanide sulfurtransferase (TST) activity (Cartini et al., 2011). RhdA was widely studied in our lab from both structural and functional point of views.

Starting from the evidence that the *rhdA* null-mutant strain (MV474) showed altered sensitivity to oxidative events (Cereda et al., 2009), I investigated the nature of the endogenous oxidative stress induced in *A. vinelandii* by the absence of RhdA. I found that in MV474 strain the ratio GSH/GSSG was misregulated, and the levels of lipid hydroperoxides were significantly increased, although defensive activities against oxidative stress damage were activated (e.g. upregulation of the *ahpC* gene, coding for Alkylhydroperoxidase C, a member of the OxyR regulon). Furthermore, *rhdA* expression was highly induced in the *A. vinelandii* strain (UW136) when the oxidative stress was performed by the incubation with the superoxide-generator phenazine methosulfate (PMS). These results demonstrated that RhdA has a role in protecting *A. vinelandii* from oxidative damage and were the subject of a publication (Remelli et al., 2010).

Therefore I addressed my study to understand how RhdA could function in protecting redox homeostasis in *A. vinelandii*. I studied, *in vitro*, the oxidation behavior of the only cysteine residue (Cys_{230}) present in RhdA. Site-directed mutagenesis showed that the Cys_{230} residue is mandatory for RhdA TST activity (Cartini et al., 2011). Combining results of TST activity assays, and thiol quantification by the use of the fluorescence probe monobromobimane (mBBr), I found that, after incubation with PMS, Cys_{230} underwent irreversible oxidation, while underwent reversible oxidation if RhdA was preincubated with thiosulfate or reduced glutathione (GSH). This latter result was taken as an indication that productive interaction with GSH, the widespread redox buffer, could be a key point on understanding RhdA biological function in *A. vinelandii*.

The RhdA/glutathione interaction was characterized using different approaches. The ability of RhdA to interact with different glutathione species of biological relevance was studied by measuring changes of the RhdA intrinsic fluorescence due to tryptophan residues surrounding the RhdA active site. In particular, RhdA is able to strongly interact with GSH (K_d = 1.5 µM), glutathione thiyl radical ($GS^{\bullet}$; K_d = 10.4 µM), a radical form of GSH, while interaction with disulfide glutathione (GSSG) is weak (K_d = 1.4 mM). According to the RhdA active site features and to the thiol chemistry, a covalent binding with GSH was excluded by mass spectroscopy analyses and by the finding that reducing agents were unable to break the RhdA/GSH complex. Moreover, the inability of RhdA to bind GSH in the presence of high ionic strength conditions suggests that RhdA/glutathione complex is stabilized by electrostatic interactions according to the *in silico* model produced by docking the interaction.

The ability of RhdA to interact with glutathione (especially with $GS^{\bullet}$) as well as the results that GSH level was lower in the mutant than in the wild-type strain, were considered for discerning the biological functions of RhdA. Only a small number of proteins can manage $GS^{\bullet}$, among them human glutaredoxin 1 and 2 (*h*Grx1; *h*Grx2) can catalyze the reaction between GSH and $GS^{\bullet}$

leading to the formation of GSSG and a superoxide radical (Starke et al., 2003). The ability of these proteins to catalyze the oxidation of glutathione is mainly due to the peculiar feature of their active site that bear a low pK_a cysteine residue (Gallogly et al., 2008) . *In vitro* assays, using $GS^{\bullet}$-generating mix as a substrate, demonstrate the ability of RhdA to catalyze GSSG production with a turnover number 180-fold higher compared to human glutaredoxin 1, the glutaredoxin that present higher activity (RhdA k_{cat}: 628 s^{-1}). The lacking in the *A. vinelandii* genome of genes coding for *h*Grx1- and *h*Grx2-like glutaredoxins (while genes for other glutaredoxins are present), together with the absence of a complete ascorbic acid biosynthetic pathway, increases the biological relevance of the RhdA ability to scavenge $GS^{\bullet}$, preventing further oxidation of $GS^{\bullet}$ to toxic and/or unrecoverable forms. Considering that $GS^{\bullet}$ is mainly produced from GSH activity of, for example, detoxification of hydroxyl radicals ($OH^{\bullet}$) produced during cellular respiration (Lushchack, 2011), it is reasonable to believe that the RhdA function in protecting redox homeostasis must be related to the maintaining of the cellular respiration rate and has been further suggested by monitoring the oxygen consumption of UW136 and MV474 crude extracts.

B. subtilis is a Gram-positive bacterium that has been taken as a model prokaryotic system because of its close evolutional relationship with pathogen Gram-positive bacteria like *B. anthracis*, (which causes anthrax), *B. cereus* (responsible of the foodborne illness), and *B. thuringiensis* that is an important insect pathogen. Analysis of the *B. subtilis* genome allowed the identification of 5 rhodanese-like proteins; 3 (YtwF, YqhL, YbfQ) are single-domain protein and 2 (YrkF and YrkH) have the rhodanese domain fused to other functional domains. Noteworthy, rhodanese-like proteins having the RhdA domain architecture (i.e. two rhodanese domains organized in tandem) are not present in the *B. subtilis* genome. *B. subtilis* rhodanese-like proteins share the structural features of the rhodanese catalytic domain: a putative catalytic cysteine residue surrounded by positively-charged amino acid residues.

In silico analyses on transcription factor binding sites revealed that YbfQ, YhqL and YtwF are putatively controlled by FurR homologs, that in *B. subtilis* are the transcription factors that controls: the iron uptake (FurR), the zinc uptake (ZurR) and the peroxide response system (PerR). Furthermore *yhqL* transcription is also putatively controlled by NagC that is related to the expression of proteins involved in the N-acetil-glucosammine (GlcNac) transport. These informations suggest that *B. subtilis* rhodanese-like proteins, or at least some of them, could be involved in the oxidative stress response system. This idea have been recently supported by transcriptome analyses in which overexpression of *ybfQ B. anthracis* homolog has been shown after induction of the oxidative stress by treatment with hydrogen peroxide (Pohl et al., 2011).

A preliminary characterization of biological function of rhodanese-like proteins in *B. subtilis* was performed analyzing phenotypic changes on the rhodanese-like quadruple null-mutant J1235 strain (Δ*yrkF*, Δ*yhqL*, *ΔybfQ*, *ΔytwF*), kindly provided by professor T. Larson, compared to the isogenic wild-type strain PS832. Whereas no visible growth differences were observed in rich medium (LB), a small, but significant, growth difference was observed in Spizizen minimal medium supplemented with 0.4% sucrose. Hydrogen peroxide challenging assays, using both sublethal and lethal stressor concentrations, indicated that J1235 strain was more prone to oxidative stress damage compared to the wild-type PS832 strain. It suggests that the absence of rhodanese-like proteins caused a chronic endogenous oxidative stress condition enhanced by growths on the minimal media. These results were further confirmed by the ~40% decrease of the aconitase activity, an oxidative stress sensitive Fe-S cluster enzyme that is generally used as a marker to evaluate cellular oxidative stress conditions. Furthermore J1235 strain exhibited a ~50% increase of the intracellular lipid hydroperoxide content suggesting membrane oxidation.

Differently from eukaryotes and most of the Gram-negative bacteria, the majority of the Gram-positive bacteria have evolved different strategies to maintain intracellular redox homeostasis that don't involve the synthesis of GSH (Fahey et al., 1978). The most thoroughly studied of these alternative compounds are mycothiol (MSH) and coenzyme A (CoA) (Rawat et al., 2007; del Cardayré et al., 1998). Recent studies on the redox-sensitive thiol proteins of *B. subtilis*, have uncovered an unknown low-molecular mass thiol in association with the transcription factor Ohr (Nicely at al., 2007) that, in eukaryotic organisms, is regulated by glutathionylation (Hermansson et al., 1990). This new molecule, named bacillithiol (BSH), shares some structural characteristics with MSH (e.g. the GlcNac and cysteine mojeties) (Newton et al., 2009), and has proven to be the *B. subtilis* major low-molecular weight thiol (Gaballa et al., 2010).

Interestingly, a decrease of both total soluble BSH (~35%) and the BSH/BSSB ratio (~40%) were observed when the *B. subtilis* J1235 strain, where rhodanese-like proteins are not expressed, was compared with the wild-type strain. These and other phenotype features (i.e. differences of low-molecular weight thiol levels; increase of lipid oxidation), make the condition observed for the *B. subtilis* J1235 strain very similar to that observed for the *A. vinelandii rhdA* null mutant strain MV474, suggesting that at least one of the rhodanese-like protein shares the biological function of *A. vinelandii* RhdA. Structural differences between RhdA and *B. subtilis* rhodaneses could be explained by the structural differences between GSH and BSH, that requires a different active site architecture. For the cell localization and the presence of FurR and NagC control elements, among the *B. subtilis* rhodanese-like proteins, YhqL is supposed to be the primary candidate that could share the same biological function with RhdA. In preliminary experiments, the Δ*yhqL* single mutant

JD0206 and the rhodanese-like quadruple null-mutant J1235 strains showed similar results about the BSH levels, further supporting the hypothesis that YhqL is the *B. subtilis* orthologous of RhdA.

In conclusion, during my PhD research project, I gave solid indications of a direct involvement of members of the rhodanese-like protein superfamily in protecting the cell from endogenous oxidative stress that can arise, for example, from cellular respiration. The maintenance of the cellular respiration is equivalent to cell survival and became critic, for example, for pathogens bacteria when under attack of the host cell opening, among others, to future implications of the rhodanese-like protein superfamily as a potential drug target for pathogen eradication.

CHAPTER 2:

Introduction

2.1 Chemistry of sulfur

Sulfur, the eighth most abundant element in humans, is an essential element for life due in large part to its chemical versatility (Beinert., 2000). Some of the unique chemical properties of sulfur can be attributed to the availability of d-orbital electrons in its binding. Elemental sulfur is typically found in rings composed of eight sulfur atoms (S_8), which is the most stable allotrope (Brown., 2000).. Sulfur is never found as a single atom due to its tendency to readily form bonds with other atoms (Beinert., 2000). The S–S bond is highly reactive to heat and radiation, but biologically-important processes typically involve bimolecular nucleophilic (S_{N2}) reactions with the S–S bond (Brown., 2000).. Another characteristic of sulfur that can be attributed to the availability of d-orbital binding is its ability to exist in various valencies and oxidation states. Sulfur has valencies of 2, 4, and 6, and oxidation states of –2, 0, +2, +4, and +6 (Brown., 2000).. The number of oxidation states available in sulfur allows it to form many oxyanions, including sulfate, sulfite and thiosulfate (Roy et al., 1970). These oxyanions are biologically active and play significant roles in cellular metabolism (Beinert., 2000). Sulfur is a critical component of proteins and coenzymes such as thiamin, biotin, molybdopterin, coenzyme A, and lipoic acid. Sulfur is found in protein and protein complexes as thiols (cysteine), disulfides (cystine), thioethers (methionine), or as a constituent of iron-sulfur clusters (Brown., 2000).. The chemical activity of sulfhydryl groups and disulfides in proteins is essential to the activity of many enzymes. It has been reported that nearly 40% of proteins lose activity when chemical reagents bind sulfhydryl groups, and disulfide bridges are important in the stabilization of the tertiary and quaternary structures of some proteins (Beinert., 2000). Many human diseases can be attributed to deficiencies in enzymes involved in sulfur metabolism (Muller., 1984), for that reason significant areas of research focus on trafficking of sulfur *via* sulfurtransferases and elucidating the pathways in which sulfur is incorporated into biologically-important molecules.

2.2 Sulfane sulfur

2.2.1 Biological significance

Sulfane sulfur atoms are sulfur atoms covalently bound in chains to other sulfur atoms and have an apparent oxidation state of 0. The highly reactive sulfane sulfur is mostly contained in sulfur compounds such as polysulfides (R-S-S_n, n > 2), thiosulfate (SSO_3^{2-}), polythionates ($^{2-}O_3S$-S_n-SO_3^{2-}), persulfides (R-S-S^-), and elemental sulfur (S_8) (Beinert., 2000; Iciek., 2001; Toohey., 1989). S_0 readily reacts with cyanide and is frequently referred to as “cyanolyzable sulfur” (Iciek., 2001, Toohey., 1989) and is supposed to be the form of sulfur incorporated into many biological compounds, including biotin, thiamin, and thiol-modified tRNA (Beinert, 2000).

It has also been suggested that S_0 plays a significant role in cellular regulation (Toohey et al., 1989), carcinogenesis (Sundaram et al., 1996), and as a key actor in protection against oxidative stress acting as an antioxidant (Iciek et al., 2001). Very little is known about the generation of S_0 but recent publication suggest that sulfane sulfur can be enzymatically produced by direct conversion of S_8 into S_7 with the concomitant formation of a glutathione persulfide (GS-SH) (Hildebrandt et al., 2008) and by the desulfydration of cyst(e)ine perfomed by cystathionases and cysteine desulfurases

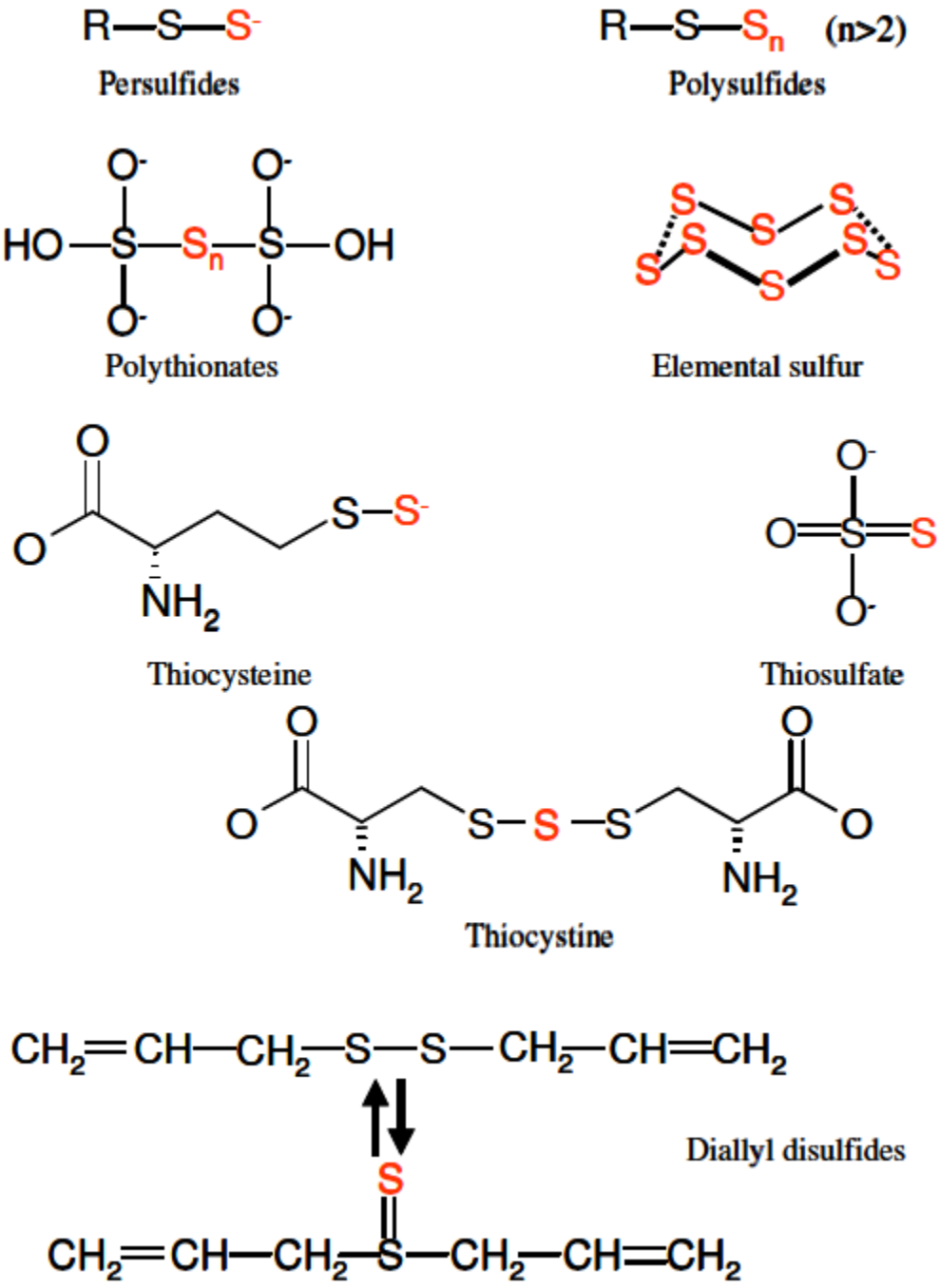

Figure Sulfane sulfur containing compounds

The conservation of sulfane sulfur carrier proteins in many species, from bacteria to human, gives evidence that supports S_0 as an important component of cellular regulatory processes (Toohey,

1989) and it is believed that the covalent modification of sulfhydryl groups in proteins by S_0 can lead to either their activation or inactivation (Iciek et al., 2001; Toohey., 1989). Although sulfur is present in many important cofactors and sulfane sulfur seems to be their building block , the cellular trafficking for delivering sulfane sulfur to these cofactors is still not fully understood (Mueller 2006).

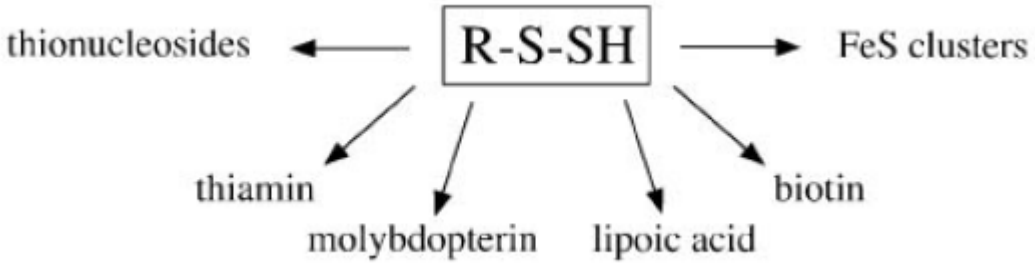

Figure sulfur compounds. Schematic representation of sulfur compounds that mandatory require sulfane sulfur as sulfur source

2.2.2 S_0 carrier proteins

Many enzymes have been characterized as sulfane sulfur carrier proteins. Examples of proteins that have been well studied include, cysteine desulfurases, cystathionase and sulfurtransferases. These proteins are distributed throughout life and allow for the transport of the highly reactive S_0 atom around the cell by forming stable protein-sulfur complexes (Toohey., 1989).

2.2.3 Cystathionase

Cystathionases, also named as Cystathionine gamma-lyases, are 5'-phosphate (PLP)-dependent enzymes involved in the irreversible methionine transulfuration pathway and in the production of cysteine and piruvate using cystathionine as substrate (Brosnan et al., 2006).

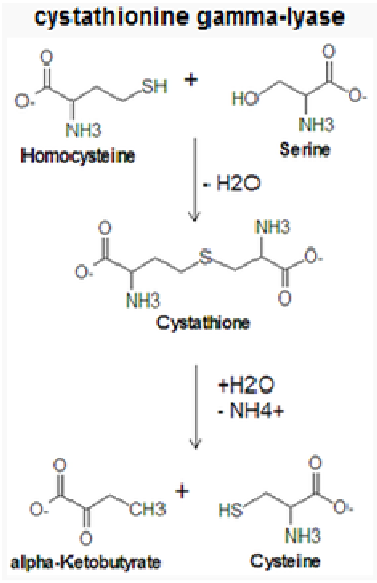

Fig cystathionase: Cysteine metabolism, cystathionases catalyze the lower reaction

The peculiarity of cystathionases resides in the ability of these enzymes to stabilize a trisulfde bond between the two catalytic cysteine residues and an extra sulfur atom thus helping the maintenance of the intracellular sulfane sulfur pool (Toohey 1989).

2.2.4 Cysteine desulfurases

Cysteine desulfurases are up to now considered as the initiator of sulfur mobilization inside the cell representing the most relevant example of a S_0 carrier proteins (Mihara et al., 2002). Cysteine desulfurases are PLP-dependent enzymes whose the *in vitro* catalytic reaction consists of the generation of a sulfane sulfur atom, that is carried on the protein catalytic cysteine (Zheng et al., 1993), by conversion of an L-cysteine to L-alanine (Mihara et al., 2002). The sulfane sulfur atom is then incorporated into essential sulfur-containing compounds through pathways that are not yet fully elucidated.

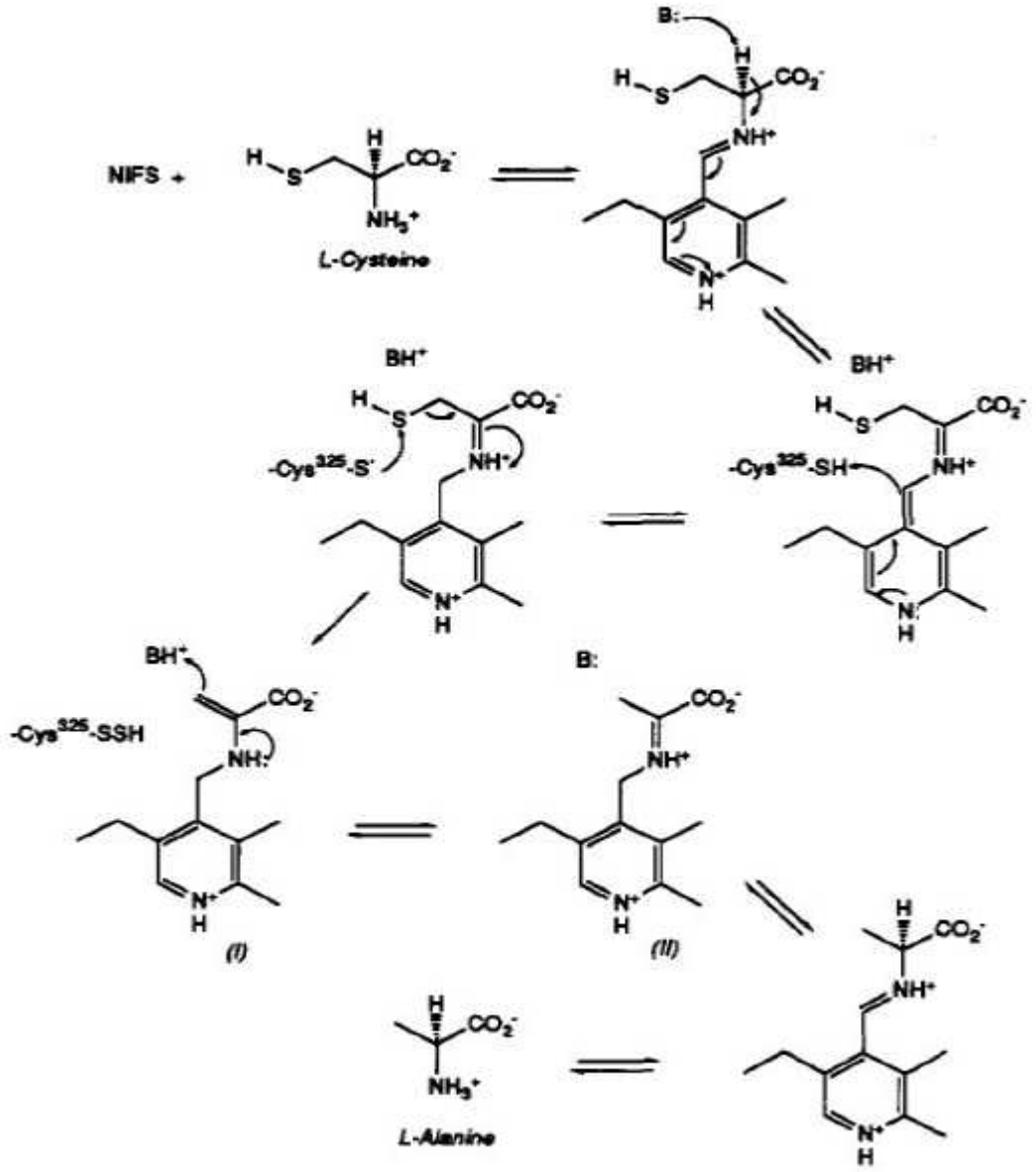

Figure cysteine desulfurase mechanism. Mechanism of NifS desulfuration

Cysteine desulfurases were first studied in the nitrogen fixation (*nif*) gene cluster of *Azotobacter vinelandii* (Mihara et al., 2002; Jacobson et al., 1989). The *nifS* gene encodes the homodimeric, PLP-dependent NifS cysteine desulfurase that is involved in the synthesis of [Fe-S] clusters specifically for the nitrogenase enzyme. The desulfuration of L-cysteine catalyzed by NifS generates an enzyme-bound cysteine persulfide, which serves as the ultimate sulfur source for the specific [Fe-S] clusters essential for the activity of nitrogenase (Zheng et al., 1993; Frazzon et al., 2002). *A. vinelandii* encodes a protein homologous to NifS named IscS (Zheng et al., 1998). IscS is a cysteine desulfurase involved in the maturation of [Fe-S] clusters within proteins that are part of general cellular processes and is known to be essential as knockouts of the gene are lethal (Frazzon et al., 2002; Zheng et al., 1998).

The mechanism for cysteine desulfuration is initiated when the cysteine substrate forms a Schiff base with PLP. The sulfur atom of the substrate cysteine is subsequently transferred to the active site cysteine residue. Thus, the enzyme generates L-alanine and contains an active site cysteine persulfide intermediate (Zheng et al., 1994). In the case of IscS from *E. coli*, the persulfide sulfur can be released as either sulfane sulfur or, in reducing conditions, as sulfide (S^{2-}), and can serve as a sulfur source for a variety of cofactors and thiolated tRNAs (Lauhon et al., 2000; Coop et al., 2003).

2.2.5 Sulfurtransferases

Sulfurtransfrases are a class of proteins characterized by the peculiarity to transfer a sulfur atom from a suitable donor to a suitable acceptor without using any cofactor either organic or not organic. Sulfurtrasferases are mandatory for the vehiculation of S_0 and were originally classified in function of their *in vitro* preferential substrate as 3-mercaptopiruvate sulfurtransferes, like SseA from *E. coli*, and thiosulfate:cyanide sulfurtransferases, like the *Bos taurus* rhodanese (RDP).

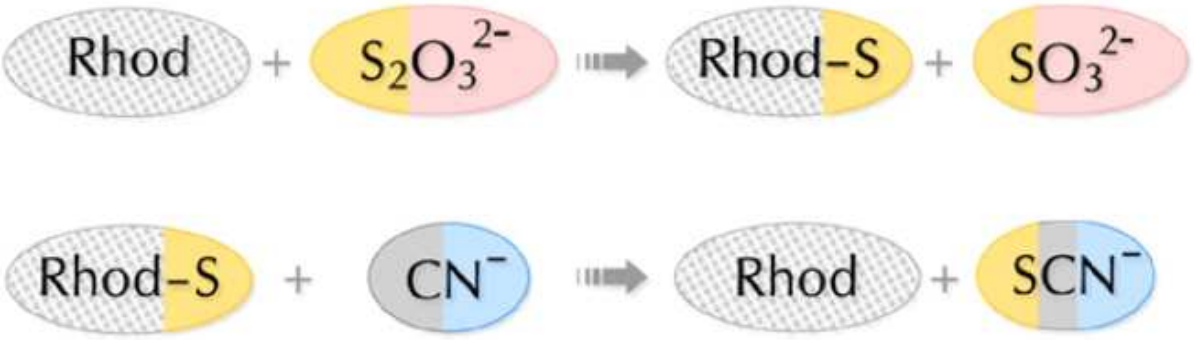

Figure sulfurtransferase activity. Schematic representation of the rhodanese *in vitro* sulfurtrasferase activity from a suitable sulfur donor to cyanide with the concomitant formation of thiocyanate.

All these enzymes have the ability to carry S_0 as cysteine persulfides or as a persulfide derivative, like the case of cystathionase that has been shown to carry S_0 in a stable trisulfide between two cysteine residues (Toohey., 1989), and can act in an independent or cooperative way. Example of cooperation in transferring sulfane sulfur atom between cystathionases and RDPs protein superfamilies has been evidenced by Szczepkowski and Wood that showed that cystathionase and rhodanese form *in vitro* a coupled enzyme system that can transfer sulfur from cysteine to cyanide, sulfite, or to other compounds (Szczepkowski et al., 1967) via the intermediate formation of thiocysteine, that has been shown to be a more efficient substrate for rhodanese than thiosulfate (Abdolrasulnia et al., 1979). This evidence suggests that the two enzymes are coupled in a

transulfuration system that utilizes thiocysteine generated from cysteine as an intermediate source of sulfane sulfur (Szczepkowski et al., 1967).

More recently a direct S_0 exchange was suggested between the rhodanese domain of ThiI and IscS in *E. coli* in which the sulfane sulfur beared by IscS, and produced by conversion of L-cysteine into L-alanine, is directly passed to ThiI for the *in vitro* biosynthesis of 4-thiouridine (s(4)U), a modified nucleotide in tRNA (Kambampati et al., 2000).

2.3 Thiosulfate:cyanide sulfurtransferase (rhodanese)

In 1933 an enzyme was characterized and catalyzed the transfer of sulfur from thiosulfate to cyanide, forming thiocyanate. The enzyme was named rhodanese from the German word for thiocyanate, *rhodanid*, by Lang (Cooper et al., 1983). Rhodanese (thiosulfate:cyanide sulfurtransferase, EC 2.8.1.1) has become one of the better-characterized sulfurtransferases. The rhodanese homology domain is a ubiquitous structural module found in a variety of proteins (Bordo et al., 2002; Bordo et al., 2000).

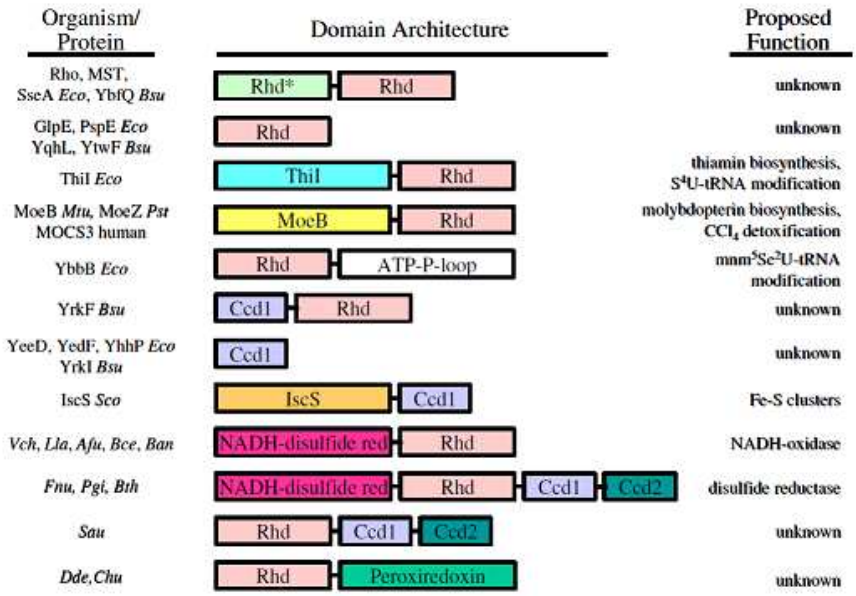

Figure Rhodanese architectures. Architectures of various catalytic rhodanese domains (Rhd), pseudo rhodanese domains (Rhd*), conservative cysteine domains (Ccd1) and predicted peroxiredoxin domains (Ccd2). ***Eco, E. coli; Bsu, B. subtilis; Mtu, Mycobacterium tuberculosis; Pst, Pseudomonas stutzeri; Sco, Streptomyces coelicolor; Vch, Vibrio cholera; Lla, Lactococcus lactis; Afu, Archaeoglobis fulgidus; Ban, Bacillus anthracis; Fnu, Fusobacterium nucleatum; Pgi, Porphyromonas gingivalis; Bth, Bacteroides thetaiotaomicron; Sau, Staphylococcus aureus; Dde, Desulfovibrio desulfuricans; Chu, Cytophaga hutchinsonii***

It was originally proposed that RDPs were involved in the detoxification of cyanide because these enzymes convert cyanide to the less toxic thiocyanate and were found at high concentrations in mitochondria (Vennesland et al., 1982). However, since RDPs are known to be ubiquitous enzymes

and to be associated with a variety of functional domains, it has been suggested that they are involved in a wide range of cellular functions (Bordo et al., 2002; Bordo et al., 2000). The rhodanese homology domain is comprised of an active site fold, containing a conserved cysteine residue, flanked by two structural motifs, CH2A and CH2B (Faumann et al., 1998). Proteins containing the rhodanese module are found in a variety of different domain architectures (Bordo et al., 2002; Bordo et al., 2000). Several well-characterized RDPs are comprised of a functional rhodanese domain fused to a structurally identical, non-functional rhodanese domain (Bordo et al., 2002; Bordo et al., 2001). RDPs have also been isolated as single-domain proteins and have been found as domains in proteins with a variety of functions (Spallarossa et al., 2001).

The 297 amino acid rhodanese from *B. taurus* is the best-characterized of the RDPs (Westley, 1981; Westley et al., 1983). Bovine rhodanese catalyzes the transfer of sulfane sulfur from thiosulfate to cyanide via a double-displacement (ping-pong) mechanism involving the formation of a cysteine persulfide at the active site.

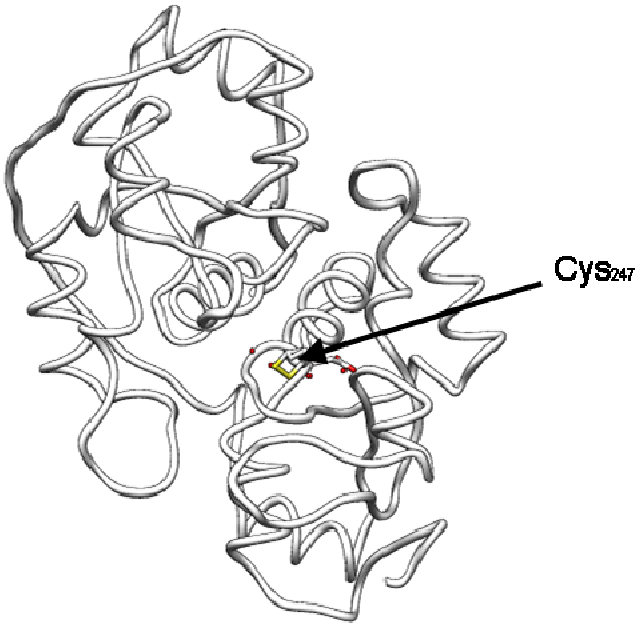

Figure bovine rhodanese. Mithocondrial bovine rhodanese 3D structure. Catalytic Cys_{247} residue is highlighted by a black arrow

Crystallographic studies reveal that bovine rhodanese is comprised of two domains of identical α/β topology (Ploegman et al., 1979; Ploegman et al., 1978). Though there is limited sequence identity between the two domains, both display a structure similarities that consist of a central five-stranded β-sheet surrounded by α-helices. The N-terminal domain is not catalytically active, whereas the active site Cys_{247} is located in the C-terminal domain. Cys_{247} can accept a sulfur from a suitable

sulfur acceptor like thiosulfate, forming a persulfide intermediate, and the enzyme cycles between this form and a sulfur-free form during its catalytic mechanism (Ploegman et al., 1978). The two forms of the enzyme (sulfur-free and persulfide) have no significant structural differences (Gliubich et al., 1996). However, the persulfide form of rhodanese is more resistant to direct oxidation (Horowitz et al., 1989). Though the first RDPs characterized consisted of two identical domains, the elucidation of entire genomes from a variety of organisms has revealed that RDPs can be found in a number of different domain architectures. The presence of single-domain rhodanese homologs supports the hypothesis that the duplication of an ancestral rhodanese gene gave rise to the two-domain RDPs (Spallarossa et al., 2001). Rhodaneses such as GlpE (Ray et al., 2000) and PspE (Adams et al., 2002) of *E. coli* demonstrate that a second N-terminal domain is not necessary for the *in vitro* catalysis. Therefore, a single-domain rhodanese module in a protein may play an important role in the regulation of the enzyme activity. This assertion is supported by known examples, including YbbB (Wolfe et al., 2004) and ThiI of *E. coli* (Palenchar et., 2000) and human MOCS3 (Matthies et al., 2004) where it has been shown that the rhodanese domain of each protein is necessary for their respective activities

2.3.1 *Azotobacter vinelandii* RhdA

A. vinelandii RhdA (Colnaghi et al., 1996; Bordo et al., 2001; Pagani et al., 2000) is a rhodanese-like protein classified as a TST because of its ability to catalyze *in vitro* the typical rhodanese reaction. The enzyme is composed of two similarly folded α/β domains, each of approximately 125 amino acids, displaying very conserved three-dimensional structure, characterized by a central parallel β-sheet surrounded by α-helices. A trace of the ancestral gene duplication is still present in the amino acid sequence of the two RhdA domains, which have 26 identical residues out of a total of 125 (20.8 % of identity).

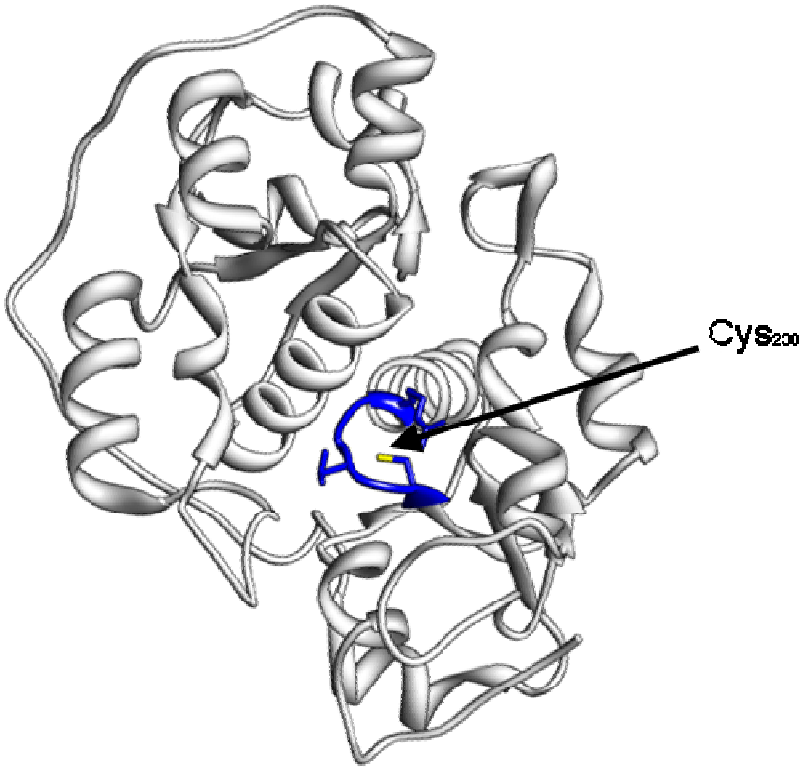

Figure *A. vinelandii* RhdA. *A. vinelandii* RhdA 3D structure, the active site is highlighted in blue while catalytic Cys_{230} residue is evidenced by a black arrow.

The active-site residue, Cys_{230}, the only cysteine residue present in the whole protein, is located in the C-terminal domain at the bottom of a shallow round pocket on the protein surface. The active-site loop adopts a semicircular, cradle-like, conformation, which allows precise positioning of the Cys_{230} sulfur atom at the bottom and in the centre of the active-site pocket.

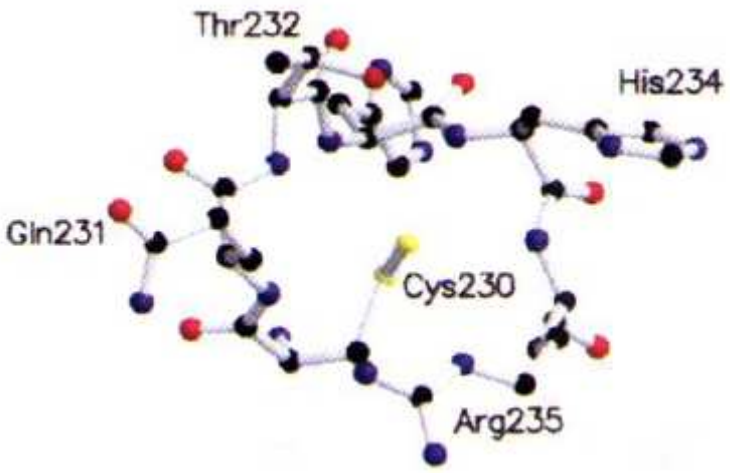

Figure RhdA active site. *A. vinelandii* active loop 3D structure (Bordo et al., 2001)

The RhdA catalytic centre has a motif (HCQTHHR), not commonly found in RDPs, that originates a strong positive electrostatic field, thus favoring stabilization of a persulfide bond on the catalytic Cys_{230} residue. This feature is due to the six peptide dipoles, from 230 to 235, radially oriented with their positive ends aiming at the centre of the catalytic pocket, thus making an active site with electrostatic and sterical properties of an anion binding site (Bordo et al., 2001).

As before stated, the RhdA active-site motif (HCQTHHR) is not currently found in rhodanese domain proteins. In RhdA, conserved catalytic cysteine is surrounded by residues that are entirely different from those found in the vertebrate enzymes (Colnaghi et al., 1996; Bordo et al., 1999). In the active site motif of the bovine rhodanese (Ploegman *et al.*, 1978), the cationic residue Lys_{249} has been identified as catalytic requirement for the sulfur transfer function (Luo et al., 1994) and replacement of Lys_{249} with an hydrophobic residue (Ala) knocks out Rhobov ability to transfer sulfane sulfur in vitro. In RhdA, the corresponding residue is Thr_{232}. When Thr_{232} was replaced with either Lys or Ala (Pagani et al., 2000), the ability to transfer sulfane sulfur from thiosulfate to cyanide increased about three-fold in both mutants as compared to that of the wild-type RhdA (Pagani et al., 2000). This result evidenced that the catalytic proprieties of RhdA are different from those of known mammalian TSTs thus leading to the hypothesis of the involvement of RhdA on processes that differs from cyanide detoxification *via* thiosulfate. Further inspections of the RhdA active-site 3D structure (Bordo et al., 2000-2001) highlighted the structural relationship with the active-site structures of Cdc25 phosphatases (Fauman et al., 1998; Reynolds et al., 1999). In Cdc25 phosphatases the active site loop [His–Cys–$(X)_5$–Arg] is one residue longer than in RhdA [His–Cys–$(X)_4$–Arg]. To prove the hypothesis that the length of the RhdA active-site loop should play a key role in substrate recognition and catalytic activity, RhdA scaffold was the starting point for producing mutants with single-residue insertion to generate the catalytic loop HCQTHAHR and HCQTHSHR. Analyses of the catalytic performances of these engineered RhdAs revealed that elongation of the catalytic loop definitely compromised the ability to catalyze sulfur transfer reactions, while it generated the ability to hydrolyze phosphorus-containing compounds (Forlani et al., 2003). Another feature of RhdA is that, after heterologous expression in *E. coli*, RhdA is purified in a mixture of persulfurated and unpersulfurated forms, and L-cysteine was identified as the most effective *in vivo* sulfur source in producing RhdA-SSH (Forlani et al., 2005). As before stated, the active-site loop of RhdA appears properly designed to stabilize its persulfurated form (RhdA-SSH), and RhdA-SSH was productively used as the only sulfur source for in vitro 2Fe-2S cluster assembly in apo-adrenodoxin (Cereda et al., 2003).

2.4 Mercaptopyruvate sulfurtransferase (MST)

Mercaptopyruvate sulfurtransferase (MST) (EC 2.8.1.2) catalyzes the transfer of sulfur from mercaptopyruvate to a variety of thiophilic compounds that include cyanide, sulfite, and thiols (Spallarossa et al., 2004). The physiological roles of MSTs are currently unknown and widely speculative (Spallarossa et al., 2004). Though not as extensively characterized as the sulfurtransferase rhodanese, MSTs from rat liver (Nagahara et al., 2004), *Arabidopsis thaliana* (Papenbrock et al., 2000), *E. coli* (Spallarossa et al., 2004), and *Leishmania major* (Alphey et al., 2003) have been studied. Kinetic studies of MSTs and RDPs show most of the MSTs transfer sulfur through a sequential mechanism (Nagahara et al., 1999), whereas RDPs do so through a ping-pong mechanism (Westley, 1983). The amino acid sequence of MSTs is similar to rhodanese sequence (up to 66% of identity) and both MSTs and rhodaneses contain a six amino acid active site loop that begins with a catalytic cysteine residue (Nagahara et al., 1995).

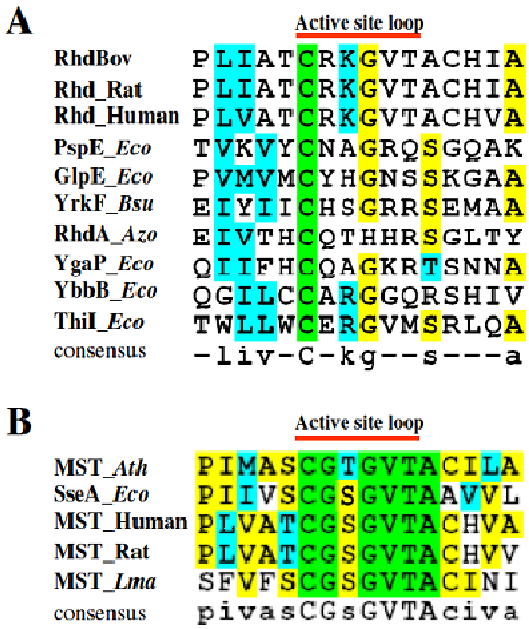

Figure active sites. Active site residues of various RDPs (A) and MSTs (B) were aligned using CLUSTALW. In green are highlighted the conserved residues, in yellow the identical residues, in light blue the similar ones while in white are highlighted the not conserved residues. RhdBov (*B. taurus*, M58561), Rhd_Rat (*R. norvegicus*, P24329), Rhd_Human (*H.sapiens*, Q16762), PspE_Eco (*E. coli*, P23857), GlpE_Eco (*E. coli*, M96795), YrkF_Bsu (*B. subtilis*, CAB14594), RhdA_Azo (*A. vinelandii*, P52197), YgaP_Eco (*E. coli*, P55734), YbbB_Eco (*E. coli*, F64781), ThiI_Eco (*E. coli*, NP_414957). (B) MST_Ath (*A. thaliana*, CAB64716), SseA_Eco (*E. coli*, JX0320), MST_Human (*H. sapiens*,P25325), MST_Rat (*R. norvegicus*, P97532), MST_Lma (*L. major*, CAC85741).

However, MSTs show little variability in the amino acid composition of the active site loops and are characterized by the consensus CG[S/T]GVT (Spallarossa et al., 2003). This is in contrast to RDPs, which tend to show substantial variability in the active site loop sequences (Bordo et al., 2000). Mutagenic studies of the MST and rhodanese active sites reveal that changes in key residues

can partially shift substrate specificities of the enzymes (i.e. an altered rhodanese displays MST activity, and *vice versa*) (Nagahara et al., 1995). The substitution of the active site serine in rat liver (Nagahara et al., 1995; Nagahara et al., 1996) MST to lysine resulted in conversion to a more rhodanese-like activity. Recently, solved structures of *E. coli* (Spallarossa et al., 2004) and *L. major* MSTs (Alphey et al., 2003) revealed 3-dimensional folding similar to RDPs and allowed for comparison of structure/function relationships between rhodaneses and MSTs.

E. coli MST (SseA), solved to a resolution of 2 Å, consists of two identical rhodanese-like domains (Spallarossa et al., 2004). Each domain is composed of a central α-helics structure surrounded by β-sheets. In the structure, the catalytic Cys_{237} appears to contain a bound persulfide sulfur. However, this is likely an artifact of the high concentration of $Na_2S_2O_3$ required for crystallization. Mass spectral and fluorescent studies indicate SseA does not maintain a stable persulfurated form, and the amino acid composition of the active site would not stabilize a persulfide sulfur (Spallarossa et al., 2004). The active site loop of SseA does not form the "cradle-like" shape observed in RDPs (Bordo et al., 2001) and the Cys_{237} is shielded from solvent in one of at least two different conformations. The two different forms of the enzyme observed varied in the conformation of loop 61-67 and were named "open" and "closed" based on the solvent accessibility of Cys_{237} (Spallarossa et al., 2004). The different forms of SseA observed might give insight into the catalytic mechanism of MSTs and explain why a ping-pong mechanism is not observed. The open form of loop 61-67 may allow Cys_{237} access to 3-mercaptopyruvate, which then can form a covalent thiosulfoxide at the active site. The sulfur would then be transferred to a nucleophilic molecule in a sequential manner (Spallarossa et al., 2004).

The structure of *L. major* MST shows that the enzyme contains three domains. The N-terminal and central domains have structures similar to rhodanese and *E. coli* MST, with the active site Cys_{253} located within the central domain. The C-terminal domain consists of about 80 amino acids and its function is unknown (Alphey et al., 2003). However, proteins with a C-terminal truncation are not stable because of an inability to fold correctly (Williams et al., 2003). The solved structure contains a sulfite molecule bound in the active site and persulfides on Cys_{253} and Cys_{331}. These modifications most likely resulted from crystallization in buffer containing thiosulfate, as was done for SseA. However, the active site loop of *L. major* MST could possibly stabilize an active site persulfide, unlike SseA (Alphey et al., 2003). The structure also reveals that the amino acids Gly_{254} and Ser_{255} (corresponding to bovine rhodanese Arg_{248} and Lys_{249}, respectively) may be important residues in determining the activity of the enzyme. Conversion of bovine rhodanese Arg_{248} and Lys_{249} to glycine and serine increases the MST activity of rhodanese (Nagahara et al., 1999), and, as

previously mentioned, conversion of the rat MST active-site serine to lysine results in an increase in rhodanese activity (Nagahara et al., 1995; Nagahara et al., 1996).

2.5 Oxidative stress

2.5.1 Origins and mechanistic aspects of the oxidative stress damage

Undergoing to oxidative stress is an unavoidable biological problem for the cellular environment because of the nature of the reaction that is an univalent electron transfer. Oxygen molecules are small enough to enter in most of the protein active sites and, if they contact redox cofactors at a lower potential than oxigen, then electron transfer can easily occur generating reactive oxygen species (ROS). The formation of intracellular ROS steady flux in an aerobe organism mostly depends from the high permeability of cellular membranes to oxygen, which intracellular concentration is equivalent to that which is immediately outside the cell (Ligeza et al., 1998), and from the ubiquitous presence of flavoenzymes that can easily interact with molecular oxygen thereby generating partially reduced oxygen species (Massey et al., 1969). For this reason microaerophilic bacteria and mammalian cells are substantially protected from oxidative stress because they grew in habitats where the extracellular compartment is consistently saturated with air.
Autoxidation events can produce two main species or ROS depending on the number of electrons that are actively exchanged. If one electron is exchanged, superoxides (O_2^-) are the most representative species produced, while the exchangement of two electrons lead to the production of hydrogen peroxides (H_2O_2). Experiments conducted on *E. coli* in order to discern the predominant intracellular sources of ROS have demonstrated that the respiratory chain is the main sources of O_2^-, while the H_2O_2 cytoplasmic source must lie outside the respiratory chain (Korshunov et al., 2006).
The natural vulnerability of organisms to ROS is exploited by plants and microbes to negatively influence the growth of their competitors. They excrete redox-cycling compounds that diffuse into nearby bacteria, where these agents generate O_2^- by oxidizing redox enzymes and transferring the electrons to molecular oxygen. Such compounds are typically viologens, phenazines, or quinones, and they can highly elevate the rate of intracellular ROS formation. Redox-cycling compounds can also generates H_2O_2 in concomitance with O_2^- due to the dismutation of this latter. Unlikely O_2^-, H_2O_2 is uncharged and can easily pass trough cellular membrane thus giving to this latter stressor a strategic advantage. For these reason organism have evolved strategies to produce and secrete high amount of H_2O_2. Lactic bacteria, as example, suppress the growth of their competitors by using lactate or piruvate oxidases to produce large doses of H_2O_2. Moreover plants and mammals activates specific terminal NADPH oxidases that produce high amount of stressor at the level of the wound site (plants) or at the level of the macrophage (mammals).

Although cells can be killed by exogenous H_2O_2, lethal doses are in the millimolar range, due to the redundancy of the protection systems, making difficult to understand which biological molecules

are the primary ROS targets and what is the damage mechanism. Clarity has emerged characterizing the phenotype of *E. coli* mutants lacking scavenging enzymes. An *E. coli* mutant strain lacking the synthesis of superoxide dismutases (SODs) has comparable anaerobic growth rate to the wild-type but has growth defects in aerobiosys due to the accumulation of O_2^- (Carlioz et al., 1986). Furthermore *E. coli* cells were poisoned by the accumulation of H_2O_2 in catalase/peroxiredoxin double mutants (Jang et al., 2007) displaying similar phenotypes to SODs mutant that stem from the inactivation of a family of dehydrateses (Flint et al., 1993). The action of either O_2^- and H_2O_2 consist in the destabilization of the uncoordinated iron atom of the $[4Fe\text{-}4S]^{2+}$ dehydratases iron-sulfur cluster that is responsible for the binding with the substrate. The O_2^- univalently oxidizes the cluster to $[4Fe\text{-}4S]^{3+}$ that spontaneously releases the catalytic iron forming the inactive $[3Fe\text{-}4S]^{+}$ cluster while H_2O_2 divalently oxidized the cluster releasing ferric iron to generate the $[3Fe\text{-}4S]^{+}$ species (Jang et al., 2007). The O_2^- and H_2O_2 are also mutagenic. H_2O_2 indirectly oxidize the DNA, by oxidizing unincorporated ferrous iron (Fe^{2+}), some of which is associated with DNA via Fenton reaction (Henle et al., 1999) .

$$Fe^{2+} + H_2O_2 \rightarrow FeO^{2+} + H_2O.$$
$$FeO^{2+} + H^+ \rightarrow Fe^{3+} + HO^{\bullet}.$$

Figure fenton reaction. Schematic representation of the two steps Fenton reaction

This reaction can occur quite easily at physiological pH value (rate constant between $5x10^5$ and $20x10^5$ M^{-1} s^{-1}) leading to the formation of hydroxyl radical (OH*) that is characterized by reacting near the site of its production because of its low diffusion rate. OH* is highly reactive toward purines leading to DNA depurination. Unlikely H_2O_2, O_2^- can not directly react with ferrous iron. DNA damage provoked by O_2^- arise from its ability to release iron from damaged dehydratases (Keyer et al., 1996). Because of the ability of iron to bind lipids and protein surface, it is probable that even this biological molecule can suffer from oxidations and could explain additional defects of both SODs and catalase/peroxiredoxin *E. coli* mutant that are unable to synthesize aromatics compounds, including amino acids, and are unable to perform normal sulfur metabolism (Carlioz et al., 1986).

Due to the different biochemical actions of O_2^- and H_2O_2 microorganisms have evolved distinct strategies to sense discrete forms of oxidative stress.

2.5.2 SoxR(S) regulator of the superoxide response.

E. coli exposure to redox cycling antibiotics causes the overexpression of manganese containing superoxide dismutase (MnSOD) (Hassan et al., 1977) which transcription was found to be regulated by the SoxR(S) system. This system is composed by two protein: SoxR is the sensor protein that detects redox stress while SoxS is the transcription factor that positively regulates about two dozen of genes including *sodA* (Pomposiello et al., 2001). SoxR is an homodimer containing one [2Fe-2S]$^{+}$ cluster per subunit that is oxidized to a +2 state by redox-cycling compounds (Ding et al., 1997) leading to conformational changes that improves promoting site accessibility to RNA polymerases. In enteric bacteria this process enhance *soxS* expression by more than 20-fold. SoxS functions as a secondary inducer that further promotes the transcription of the SoxR(S) regulon. It seemed reasonable to deduce that the SoxR(S) system is activated by O_2^- due to the ability of this ROS to directly oxidize iron-sulfur cluster and because this system regulates *E. coli* superoxide dismutases expression. Gram-negative bacteria commonly synthesize both cytoplasmic and periplasmic isozymes of SOD as their frontline defense against O_2^-. *E. coli* contains two cytoplasmic SOD isozymes, one each of the manganese- and iron-cofactored types (MnSOD and FeSOD). It also secretes a single copper, zinc-cofactored enzyme (CuZnSOD, also called SodC) to the periplasm. Because O_2^- does not easily cross membranes at neutral pH (Lynch et al., 1978), O_2^- does not flow between these two compartments, and the physiological roles of the cytosolic and periplasmic enzymes can be considered separately. This arrangement is common, and it is ancestral to the mitochondrial MnSOD and cytoplasmic CuZnSOD of eukaryotes. Although SOD exhibits a rate constant that approaches catalytic perfection, bacteria synthesize it in abundance thus further indicating that both abundance and high catalytic activity are essential to protect labile protein iron-sulfur clusters to superoxide anion mediated oxidation.

2.5.3 The OxyR and PerR regulators of response to hydrogen peroxide.

The OxyR regulator belongs to the LysR family of transcription factors and was firstly evidenced in Salmonella mutants hyperresistent to H_2O_2 (Christman et al., 1985). OxyR is a repressor and transcriptional activation of the OxyR regulated genes depends from a mechanism that involves a two step oxidation. H_2O_2 directly oxidize the conserved cys residue Cys_{199} to a sulfenic acid form promoting the formation of a disulfide bond with the Cys_{208} residue inducing a three-dimensional protein reorganization (Zheng et al., 1998). Due to the ability of H_2O_2 to induce DNA damage at low intracellular concentration the OxyR sensitivity to oxidation has to be calibrated to nM H_2O_2 doses. The stop of the induction is given by the reduction at the Cys_{199}-Cys_{208} disulfide bond that allow OxyR to recover its inactive structure. This specific disulfide bond can either be reduced by

glutaredoxin 1 through sulfur exchange reaction (Zheng et al., 1998). Because glutaredoxin 1 and glutathione reductase gene expression is under OxyR control the system comprises a negative feedback mechanism. Although the OxyR system is widespread among bacteria, the Gram-positive bacterium *Bacillus subtilis* uses a distinct H_2O_2 sensor mechanism (Bsat et al., 1996) based on the PerR regulator. The PerR protein can bind a single ferrous iron atom, and in this form, it is active as a transcriptional repressor. Upon exposure to H_2O_2, the iron atom is oxidized in a direct Fenton reaction that generates a ferryl and/or hydroxyl radical. This species covalently oxidizes one of the metal-coordinating histidinyl residues (Lee et al., 2006), and this modification likely facilitates ferric iron dissociation and blocks the reloading of ferrous iron. The demetallated protein lacks DNA-binding activity, allowing the induction of the genes whose transcription it normally blocks.

The OxyR and PerR transcriptional factors regulates the expression of the hydrogen peroxide response machinery in which the primary actor is the peroxiredoxin AhpCF a two component NADH peroxidase (Parsonage et al., 2005). H_2O_2 oxidizes Cys_{46} of AhpC to a sulfenic acid, which then condenses with Cys_{165} to form a Cys_{46}-Cys_{165} disulfide bond. Exchange reactions with other AhpC cysteinyl residues reduce that bond at the expense of the creation of a second disulfide. This bond, in turn, is reduced upon reversible binding of the NADH-reducible flavoprotein AhpF. The Ahp system activity is so high that is able to control the steady intracellular concentration of H_2O_2 to 20 nM even if its rat production is around 15 $\mu M\ s^{-1}$ (Seaver et al., 2001). When higher doses of H_2O_2 are present in the cell, Ahp system is saturated and intracellular hydrogen peroxide concentration rises until 0.1 µM inducing OxyR mediated oxidative stress response (Parsonage et al., 2005). Catalase is strongly induced, and it becomes the primary scavenging enzyme. The *katG*-encoded catalase of *E. coli* exhibits a high K_m, so it is not saturated by even millimolar doses of H_2O_2 (Hillar et al., 2000).

Table 1 Selected genes induced by the SoxRS system[a]

Gene	Enzyme or activity
Oxidant-resistant dehydratase isozymes	
fumC	Fumarase C
acnA	Aconitase A
Suspected cluster repair	
yggX	Fe/S cluster repair protein?
zwf	Glucose-6-phosphate dehydrogenase
fpr	NADPH:flavodoxin/ferredoxin oxidoreductase
fldA	Flavodoxin A
fldB	Flavodoxin B
Drug efflux and/or resistance	
acrAB	Drug efflux pump
tolC	OMP component of drug efflux pump
micF	OmpF antisense sRNA
marAB	Multiple antibiotic resistance operon
nfnB	Nitroreductase
rimK	Modification of ribosomal protein S6
Other	
nfo	Endonuclease IV
fur	Iron-uptake regulatory protein
sodA	Manganese-containing superoxide dismutase
ribA	cGMP hydrolase

[a]Sources: Pomposiello et al. (29) and references within.

Table 2 Members of H_2O_2-stress regulons[a]

Role	*Escherichia coli* (OxyR response)	*Bacillus subtilis and/or Staphylococcus aureus* (PerR)[b]
H_2O_2 scavenging	AhpCF	AhpCF (*B.s.*, *S.a.*)
	Catalase G	Catalase A (*B.s.*, *S.a.*)
		Bcp (thiol peroxidase) (*S.a.*)
Heme synthesis	Ferrochetalase	HemAXCDBL (*B.s.*)
FeS cluster assembly	SufABCDE	
Iron scavenging	Dps	MrgA (Dps) (*B.s.*, *S.a.*)
		Ferritin (*S.a.*)
Iron-import control	Fur	Fur (*B.s.*, *S.a.*)
Divalent cation import	MntH	MntABC (*S.a.*)
		ZosA (*B.s.*)
Disulfide reduction	Thioredoxin C	Thioredoxin reductase (*S.a.*)
	Glutaredoxin A	
	Glutathione reductase	
	DsbG (periplasmic reductase)	
Unknown function	Several	Several

[a]Sources: Zheng et al. (42), Kehres et al. (141), Helmann et al. (125), Horsburgh et al. (130).
[b]*S.a.*: Induced in *Staphylococcus aureus*. *B.s.*: Induced in *Bacillus subtilis*.

Figure oxidative stress regulated genes (Imlay et al., 2008 and references therein).

2.6 Glutathione function as main antioxidant non-enzymatic system.

2.6.1 Glutathione molecular characteristics allow its participation to redox reaction.

Other than specific protein pathways, another oxidative stress response mechanism, in either eukaryotic and prokaryotic cells, is related to glutathione. Glutathione is present in relatively high concentrations in all eukaryotic cells while in prokaryotic cells it is found mainly in Gram-negative bacteria, including *E. coli*. Gram-positive bacteria does not synthesize glutathione, with the exception of some *Streptococcus* and *Enterococcus* species (Fahey et al., 1978).

Glutathione is a tripeptide (L-γ-glutamyl-L-cysteinyl-glycine, molecular mass 307 daltons) characterized by having two negatively charged carboxyl groups and a positively charged amino group at physiological pH values: The presence of the γ-glutamyl bond protects the tripeptide from degradation by intracellular peptidases, and the sulfhydryl group of cysteine can serve as an electron donor, endowing glutathione with reducing properties and ability to remove free radicals.

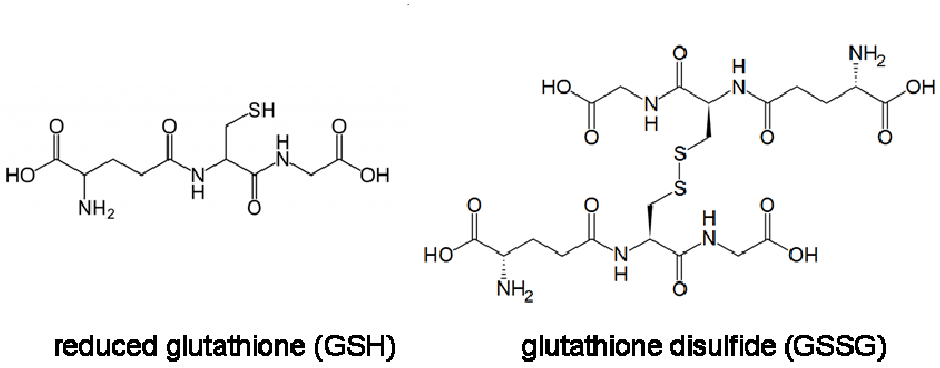

Figure glutathione: Reduced glutathione (GSH) and glutathione disulfide (GSSG) chemical structures

The peculiar characteristics of GSH allow this molecule to participate in various types of reactions involving electron exchanges that can be summarized as follow. One electron reaction of reduced glutathione (GSH) with free hydroxyl radicals (OH*) results in the formation of a thiyl radical, (GS*), that further can react, *in vitro*, with the thiolate form of GSH leading to the production of glutathione disulfide (GSSG) (Starke et al., 2003). A second type of redox reaction in which glutathione participates is thiol–disulfide exchange. This reaction plays a key role in the formation of protein disulfides (GSSR) and may be an important element in regulation of biological processes (Kosewer et al., 1987). A third type of redox reaction involves two-electron oxidation of GSH with the formation of an intermediate reacting with a second identical or non identical molecule to form glutathione disulfide GSSG or mixed disulfide, respectively.

GSH is synthesized in all cell types via two sequential ATP-dependent reactions catalyzed by γ-glutamylcysteine synthetase (γ-GCS) (EC 6.3.2.2) and GSH-synthetase (GS) (EC 6.3.2.3). γ-GCS catalyzes the formation of a peptide bond between the γ-carboxyl group of glutamate and the α-amino group of cysteine. Glutathione synthetase forms the peptide bond between the α-carboxyl of cysteine in γ-glutamylcysteine and the α-amino group of glycine. In bacteria, as in other organisms, GSH synthesis is limited by GSH feedback inhibition and by the bioavailability of L-cysteine and is stimulated by the addition of cysteine or its precursors into the medium (Loewen et al., 1979). The essential role of cysteine in GSH synthesis is related to cysteine susceptibility to produce OH* by Fenton reactions with ferric iron in the presence of H_2O_2. So, under normal conditions bacteria and other cells maintain a very low intracellular pool of cysteine (<200 μM) (Park et al., 2003) and require a nontoxic reserve form of cysteine, such as GSH.

2.6.2 Glutathione status define cells redox conditions.

The glutathione status is defined as the concentration of total glutathione and the ratio between its different forms in the cell (Kosewer et al., 1978). The most important forms of glutathione are

reduced GSH, GSSG, and mixed disulfides: mainly GSS-protein, and mixed disulfides with low molecular weight SH compounds, such as cysteine, α-pantetheine, and coenzyme A (CoA). *In E. coli* cells, 99.5% of glutathione exists in the reduced form. The concentration of GSSG is 0.17-0.33% of the total intracellular glutathione, and the ratio GSH/GSSG = 300-600. The level of mixed disulfides does not exceed 1% (1.5-2% of total glutathione is excreted into the medium) (Fahey et al., 1978; Smirnova et al., 2000). Glutathione status depends on the dynamic balance between its synthesis, decomposition, transport, oxidation, and reduction, so it can vary depending on what reaction prevails, which, in turn, depends on cellular state and environmental conditions. Changes in glutathione status might be observed under both normal physiological situations and stresses or result from genetic defects or the reaction of some chemicals. The most significant changes in GSH status are observed in *E. coli* mutants in genes encoding enzymes of glutathione metabolism. The absence of glutathione reductase (GR), the enzyme devoted to the NADPH-dependent reduction of GSSG, results in increased fraction of GSSG: although the level of GSH remains almost unchanged, the ratio GSH/GSSG decreases almost two-fold. The most appreciable changes in glutathione status are observed in cells deficient in glutathione reductase, catalase, and GSH synthesis, in which the concentration of GSSG and mixed disulfides increases by more than ten-fold (Alonso-Moraga et al., 1987). Irreversible changes in glutathione status appear resulting from inhibition of synthesis, covalent binding, or irreversible efflux of glutathione that are prominent in induced oxidative stress conditions. Most existing data concern changes in the level of reduced glutathione, whereas the status of other glutathione forms in the cell under various influences remains far less studied.

2.6.3 Glutathione participation in the oxidative stress response system.

The glutathione high intracellular concentration, its redox properties, its resistance to auto-oxidation and its ability to maintain the reduced state make this molecule the most important redox buffer. In fact the intracellular GSH concentration is between 500 and 1000 times higher compared to the one of NADPH and other cellular redox systems suggesting that changes in glutathione redox states can directly reflects changes in the cellular redox status (Shafer et al., 2001).

Glutathione can be involved directly or indirectly in the oxidative stress response machinery. The indirect participation is recognized in the formation of glutathione conjugates or in the transcription regulation *via* formation of glutathione mixed disulfide molecules.

Formation of glutathione conjugates. Because of its nucleophilic properties GSH can react with a large number of electophilic components to produce GSH conjugates (Kosower et al., 1978). The reaction of conjugate formation can develop either spontaneously or can be catalyzed by enzymes belonging to the superfamily of glutathione-S-transferases (GST). GST protein super-family can be

divided in four classes depending on substrate specificity and on amino acid sequence. Although eukaryotic organisms possesses α, μ, π and ɵ classes, the ɵ class is the only one present in the prokaryotic system. The GSTs implication in protecting against oxidative stress has been highlighted by studies on *E. coli*, that possesses nine GST-like proteins (Vuilleumier., 1997). These studies evidenced that the presence of GSTs heighten the bacterial resistance to antibiotics (Perito et al., 1996), some GSTs possesses alkylperoxidase-like activity (Nishida et al., 1994) and that GSTs are involved in the detoxification of peroxides as well as herbicides end pesticides (Vuilleumier., 1997). The GSTs-mediated or spontaneous formation of glutathione-S-conjugates is a conserved mechanism of xenobiotic detoxification in either bacteria and eukaryotic cells that ends with the excretion of the conjugated molecule in the media.

Transcription regulation and enzyme protection via formation of glutathione mixed disulfide. The presence of a redox-sensitive switch in repressors, like OxyR and OhR, implies their activation after the formation of a sulfenic intermediate (as described before), makes them implicit targets for redox regulation with the participation of thiol-containing substances. Due to its high intracellular concentration and its peculiar characteristics, glutathione can be considered one of the effective substrates for the broader concept of protein-S-thiolation (which, as described in Klatt et al., 2000, involves the formation of mixed disulfide between proteins and either glutathione, cysteine and other non biological low molecular weight thiols), that in the case of glutathione is specifically named glutathionylation. In bacteria protein glutathionylation can either be used as a mechanism of protection of redox sensitive catalytic cysteine residues or can be used as a mechanism of transcription regulation. In the presence of diammide or other redox cellular-system damaging-compounds, prokaryotic cells react with the increase of protein glutathionylation in order to prevent irreversible oxidation of sensitive proteins (Miranda-Vizuete et al., 1996). Furthermore the transcription repressor OhR, that is involved in the response against organic hydroperoxides, has been purified in association with glutathione (Gaballa et al., 1990) indicating that glutathionylation its essential for its regulation. Glutathione can be directly involved in the response against peroxide mediated oxidative stress because recent studies has evidenced that the activation of OxyR can be associated with the glutathionylation of this protein (Kim et al., 2002). Glutathionylation is a reversible protein modification in fact deglutathionylation may occurs either non-enzymatically or can be mediated by enzymes like thioredoxins, glutaredoxins or protein disulfide isomerases (Jung et al., 1996).

Reduced glutathione can directly scavenge oxygen radicals. As stated before GSH can directly react with hydroxyl radicals, produced by Fenton reactions, exchanging one electron and leading to the production of OH^- and glutathione thiyl radical (GS*). Although the presence of GS* have been

only supposed *in vivo*, due to its *in vitro* ability to further oxidize to the sulfinic or sulfonic form (Wardmann et al., 1995) or to undergoes to molecular rearrangement leading to the formation of a C-centered glutathione radical (*GS^-) (Hofstetter et al., 2010), this radical has be found to enhance the *in vitro* rate of proteins glutathionylation performed by human glutaredoxin 1 and 2 (Starke et al., 2003; Gallogly et al., 2008). Furthermore the ability of human glutaredoxin 1 (HGRX1) to catalize the *in vitro* production of GSSG starting from a glutathione thiyl radical mixture has been firstly evidenced by Starke and colleagues in 2003 underlining the biological importance of the GSH recycling in protecting against hydroxyl radical poisoning.

2.6.4 In the bacteria glutathione is the most representative low molecular weight thiol but not the only one.

Although glutathione is the most produced low molecular weight (LMW) thiol in either eukaryotic organisms and Gram-negative bacteria some Gram-positive bacteria have evolved different strategies to control redox homeostasis involving different compounds.

In Actimomycetes the major LMW thiol is not GSH but mycothiol (MSH) (Newton et al., 1996). MSH was firstly evidenced as disulfide by Sakuda and co-workers (Sakuda et al., 1994) in Streptomyces species. Its chemical structure consist in 2-(N-acetylcysteinyl)amido-2-deoxy-α-D-glucopyranosyl-myo-inositol and was later identified and characterized as the most representative LMW thiol in *Mycobacterium bovis* (Spies et al. 1994), taking the trivial name of mycothiol. The unusual properties of MSH make it weakly susceptible to copper ion-catalyzed autoxidation (Newton et al., 1995) thus leading to the hypothesis that MSH may be an analogous of GSH in protecting cells against oxidative stress damage.

Another LMW thiol that shares characteristics with both GSH and MSH was described by Newton and co-workers in 2009 (Newton et al., 2009). This compound appears to be the major LMW thiol in Bacilli and has been named bacillithiol (BSH). Although the biosynthetic pathway of BSH and the chemical structure of the compound suggests analogies to MSH rather than GSH (Gaballa et al., 2010), BSH can be considered as an analogous of GSH because it was firstly purified in concomitance with OhR, which functionality is regulated by bacillithionylation.

Other Gram-positive bacteria did not evolve an ubiquitous antioxidant compound sharing the peculiar characteristic of GSH, MSH or BSH preferring to specialize different molecules. The most rapresentive example of bacterium using this latter strategy is *Staphylococcus aureus* in which, although the antioxidant activity is performed by CoA and a specific CoA disulfidereductase (delCardayre et al., 1998). CoA cannot function as a protected cysteine reservoir due to cysteine decarboxilation during CoA biosynthesis.

2.7 Relevance of controlling redox homeostasis in bacteria.

Most cells possesses strategies to produce and detoxify ROS. In standard conditions the protection mechanisms are devoted to maintain a low concentration of ROS, due to the high toxicity of this class of molecule. However in some cases, like the oxidative stress condition, these protection mechanisms are overridden by a rapid and transient huge production of ROS namely "oxidative burst". The oxidative burst has been evidenced like one of the ubiquitous cellular protection mechanism against pathogen infection and has been largely studied in both mammalian phagocytes (Segal et al., 1993) and plant systems (Doke et al., 1996).

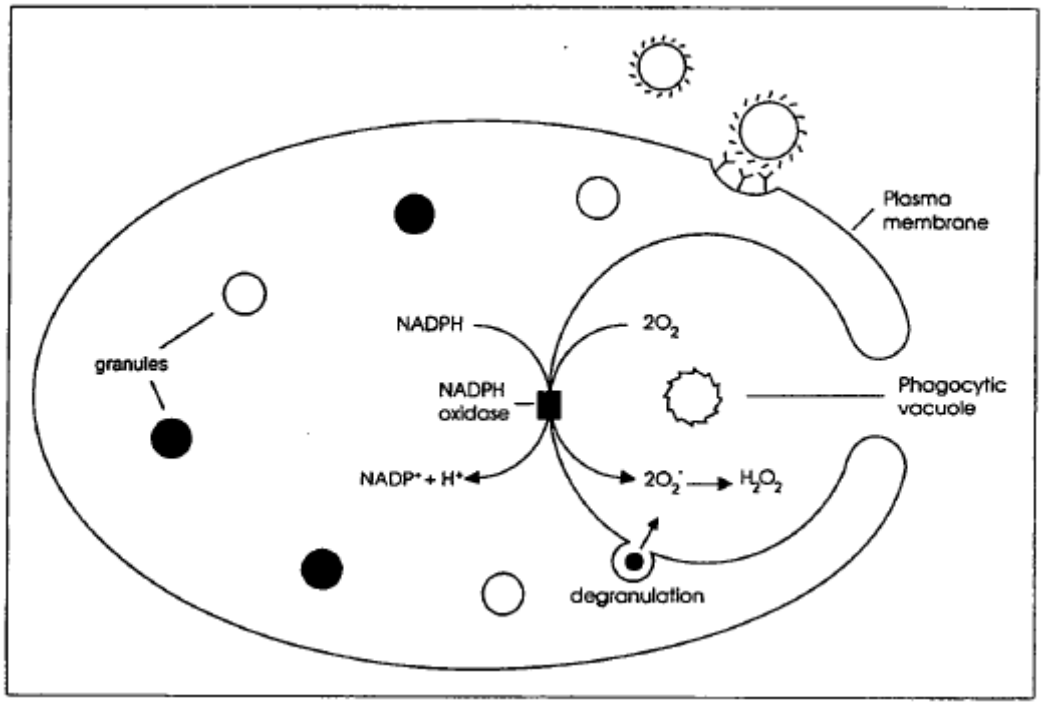

Figure oxidative burst: Schematic representation of microbes phagocytosis The NADPH oxidase is activated in the vacuolar membrane, generating superoxide anions in the lumen. Degranulation of cytoplasmic granules leads to the release of bactericidal proteins inside the vacuole (Wientjes et al., 1995).

A central role in the oxidative burst enhancement is played by the enzyme NADPH oxidase and by transferrin. The activation of the NADPH oxidase allows the cell to pump high doses of superoxide anion into the vacuole creating an oxidative environment while transferrin, that is a ferric iron storage protein, enters in the vacuole via endocytosis and releases the ferric iron, due to the acid pH of the vacuole, thus eliciting ROS production *via* Fenton reaction. The production of hydroxyl radicals leads to membrane depolarization via lipid oxidation thus inducing the pathogen cell death . Pathogens have evolved effectives strategies to overcome the host defense. As described and reviewed in Collins (2003), *Mycobaterium tubercolosis* and *Salmonella thiphymurium*, for example, have the ability to secrete siderophore that binds ferric iron leading to its internalization thus

increasing intracellular iron content. The overload of iron increases exponentially the pathogen virulence thus inducing an early development of the symptoms.

2.8 Rhodanese-like protein involvement in protecting against oxidative stress.

The involvement of RDPs in the oxidative stress response machinery has been firstly evidenced by Nandi and co-workers in 1998 (Nandi et al., 1998). Nandi and colleagues evidenced that reduced thioredoxin, one of the best characterized player in the antioxidant machinery, can be the sulfur acceptor of the sulfanic sulfur mobilized by the bovine rhodanese, and they formally proposed a mechanism involving as a donor substrate the physiological compound alanine thiosulfonate. Starting from this data, the first evidence of a rhodanese-like protein directly involved in the oxidative stress response machinery was observed comparing the reduced thioredoxin dependent rhodanese activity of the bovine rhodanese isoforms. This study evidenced that the less negative isoform of the bovine rhodanese can act as a thioredoxin oxidase catalyzing the direct oxidation of reduced thioredoxin by reactive oxygen species thus suggesting a role in intramithocondrial oxygen free radical detoxification (Nandi et al., 2000). The mechanicistic of the reaction involves the formation of a sulfenic cysteine residue on the rhodanese that leads to the oxidation of the thioredoxin and has been deeply studied by Nagahara and colleagues in 2005 leading to the conclusion that the mild oxidation of the cysteine catalytic residue can function as a post translational modification that control the redox homeostasis by decreasing the rhodanese activity in a way to increase the cysteine availability promoting the synthesis of glutathione (Nagahara et al., 2005). Traditional biochemical characterization has highlighted the *in vitro* correlation between RDPs and the control of the redox homeostasis although *in vivo* evidences are still lacking. The *in vivo* evidence of a rhodanese-like protein involvement in protecting against oxidative stress was observed in the Gram-negative bacterium *A. vinelandii*. *A. vinelandii* possesses 14 ORFs coding for putative RDPs but just one protein, named RhdA, is responsible of ≈ 90% of the in vitro TST activity (Cartini et al., 2011; Colnaghi et al., 1996). The production of a null mutant *A. vinelandii* strain in which the *rhdA* gene was inactivated by deletion (Colnaghi et al., 1996) highlighted the susceptibility of this latter strain to oxidative stress damage induced by incubation with the mixed radical generator phenazine methosulfate (PMS) (Cereda et al., 2009) suggesting a direct involvement of this rhodanese-like protein in managing redox homeostasis. A new impulse in this field of study has been given by the high trough-put analyses of the bacterial transcriptome after inducing the oxidative stress. Preliminary data are now arising from both Gram-negative and positive bacteria, as example in *B. anthracis* a rhodanese-like protein (*ybfQ*) is highly induced in hydrogen peroxide oxidative stress condition (Pohl et al., 2011).

CHAPTER 3:

Material and Methods

3.1 Strains list

Bacterial strains used in this work are listed in the table below:

Bacterial species	Strain	Genotype	Reference
A. vinelandii	UW136	Wild Type	Bishop et al., 1977
A. vinelandii	MV474	*rhdA* null mutant	Colnaghi et al., 1996
B. subtilis	PS832	Wild type	D.L. Popham
B. subtilis	J1235	ΛYhqL; ΛYbfQ; ΛYrkF; ΛYtwF	T.J. Larsonn
B. subtilis	JD0206	ΛYhqL	T.J. Larsonn
E. coli	BL21(DE3)	F^-dcm omp hsdS($r_b^-m_b^-$)gal λ(DE3)	Studier et al. 1990
E. coli	BL21(pREP4)	rhdA	Colnaghi et al., 1996

Table strains list. Bacterial strains used in this work

Strain aliquots were resuspended in a 25% glycerol solution and stored at -80°C until use.

3.2: Bacterial strains and Growth Conditions.

3.2.1 *A. vinelandii*

The *A. vinelandii* strains used in this study were UW136 and a derivative of UW136 (MV474) in which disruption of the *rhdA* gene was achieved by the insertion of a KIXX cassette, following deletion of 584 bp as described in (Colnaghi et al., 1996). Cells were grown aerobically in Burk's medium (Newton et al., 1953) for 24 h at 30°C, supplemented with 15 mM ammonium acetate and 1% sucrose or 0.2% gluconate. When the optical density reached OD_{600} = 2.0, the cells were spun down at 3800 ×*g* for 10 min, and stored at –80 °C. For oxidative stress induction, cells were grown in the above conditions up to OD_{600} = 0.800, then the cultures of either UW136 or MV474 strains were divided into two equal samples one of which was treated with phenazine methosulfate (PMS, final concentration 15 μM).

3.2.2 *B. subtilis*

The bacterial strains used were *B. subtilis* wild-type PS832 and its two derivatives: J1235 mutant strain bearing the deletion of 4 genes coding for rhodanese-like proteins (*yhqL::spc, ytwF::erm, yrkF::erm::cat, ybfQ::kan*) and JD0206 mutant strain bearing the deletion of *yhqL* (*yhqL::spc*). *B. subtilis* strains were cultivated under vigorous agitation (250 rpm) at 37°C in either LB media or Spizizen minimal media (2 g/L NH_4SO_4, 14 g/L K_2HPO_4, 6 g/L KH_2PO_4, 1 g/L $Na_3Citrate*2H_2O$; 0.0125 g/L $MgCl_2*6H_2O$, 0.00055 g/L $CaCl_2$, 0.00135 g/L $FeCl_2*6H_2O$, 0.0001 g/L $MnCl_2*4H_2O$,

0.00017 g/L $ZnCl_2$, 0.00004 g/L $CuCl_2*2H_2O$, 0.00006 g/L $Na_2MoO_4*2H_2O$, 0.00006 g/L $CoCl_2*6H_2O$) in which the carbon source was substituted with 0.4% (w/v) sucrose. For enzymatic assays, sporulation assays and low molecular thiols quantification cells were synchronized by cultivation until early exponential phase (0.1 OD) and then subcultured until an optical density at 600 nm (OD_{600}) of 1.0 ± 0.1. Media was removed by centrifugation (3800*xg*, 15 min, 4°C) and cell pellets were stored at -80°C until use.

3.2.1.1. Hydrogen peroxide challenges

Experiments were performed as described by Murphy et al. (1987) with minor modifications. *B. subtilis* PS832 and J1235 cells were synchronized as described before and grown in LB medium until middle exponential phase ($O.D_{600nm}$ = 0.5) . Aliquots (5 mL) were then taken and incubated with the chosen concentration of H_2O_2 (from 1 to 100 mM) for 20 min at 37°C under shaking (200 rpm). After H_2O_2 treatment cells were serially diluted in fresh LB medium and 10 µL of every dilution was plated on LB and grown overnight (37°C) for the determination of colony forming unit (CFU). Growth with sublethal concentration of H_2O_2 were performed adding the hydrogen peroxide solution directly to the *B. subtilis* LB coltures (0.058 – 0.5 mM concentration range) in early exponential phase (Hellman et al., 2003). Growth changes were then monitored by controlling the optical density at 600 nm every 30 min for 6 h.

3.2.1.2 Sporulation assay

Sporulation assays were performed on synchronized PS832 and J1235 *B. subtilis* coltures prepared as described before. After synchronization cell growth was monitored by measuring the optical density at 600 nm for 24 h. Aliquots (1 ml) were taken after 2.5, 8 and 24 h and serially diluted in fresh LB medium. Dilution were plated (10 µL) on LB agar before and after 30 minute incubation at 65°C (wet heat) to allow the killing of the vegetative cell fraction. Plates were incubated overnight at 37°C and the survived cells were counted and expressed as CFU.

3.2.3 *E. coli*

For protein overexpression, the *Escherichia coli* strain, BL21[pRep4], was grown in Luria-Bertani medium (containing 100 µg/ml ampicillin and 25 µg/ml kanamycin) at 37°C and, when D_{600} = 0.4, 1 mM isopropyl β-D-thiogalactoside (IPTG) was added. After further 4 h-growth, cells were collected and used for protein purification.

3.3 Molecular biology techniques

Total RNA was isolated using the NucleoSpin® RNA II kit (Macherey-Nagel, Düren, Germany) according to manufacturer's protocols. Reverse transcription was performed on 1200 ng of total RNA, using RevertAid™ H Minus M-MuLV RTase (Fermentas), RiboLock™ RNAse inhibitor (Fermentas), and reverse primers. Primers were: RhdAWR1FOR (5'-ACAACTGGAAAGCCTGTTCG-3') and RhdAWR1REV (5'-CCTTGGCGATCAGGTAGGT-3') for the amplification of *A. vinelandii rhdA* (703771-702956 nucleotide region of GenBank® GI: 7759697), 16SFOR (5'-ACCGCATCCAAAACTACTGG-3') and 16SREV (5'-CACCGGCAGTCTCCTTAGAG-3') for the amplification of *A. vinelandii 16S rRNAs* (177422-178956 nucleotide region of GenBank® GI: 7759149), AhpCFOR (5'-CCTACCACAACGGCAAGTTC-3') and AhpCREV (5'-AGATCCAGGGACGGCTTC-3') for the amplification of *A. vinelandii ahpC* (4662884-4663447 nucleotide region of GenBank® GI: 7763457). Quantitative reverse transcription real-time PCR (qRT-PCR) was carried out using the SYBR® Green Supermix (Bio-Rad) in a final volume of 20 µL. For each reaction were added the cDNA (obtained from 2 ng total RNA), 0.25 µM of each primer, 5 % dimethyl sulfoxide (DMSO). Amplification conditions were: 95 °C for 4 min, followed by 45 cycles consisting of 95 °C for 40 s, 59 °C for 40 s, 72 °C for 40 s. Each qRT-PCR was performed in triplicate. Negative controls were performed with 2 ng of non-reverse transcribed RNA as template, and in the absence of template. In positive controls, *A. vinelandii* genomic DNA (190 ng, extracted from *A. vinelandii* cell cultures using a proteinase-K-based minipreparation) was used as template. Data were elaborated according to Livak and Schmittgen (Livak et al., 2001) using *16S* rRNA as reference.

3.4 Low molecular weight thiol determinations

3.4.1 *A. vinelandii*

Measurement of the levels of glutathione was performed by a monobromobimane HPLC method (Riemenschneider et al., 2005) using 50 mg (fresh weight) cell samples. This method measures the DTT-reducible and the reduced forms of free glutathione.

Disulfide glutathione was measured using 120 mg (fresh wt.) cell samples in a Beckman P/ACE MDQ capillary electrophoresis system (Palo Alto, CA, USA) equipped with a UV absorbance detector set at 200 nm according to [28]. The fused-silica capillary (65 cm x 75 µm I.D.) was maintained at 28°C, samples were injected by pressure (2.07 kPa) for 10 s and separated at 30 kV. The background electrolyte contained 100 mM boric acid and 25 mM Tris pH 8.2. Data were collected and processed with a 32 Karat™ Beckman software.

3.4.2 *B.subtilis*

Levels of intracellular bacillithiol were quantified using HPLC based mBBr method described for *A. vinelandii* with minor modification. Cells were grown in Spizizen minimum media as described above . Aliquots (≈ 300 mg wet cells) were collected and dissolved in 1600 µL of 50mM Tris, 100 mM NaCl pH 7.2 buffer. Cells were distrupted by sonication (6 min, power 5 W) and divised in 3 aliquots. For total soluble thiol samples were incubated with HCl (final concentration 100 mM) to allow protein precipitation and 50 uL of sample (≈ 9.4 mg wet cells) was treated as described in (Remelli et al 2010). To quantify soluble oxidized thiols the method previously described was modified: Prior to DTT incubation samples were incubated for 1 h with 2mM Iodacetamide and then treated with 1mM DTT. Total intracellular thiols were quantified incubating the samples with 1 mM DTT prior to acid precipitation.

Separation and quantification of mbbR (Sigma Aldrich) derivatized low molecular weight thiol was achieved with High performance liquid chromatography (HPLC) system (Waters) using a Zorbax SB-C18 (4.6 x 150 mm; 5-micron; Agilent) coupled with a fluorescence detector (λ_{exc}: 380nm; λ_{em}:480nm). Separation was achieved at a flow rate of 0.6 mL/min using a linear gradient as described in (Newton et al., 2010). BSH retention time was 11.4 ± 0.2 min while unreacted monobromobimane and DTT retention time were respectively 2.8 and 27 min. Amounts of intracellular BSH was calculated plotting the peak areas against a standard curve generated derivatizing known amount of pure compound (BSH was gently given from Tim Hellman).

3.5 Protein and lipids extractions

3.5.1 *Azotobacter vinelandii* proteins and lipids extraction

Cell-free extracts were prepared by sonication (five 30 s pulses with intermitted 1 min cooling periods in Soniprep 150, UK) in 10 mM Tris-HCl, 100 mM NaCl (pH 8), and cell debris was removed by centrifugation (30 min at 10000 ×*g*).

For intracellular PMS determinations 100 mg cells (wet weight) were washed twice with 1 ml of 10 mM Tris-HCl, 100 mM NaCl (pH 8) buffer and then dissolved in 900 µl of 0.1M HCl in dH_2O. Cells were disrupted by vortexing (10 cyckes: 1 min vortexing and 1 min rest in ice) and fresh extracts were used for the analysis.

Total lipids were extracted using Bligh and Dyer methods with some modifications. In short 100 mg of *A vinelandii* cells (wet weight) were dissolved in 1.9 mL of (1:2 $CHCl_3$:MetOH) and vortexed for 3 min. After vortexing 0.63 mL of $CHCl_3$ and 0.63 mL of dH_2O were added and the sample was vortexed again for 5 min. The organic phase was isolated by centrifugation (5 min 5000

rpm 4°C) and then recovered using a glass Pasteur. After been washed twice with 2 volumes of dH_2O the organic phase was directly submitted to lipid hydroperoxides content estimation.

3.5.2 Bacillus subtilis proteins and lipids extraction

One liter of cells were collected as described above and resouspended, in the absence of oxygen, in 5 mL of 10 mM Tris-HCl, 100 mM NaCl (pH 8) degased buffer. Cells were broken by French press and protein extract were clarified by centrifugating for 35 min., 6000 *x* g at a temperature of 4°C.

Total lipids were extracted using Bligh and Dyer method (Bligh et al., 1959). In short 100 mg of *B. subtilis* cells (wet weight) were dissolved in 1.9 mL of (1:2 $CHCl_3$:MetOH) and vortexed for 10 min. After vortexing 0.63 mL of $CHCl_3$ and 0.63 mL of dH_2O were added and the sample was vortexed again for 10 min. The organic phase was isolated by centrifugation (15 min 5000 rpm 4°C), recovered using a glass Pasteur and directly submitted to lipid hydroperoxides content estimation.

3.5.3 RhdA purification

His-tagged RhdA and RhdA-Cys^{230}Ala were expressed in *E. coli* strains (BL21[pRep4]) harbouring pQER1 (Pagani et al., 2000) and pQER1MP (Cartini et al., 2010) respectively, and purified by Ni-NTA affinity chromatography (Cartini et al., 2010). Sulfane sulfur-deprived RhdA was prepared by cyanide treatment as previously described in Forlani et al. (2005).

3.6 Determination of the protein concentration

Protein concentration of complex samples was determined by the Bradford assay (Bradford et al., 1976) using bovine serum albumin as standard. RhdA protein concentration was estimated by 280 nm absorbance using $\varepsilon = 1.313\ mg^{-1}\ cm^{-1}$ coefficient (Colnaghi et al., 1996).

3.7 Reagents preparation

3.7.1 Glutathione thiyl radical preparation.

Glutathione thiyl radical (GS*) was prepared starting from reduced glutathione (GSH) using the horseradish peroxidase (HRP) generating system as described in (Sipe et al., 1997) with minor modifications. Reaction mixture, containing 90 nM HRP (Sigma, type II, 188 U mg^{-1}), 0.5 mM phenolphthalein, 0.25 mM H_2O_2, and 5 mM GSH in 50 mM phosphate buffer (pH 7.4), was incubated for 2 min at room temperature and immediately used for enzymatic assays.

3.7.2 FOX2 reagent preparation

FOX2 reagent was used to quantify lipid hydroperoxides content and was prepared as described in (Wolff., 1994). Ammonium ferrous sulphate hexahydrate (2.5 mM) was dissolved in H_2SO_4 (250 mM). An aliquot (25-ml) of this solution was then mixed with 19 mg of xylenol orange previously dissolved in 50 ml of methanol. The volume of the mixture was finally completed to 250 ml with methanol. Concentrations of xylenol orange, ammonium ferrous sulphate hexahydrate, and H_2SO_4 were 100 µM, 0.25 mM, and 25 mM, respectively. FOX2 reagent was freshly prepared before every assay.

3.8 RhdA Cys_{230} oxidation studies

RhdA Cys_{230} residue oxidation studies were performed on RhdA either sulfur loaded of unloaded samples prepared as described in Forlani et al., 2005. A 16.12 µM (0.5 mg/mL) RhdA solution (10 mM Tris, 100 mM NaCl pH 8) was incubated with PMS (molar ratio 1 :1). Time point were taken and PMS incubation was stopped by precipitating RhdA with 100% cold acetone. After 30 min incubation at -20°C protein pellet was recovered and suspended in 100 µL of 100 mM Tris-HCl buffer pH 7.5 and derivatized with monobromobimane (mBBr). Reversible oxidation was tested by treating same of the sample replicates with the reducing agent 2-mercaptoethanol (BME) (incubation whit 4mM BME for 30 min 4°C) prior to cold acetone precipitation.

RhdA thiol derivatization was performed by incubating RhdA samples with 2mM mBBr for 30 min in the absence of light sources. Derivatization was stopped by adding to the sample 10 µL of 100 mM Tris-HCl pH 7.5 supplemented with 10% (w/v) sodium dodecilsulfate (SDS). RhdA was recovered by acetone precipitation as described before, suspended in 10 mM Tris-HCl (pH 7.5) buffer and used for SDS-page or fluorimetric analyses.

3.9 Enzymatic assays

3.9.1 Thiosulfate:cyanide sulfurtransferase activity(TST)

TST activity was tested by the discontinuous method described in (Sorbo, 1953) that quantitates the product thiocyanate, based on the absorbance of the ferric-thiocyanate complex at 460 nm (ε = 2890 M^{-1} cm^{-1}). One unit (U) of TST activity is defined as the amount of enzyme that produces 1 µmol thiocyanate per min at 37°C.

3.9.2 GS*-scavenging activity assay

GS*-scavenging activity assay was performed according to (Starke et al., 2003) with minor modifications. Reaction mixture containing 0.1 mM NADPH, 0.8 U baker yeast glutathione oxido-reductase (GOR; Sigma, 230 U mg^{-1}), various amounts of RhdA (1-18 nM) in 50 mM sodium-phosphate buffer (pH 7.4) (final volume 900 µl) was incubated for 5 min at 25 °C. Reaction was initiated by addition of 100 µl of GS* premade mixture (see: "Glutathione thiyl radical preparation"). Controls omitting RhdA or GS* mixture were performed in parallel. NADPH oxidation (stoichiometric to glutathione disulfide formation) was monitored at 340 nm (ε = 6220 M^{-1} cm^{-1}). For calculation of apparent kinetic parameters, initial rates of reaction at different amounts of GS* premade mixtures were measured, and values of K_m and V_{max} were calculated using non-linear regression curve (SigmaPlot, SPSS Inc., Chicago, IL, USA). For anaerobiosis studies oxygen was substituted with argon in each component of the mixture. One unit (U) of GS*-scavenging activity is defined as the amount of enzyme that produces 1 nmol GSSG per min at 25 °C.

3.9.3 Lipid hydroperoxides assay

Lipid hydroperoxides content was quantified according to (Griffiths et al., 2000). In short 200 µL of the organic phase containing total cellular lipids were directly mixed with 1 mL of FOX2 reagent (prepared as described above). Sample was mixed by vortexing and then incubated in the dark for 1h. After incubation lipid hydroperoxides content was determined spettrofotometrically recording the 560nm absorbance and using the molar absorption coefficient derived from standard linoleate hydroperoxide (ε= 6.0 x 10^4 M^{-1} cm^{-1}, Gay et al., 1999).

3.9.4 Catalase activity assay

Catalase activity was tested by using the discontinuous method described in (Sinha. 1972) that quantities the H_2O_2 based on the formation chromic acetate that present an absorbation maximum at 570 nm. One unit (U) of catalase activity is defined as the amount of enzyme that consumes 1 µmol of hydrogen peroxides per min at room temperature.

3.9.5 Aconitase activity assay

Aconitase assays were prepared in 1-ml quartz cuvettes (sealed airtight with rubber septa) containing 700 µl of 100mMTris-HCl buffer at pH 8.0 and 0.1mg of anaerobic crude extract . The reaction was initiated with the addition of 25 mM sodium citrate, and activity was monitored at 240 nm (Saas et al., 2000).

3.9.6 Quantification of the oxygen consumption in crude extracts

Oxygen consumption was quantified by oxygraph. Experimental condition were 25°C, 400 rpm, 101.1 kPa. 100 µL of protein extracts in 10mM Tris, 100 mM NaCl pH 8 buffer were diluted to a final volume of 2.1 ml in the same buffer and oxygen consumption was monitored for 30 min with an without the addition of overexpressed RhdA. Before every set of analyses the instrument was calibrated by monitoring the buffer oxygen concentration before (100%) and after (0%) the addition of 10 mg of sodium dithionite ($Na_2S_2O_4$).

3.10 *In silico* analyses

3.10.1 Docking analyses

Docking analyses were performed with Argus Lab software (Argus Lab 4.0.1, Planaria software LLC, Seattle, WA, U.S.A.; http://www.arguslab.com), using Lamarckian genetic algorithm scoring functions with 0.1 Å grid resolution, a 15 Å-edged box centered on Cys^{230} residue, and flexible ligand mode (other parameters were kept with default values). Docking analyses were performed against RhdA structure (pdb ID: 1h4k) as template.

Theoretical calculation of Cys^{230} residue pK_a values was carried out using the program PROPKA 2.0 (Li et al., 2005; Bas et al., 2008) by using the crystal coordinates of the deposited RhdA structure (pdb ID: 1h4k).

3.10.2 Transcription factors prediction

Trancription factor consensus sequence retrieval was performed by using the online software BPROM (http://linux1.softberry.com/berry.phtml) on specific *B.subtilis* gene sequence deposited in the NCBI *(*www.ncbi.nlm.nih.gov).

3.11 Spectrofluorimetric measurements

Fluorescence measurements were carried out in a Perkin–Elmer LS-50 instrument, and data were analyzed as previously described (Pagani et al., 2000). RhdA intrinsic fluorescence spectra experiments (λ_{exc} = 280 nm) were carried out at 25 °C in 50 mM Tris–HCl, 100 mM NaCl (pH 7.4) in the presence of 2 µM RhdA, and 50 µM glutathione (GSH, GS* or GSSG). Where it is stated, to remove unbound glutathione, 8-fold concentrated mixtures were subjected to a gel filtration step (Sephadex G-50; 1.5 × 10 cm column) before the fluorescence measurements. For the evaluation of the dissociation constant (K_d) of RhdA/glutathione bindings, changes of intrinsic fluorescence (λ_{exc} = 280 nm, λ_{em} = 342 nm) were monitored after sequential additions of 0.1 µM glutathione species or thiosulfate. Figures of intrinsic fluorescence changes were normalized for protein concentration

and assay volume. K_d values were calculated by fitting intrinsic fluorescence changes to a non-linear regression curve (SigmaPlot, SPSS Inc., Chicago, IL, USA).

3.11.1 Thermal stability

Thermal stability of either RhdA-SH and RhdA/GSH adduct were monitored as a change of the tryptophan residues fluorescence (λ_{ex} 280nm; λ_{em} 340nm) by using a LS-50 PERKIN ELMER spectrofluorimeter equipped with a Peltier device. Samples were gradually heated to 65°C at 0.5°C/min.

3.12 Protein electrophoresis

3.12.1 SDS-PAGE

Denaturing gel electrophoresis was performed according to Leammli (Leammli., 1970) on purified RhdA both mBBr derivatized or not forms denatured in Leammli buffer without the addition of 2-mercaptoethanol. Gels were either directly acquired under transUV light or after staining with Branson-Coomassie (Holtzhauer ., 2006).

3.12.2 2D gel electrophoresis

2D gel electrophoresis was performed according to Cereda et al., 2007 with minor modifications. Isoeletric focalization was performed on 7 cm strips (Immobiline^{TM} DryStrip gels pH 4-7, Amersham Biosciences) after overnight sample rehydratation (6M Urea, 3M thiourea, 2% CHAPS, 0,05% 4-7IPG buffer (Amersham), 10 mg/mL DTT, 0,005% BBF) using the following protocol step: 70V for 60h, 200V for 45 min, 500V for 30 min, 1000V 30 min, 2000V 30 min, 3000V for 150 min. After equilibration in DTT (1%) and iodoacetamide (4%), the focused proteins were separated in a vertical SDS-polyacrylamide gel using 12% (W/V) polyacrylamide resolving gel and 4% stacking gel. Separation was performed in a Bio-Rad system using constant amperage (16 mA per gel). Gels were stained using Blue coomassie standard protocol and stained gels were digitalized using an EPSON Expression 1680 Pro scanner (Epson, Milan, Italy) and spots densitometry ($\%V_{spot}/V_{total\ spots}$) was calculated by using the ImageMaster 2D Platinum software (Amersham Biosciences).

3.13 Mass spectrometry analyses

3.13.1 Mass spectrometry analysis of whole proteins

Proteins were desalted using C4 ZipTips (Millipore) following the standard protocol given by the company. For MS analysis, the protein (1 µM) in ESI buffer (50% acetonitrile, 50% Millipore water, 0.1% formic acid) was injected into the mass spectrometer (micrOTOF-Q II, Bruker Daltonics) with a flow rate of 3 µl min^{-1} using a syringe pump (KD Scientific) and the ESI sprayer from Bruker Daltonics with 0.4 bar nebulizer gas and 4 µl min^{-1} dry gas heated to 180°C. Each sample was measured for 5 min and an average spectrum was calculated using the DataAnalysis software (Bruker Daltonics). The mass of the protein was determined using the charge state ruler of DataAnalysis.

3.13.2 Mass spectrometric analysis of protein spots

LC-ESI Q-ToF analyses were carried out with an Easy-nLC system (Proxeon) coupled to a micrOTOF Q II MS (Bruker Daltonics). In-gel digestion was carried out as described in Klodmann et al. 2010. Peptides digested with trypsin were resolved in 20µl LC sample buffer (2% Acetonitrile, 0.1% FA in H_2O) and 15µl were injected into the LC-MS system.

For LC separation, a two column setup with a C18 reversed phase for hydrophobic interaction of peptides was used. Precolumn: Proxeon EASY-PreColumn (L = 2 cm, ID = 100 µm, ReproSil-Pur C18-AQ, 5 µm, 120 A); Analytical column: 10 cm Proxeon EASY-Column (L = 10 cm, ID = 75 µm, ReproSil-Pur C18-AQ, 3 µm, 120 A). The LC gradient started with 95% solution A (H_2O + 0.1% FA) and the proportion of solution B (Acetonitrile + 0.1% FA) was continuously increased for 10 minutes to 50% B. This ratio was applied for 3 minutes. Solution B then was again continuously increased for 20 minutes to finally 95% B and 5% A. MS/MS fragmentation was carried out automatically. Therefore, the software selected up to 3 peptides of highest intensity (with a minimal intensity of 3000 counts) in the MS precursor scan. For data processing DataAnalysis software from Bruker Daltonics was used. Database search was carried out with ProteinScape (Bruker Daltonics) and the MASCOT search engine in the NCBInr database.

CHAPTER 4:

Aim of the work

Bacteria, either Gram-negative or Gram-positive, are characterized by the ability to grow in stressful conditions in order to colonize hostile environments. This peculiarity can be seen as a positive feature because it allows the usage of bacteria in industrial processes (i.e. drug production) and in bioremediation (i.e xenobiotics degradation) but can also be seen as a negative feature because it contributes to the virulence of pathogen bacteria.

One of the most common and dangerous source of stress is driven by reactive oxygen species (ROS) because of the size of oxygen, that can easily pass trough both the cellular wall and membrane, and because of the nature of the reaction that is an univalent electron transfer. ROS-induced oxidative stress can easily lead to cell death because proteins, DNA and lipids are sensitive target for oxidation that suppresses or modifies their physiological functions.

The ROS toxicity is exploited by eukaryotic cells as a way to overcome bacterial colonization (i.e. oxidative burst) and pathogen bacteria have answered this by evolving sensitive mechanism to overcome ROS poisoning (that results in ROS detoxification) in order to maintain their redox homeostasis.

Although most of these defensive mechanisms have been deeply studied and the direct players in ROS detoxifications, either enzymes (catalases for hydrogen peroxide; superoxide dismutases for superoxide anion) or not (reduced glutathione for hydroxyl anion), have been already characterized, the way these players are recycled by the cell is still matter of studies, furthermore new mechanisms and new players are still emerging.

Members of the rhodanese-like proteins superfamily (RDPs) are widely distributed in either prokaryotic and eukaryotic organisms and, although characterized RDPs are formally described as sulfurtransferases (E.C. 2.8.1.x), emerging studies are correlating these proteins to the oxidative stress management system because of their redox-sensitive thiol residues (Nandi et al., 1998; Nandi et al., 2000; Nagahara et al., 2005; Cereda et al., 2007; Cereda et al., 2009).

In order to confirm RDP involvement in the oxidative stress response system and to gather information about the redox homeostasis maintaining mechanism in which RDPs are involved, my research has been devoted to the study of two prokaryotic model systems: the *Azotobacter vinelandii* system and the *Bacillus subtilis* system. In particular, among the 14 putative RDPs of *A. vinelandii*, RhdA involvement in protection against oxidative stress events has already been suggested (Cereda et al., 2009). My work will be focused in framing this role by analyzing the expression of specific physiological markers (i.e OxyR controlled genes expression and levels of glutathione), and by identifying specific RhdA partner(s) in order to elaborate a rational mechanism for RhdA involvement in maintaining redox homeostasis. Furthermore the acquired information

will be used as “pin point” in the *B. subtilis* system in order to widen the biological relevance of the RDPs in protecting the cell against ROS.

CHAPTER 5:

Azotobacter vinelandii results

Chapter 5.1 The absence of RhdA leads to an internal oxidative stress problem

Like other bacteria *A. vinelandii* can either use the Embden-Meyerhof-Parnas or the Entner-Doudoroff glycolytic pathway to produce energy in function of the given the carbon source. The Embden-Meyerhof-Parnas pathway (i.e. classic glycolysis) has an high production of energy, in the form of ATP and NAD(P)H, while the Entner-Doudoroff glycolytic pathway is less effective. Replacing sucrose with gluconate in the Burk medium for the *A. vinelandii* growth, the Entner-Doudoroff glycolytic pathway is forced to be switched on, highlighting an internal oxidative stress problem (Cereda et al., 2009).

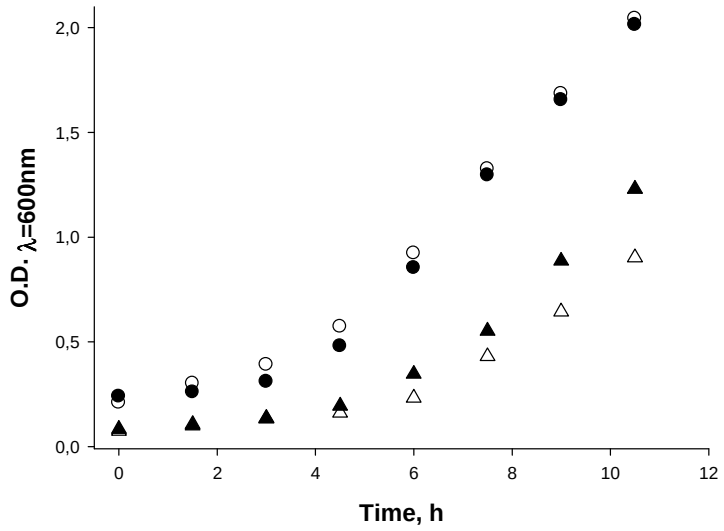

Figure growth curve: UW136 and MV474 *A. vinelandii* strains growth curve in burk medium supplemented with sucrose as carbon source (circles) or gluconate (triangles). UW136 experimental points are presented as full symbols while MV474 experimental points are presented as empty symbols.

In figure, *A. vinelandii* wild-type (UW136) and *rhdA* null mutant strain (MV474) growth curves are compared using either sucrose or gluconate as carbon source. In the case of sucrose growth (BSN; circles) no differences were displayed, while using gluconate as carbon source (BGN) the growth behavior of the two strain was clearly different (triangles), being the growth rate of the MV474 strain lower than that of wild-type strain. The MV474 strain appears to be more influenced by the impaired ability of producing NAD(P)H, proper of the Entner Doudoroff glycolytic pathway, suggesting an internal oxidative stress problem correlated with the absence of RhdA.

Solid proofs about an oxidative stress problem linked to the RhdA deficiency were given by previous works already published by our lab in which gluconate growth condition was correlated with the variations, in the MV474 strain, of two typical markers for oxidative stress conditions: depletion of the aconitase activity, and increase of the free intracellular iron content (Cereda et al., 2009, Remelli et al., 2010).

In order to have a measure of the oxidative stress caused by the absence of the rhodanese-like protein (RDP) RhdA in *A. vinelandii* cells, we quantified the amount of free intracellular reduced glutathione and glutathione disulfide.

Strain	**BSN**			**BGN**		
	Glutathione (nmol/mg cells)		GSH/GSSG	glutathione (nmol/mg cells)		GSH/GSSG
UW136	1.17 ± 0.02		136.4 ± 3.6	0.51 ± 0.01		38.2 ± 0.4
MV474	0.83 ± 0.02	**	80.6 ± 1.0	0.32 ± 0.01	**	20.4 ± 0.2

Table glutathione levels: Levels of glutathione, quantified as described in material and methods, has to be intended as the sum of reduced and DTT-reducible glutathione and were quantified in UW136 and MV474 strains growth either in BSN or BGN media.

As shown in the table, levels of glutathione significantly decreased in MV474 strain in both the tested conditions. Furthermore, when the carbon source was gluconate, levels of glutathione decreased by ≈ 29% in the wild-type strain while decreased by ≈ 37% in the *rhdA* null mutant strain. The results observed in the MV474 strain let us to conclude that oxidative stress is enhanced, by the absence of RhdA. The lower glutathione levels observed in BGN respect to BSN could be due to the oxidative stress condition induced by the growth in gluconate medium.
The internal oxidative stress condition was further confirmed by analyzing the GSH/GSSG ratio. In the MV474 strain, this ratio decreased by ≈ 45% (41 to 47%) in both the growth conditions, indicating a shift of the redox equilibrium to a more oxidized state correlated to the RhdA absence.
This shift resulted in a growth impairment when carbon source is gluconate but no growth rate changes are observed when the carbon source was sucrose (figure growth curve). It suggests that, in standard growth conditions, GSH consumption is enough to overcome the oxidative stress that results from RhdA absence because of the high production of ATP and NAD(P)H that are mandatory for GSH *de novo* synthesis.

In *A. vinelandii*, as in many other Gram-negative bacteria, the expression of the oxidative stress response system is under the control of the OxyR regulator. The *ahpC* gene, coding for the alkyl hydroperoxidase C, is one of the most recognized member of the OxyR regulon, together with catalase A and glutathione reductase, and its expression can be used as a marker to gather information about the activation of the oxidative stress response system.

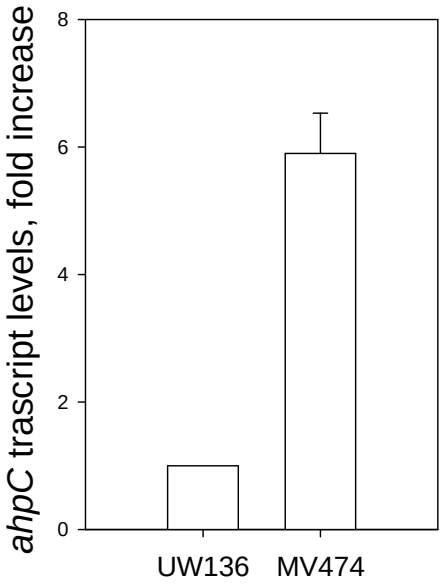

Figure *ahpC*. *ahpC* expression was quantified via qRT-PCR in the *A. vinelandii* UW136 and MV474 strains. The *16S rRNA* level was used as internal calibrator, and the value from cells grown with sucrose was chosen as standard condition. The data are the mean ± S.D. from three separate growth experiments.

Expression of *ahpC* gene was significantly ($p < 0.01$) higher in the *rhdA* null mutant strain, compared to the wild-type expression level (Fig. *ahpC*), indicating that, in order to overcome oxidative stress, MV474 strain activates the overexpression of the oxidative stress related proteins. Further experiments were conducted on the quantification of the preferential substrate of AhpC, the lipid hydroperoxides (Wang et al 2004). Lipids are one of the most representative components in cell membrane and are easy target for oxidative stress damage (Halliwell et al., 1984). In particular, in bacteria, cellular respiration is compartmentalized at the level of the periplasmic space in a way to form a protonic gradient that is mandatory for respiration (Haddock et al., 1977)**.** Under oxidative stress conditions, the oxidation of lipids perturbs the membrane integrity that can result in a decrease of cellular respiration leading to apoptosis (Wang et al 2004).

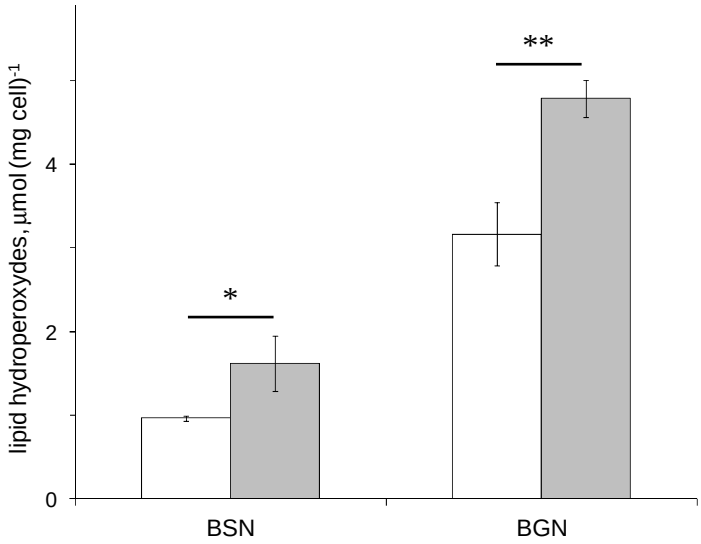

Figure Lipid hydroperoxides. Lipid hydroperoxides concentration in *A. vinelandii* cells. Lipid hydroperoxides were detected, after incubation with FOX2 reagent, in wild-type (UW136; white bars) or in *rhdA* null mutant (MV474; grey bars) *A. vinelandii* strains grown in Burk's medium containing sucrose (BSN) or gluconate (BGN) as carbon source. Data are the mean of three independent replicates ± standard deviation. Differences significant for a $p < 0.05$ (*) and $p < 0.01$ (**) are indicated (Student's *t* test).

Using sucrose as carbon source, lipid hydroperoxides content was almost not detectable in UW136 wild-type strain, while in the MV474 strain lipid hydroperoxides were significantly accumulated ($p < 0.01$). Levels of lipid hydroperoxides drastically increased when the carbon source was gluconate further supporting the data showed earlier and pointing the attention on a perturbation of the cellular respiration apparatus due to the absence of RhdA.

RhdA addition	µmol (O_2 consumed) ml^{-1} min^{-1}	
	UW136	MV474
–	0.37 ± 0.03	0.32 ± 0.02
+	0.34 ± 0.02	0.33 ± 0.04

Table oxygen consumption: The oxygen consumption of A. vinelandii UW136 and MV474 crude extracts was directly quantified *via* oxygraph as described in material and methods before (-) and after (+) the addition of 5 µM purified RhdA.

The perturbation of the MV474 strain respiration was further confirmed by comparing the oxygen consumption rate of *A. vinelandii* UW136 and MV474 strains grown in standard conditions (BSN). Rates of O_2 consumed by crude extracts of the MV474 strain were lower compared to the UW136 strain (table oxygen consumption). Further experiments suggests that the exogenous addition of purified RhdA to crude extracts did not significantly help *A. vinelandii* MV474 strain to recover the ability to consume molecular oxygen to the levels of the UW136 strain while an extra RhdA

supplement to the wild-type strain did not increase the consumption oxygen suggesting that the addition of the sole RhdA is not enough to restore the respiration rate to the level measured in the UW136 strain.

To have further insight on *A. vinelandii* physiological adaptation to the absence of RhdA, we characterized, by using the 2D-GE technique coupled to mass spectrometry, the changes on protein pattern correlated directly or indirectly to the lack of RhdA.

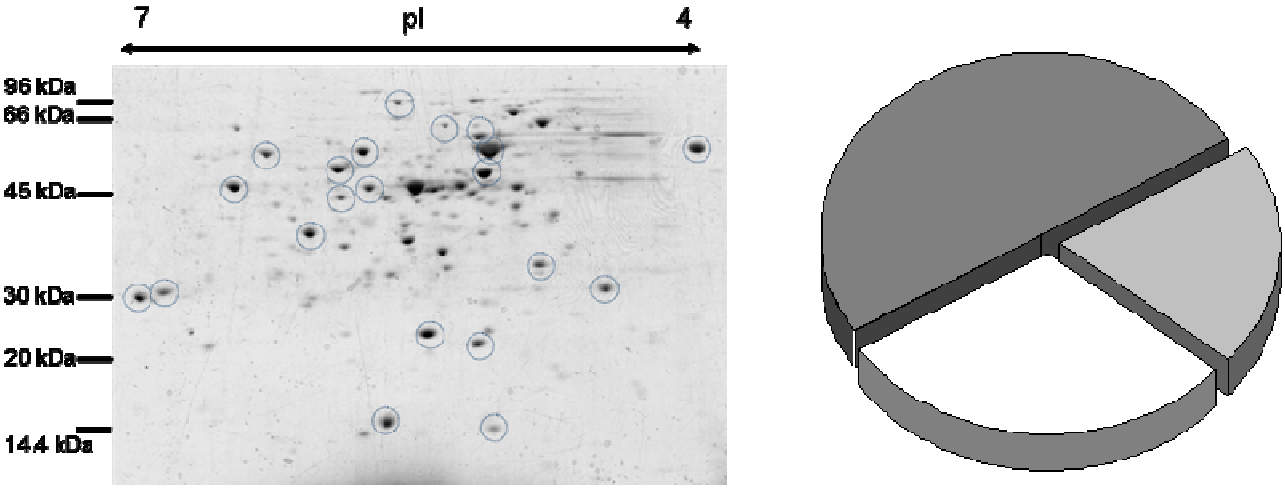

Figure MS. Representative 2D-GE of the *A. vinelandii* proteome. Inside circles are highlighted protein spots which expression changes in the MV474 strain and identified by MS as described in material and methods. The pie diagram is representative of the putative annotated functions of the identified proteins. Proteins involved in energy production are presented in dark grey, protein involved in biosynthetic processes are presented in white while protein involved on oxidative stress response are presented as light grey

The absence of RhdA leaded to significant alterations of the general protein profile pattern. In particular more than 25 proteins were differently accumulated and 16 of them were successfully identified by MS analyses. Almost 50% of the identified protein are involved in energy metabolism such as malate dehydrogenase (C1DHR4_AZOVD) and subunits a and b of the ATP synthase (C1DND5_AZOVD, C1DND3_AZOVD). The other 50% is almost equally divided in proteins implied in amino acid biosynthesis, like ILVC_AZOVD, annotated as a putative keto-acid reductoisomerase involved in branched amino acids biosynthesis, and in proteins directly involved on defending the cell against the oxidative stress, like C1DHW8_AZOVD, annotated as alkyl hydroperoxydase C.

Chapter 5.2 RhdA behavior in oxidative stress conditions induced by phenazine methosulfate

In chapter 4.1 we assessed that the absence of RhdA leads to an internal oxidative stress problem in standard growth conditions (sucrose), causing the earlier activation of the oxidative stress response machinery (e.g. overexpression of the *ahpC* gene and AhpC accumulation in the MV474 strain), the depletion of the glutathione pool and the accumulation of lipid hydroperoxides. When the *A. vinelandii rhdA* null mutant strain (MV474) was restrained to switch on the Entner-Doudoroff glicolytic pathway (gluconate as sole carbon source), the internal oxidative stress condition resulted to be even more severe leading to growth deficiencies, a stronger decrease of the free glutathione pool, and a significantly increased levels of lipid hydroperoxides.

To better clarify RhdA function in protecting *A. vinelandii* against oxidative stress we artificially induced oxidative stress *via* the addition of the superoxide generator phenazine methosulfate (PMS) at a final concentration of 15 µM.

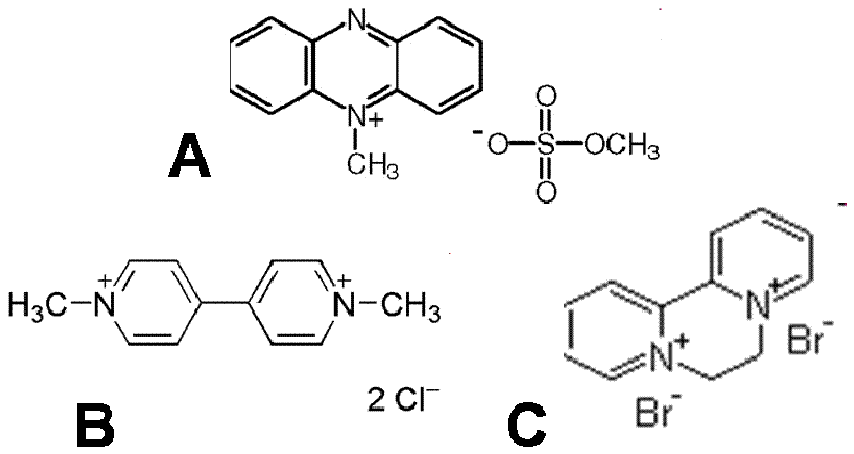

Figure PMS: Chemical structures of the oxidizing agent phenazine methosulfate (A), paraquat (B) and diquat (C)

The superoxide generator PMS has been chosen for different reasons: PMS generates mixed oxygen radicals (Huang et al., 2009) and not only peroxides; PMS shares a similar chemical structure to paraquat and diquat, two of the most extensively used herbicides until the late ’90s (figure PMS); PMS chemical stability is higher, compared to hydrogen peroxide, allowing us to perform long-timed growth curves at sublethal PMS concentration until the achievement of the early stationary phase. Furthermore, PMS owns peculiar spectroscopic features depending on its redox status (Huang et al., 2009), the oxidized form possesses a peculiar absorbance maximum at 347 nm. This latter characteristic has been exploited to determine the presence of PMS inside the *A. vinelandii* cells and in the growth medium.

As reported in Cereda et al. (2009), the addition of 15 µM PMS to the BSN medium in the late exponential *A. vinelandii* growing phase ($O.D._{600\ nm}$ = 0.6-0.8) drastically reduced *rhdA* null mutant strain (MV474) fitness while the wild-type strain grow rate is unaffected. Starting form this evidence, we exploited PMS spectroscopic properties to highlight differences in its reducing behavior in crude acid-extracts of UW136 and MV474 strains.

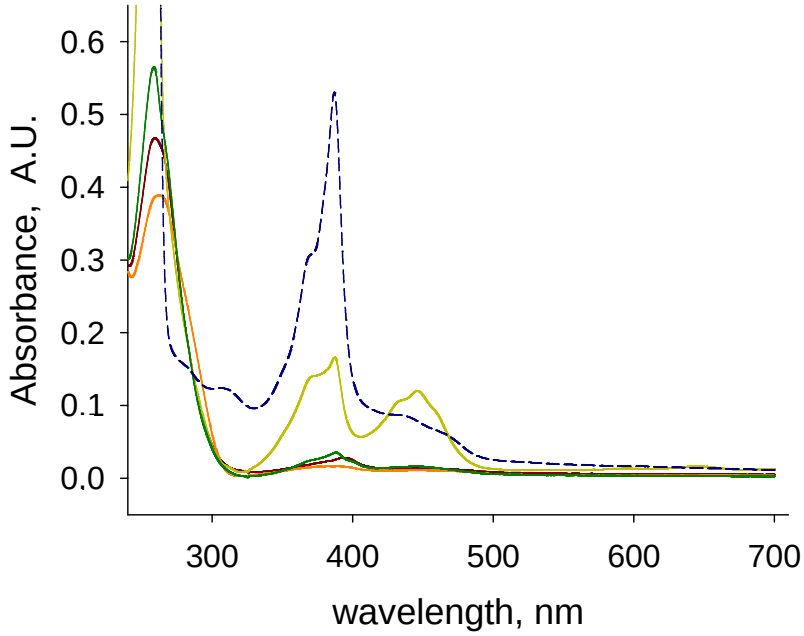

Figure intracellular PMS. Absorbance spectra of acid-extracts of 100 mg *A. vinelandii* UW136 and MV474 cells grown in standard (dark red and green lines) or in PMS-induced oxidative stress conditions (orange and yellow lines). As control, the absorbance spectrum of 25 µM PMS water solution (dashed blue line) is reported.

After 10 hour exposure to 15 µM PMS no peak at 387 nm are recordable in the UW136 wild-type strain (orange line) suggesting that the oxidative stress agent is completely reduced while in the *rhdA* null mutant strain (MV474) the 387 nm absorbance peak is still present (dark yellow line) suggesting that PMS is only partially reduced. These data led us to elaborate two independent but equally important considerations: the oxidative stress agent PMS is imported by *A. vinelandii* cells leading to the internal formation of mixed oxygen radicals; RhdA presence, directly or indirectly, allows PMS detoxification *via* its reduction**,** evidenced by the formation of the PMS semireduced intermediate that has the peculiar characteristic to absorb the light at 452 nm.

These considerations apparently doesn't agrees to what stated in the previous chapter, in which we assessed that the absence of RhdA lead to an internal oxidative stress problem that results in an earlier activation of the oxidative stress response machinery, but, if we consider what is normally controlled by the OxyR regulon in *A. vinelandii* (table OxyR-controlled genes), the inability of the

MV474 strain to reduce PMS could be explained by the mixed nature of the radicals produced by the oxidative stress agent (mostly peroxides and superoxide).

	E. coli	*A. vinelandii*	
H_2O_2 scavenging	*ahpC*	*ahpC*	GeneID: 7763457
	ahpF	*ahpF*	GeneID: 7761540
	katG	*katG*	GeneID: 7759544
Heme synthesys	*hemH*		
FeS clusters assembly	*sufA*		
	sufB		
	sufC		
	sufD		
	sufE		
Iron scavenging	*dps*		
Iron import control	*fur*	*fur*	GeneID: 7763174
Divalent cation import	*mntH*		
Disulfide reduction	*trxC*	*trxA*	GeneID: 7763605
	grxA	*grxC*	GeneID: 7760341
	gor	*gor*	GeneID: 7761415
	dsbG		
Unknown function	Several	Several	

Table OxyR-controlled genes. List of OxyR-controlled genes in *E.coli* (Imlay et al., 2008) and *A. vinelandii* (blast analyses starting from the *A. vinelandii* putative OxyR binding site: 5^1-A/GTAnG/CGnnnnAnCnA-3^1)

To deepen the involvement of RhdA in the management of PMS inside the cell we quantified *rhdA* gene expression, using a qRT-PCR approach, in wild-type strain in BSN and BGN media with an without 10-h PMS incubation.

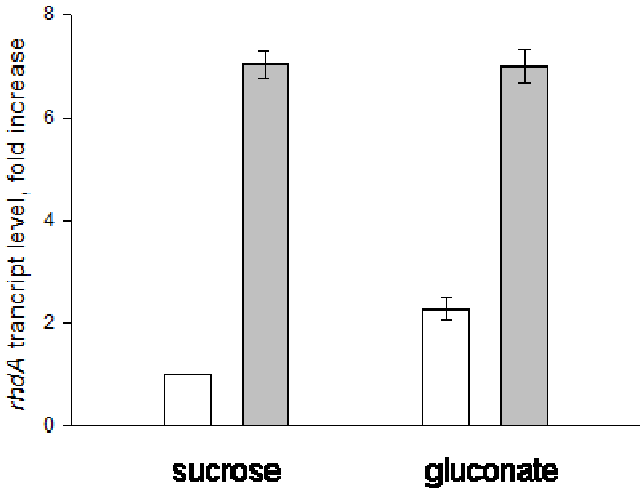

Figure *rhdA*-transcript levels Influence of the exposure to phenazine methosulfate (PMS) on the relative abundance of *rhdA* transcript in *A. vinelandii* UW136 strain. Quantitative real time RT-PCR (qRT-PCR) analyses were performed on total RNA of *A. vinelandii* grown with sucrose (BSN) and gluconate (BGN) as carbon source in the absence (white) and in the presence (grey) of the stressor PMS. The *16S rRNA* level was used as internal calibrator, and the value from cells grown with sucrose was chosen as standard condition. The data are the mean ± S.D. from three separate growth experiments.

Considering as a standard condition the *rhdA* expression level in BSN we compared, using the Livak method (Livak et al 2001), the expression rate in oxidative stress condition (grey bars) together with its expression in BGN media. The *rhdA* gene is overexpressed (around 2.2 fold) when the carbon source used was gluconate indicating a stress-dependent regulation of *rhdA* expression and corroborating the hypothesis that RhdA is actively involved in recovering from oxidative stress. Furthermore *rhdA* expression dropped up to a similar high level in PMS induced oxidative stress condition, no matter the carbon source supplied to the media. This latter result suggests that the oxidative stress induced by PMS leaded to a complete misregulation of *rhdA* response machinery that works at its maximum potential. This assumption, confirmed by the strong overexpression also evidenced for *ahpC* gene (chapter 4.1), led us to investigate on the functionality of RhdA in oxidative stress condition *via* enzymatic assay.

As reported in literature RhdA is a member of the thiosulfate:cyanide sulfurtransferase (TST) superfamily (E.C. 2.8.8.1) responsible of 90% of the TST activity of *A. vinelandii* (Cartini et al. 2011, Colnaghi et al 1996). For this reason the *in vitro* TST assay described by Sörbo (Sörbo et al 1953) can be used as a marker to study RhdA functionality in standard and PMS-induced oxidative stress conditions.

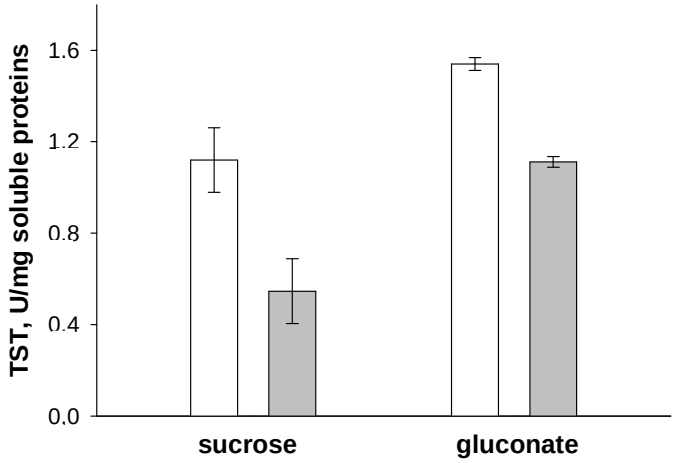

Figure *in vitro* TST activity. Effect on thiosulfate:cyanide sulfurtransferase (TST) activity of the exposure to phenazine methosulfate (PMS) of *A. vinelandii* UW136 strain. TST activity was measured in cell-free extracts from *A. vinelandii* grown with sucrose or gluconate as carbon source either in the absence (white bars) or in the presence of 15 µM PMS (grey bars). The data are the mean ± S.D. from three separate growth experiments.

Analyzing the TST activity of *A. vinelandii* coltures grown either in BSN or BGN media (white bars), we confirmed the *rhdA* expression results: in BGN media the TST activity was higher than in BSN according to the *rhdA* overexpression. When oxidative stress conditions were induced by PMS (grey bars), TST activity decreased, nonetheless *rhdA* expression dramatically increased in the same condition. The *rhdA* overexpression seems to be a response for the RhdA loss of functionality probably caused by its oxidation by PMS.

Chapter 5.3 RhdA Cys_{230} residue oxidation behavior in PMS induced oxidative stress conditions.

The publication of RhdA 3D crystallographic structure (Bordo et al., 2001; 1h4K.pdb) allowed us to predicts the redox sensitive region of RhdA. In particular, the RhdA active site (HCQTHHR) can be easily oxidized, *in vitro*, because of its exposure to the solvent and because of the presence of the redox sentisitive thiol residue of the Cys_{230}, the only cysteine residue present in the protein. These data were supported by previous works in which the *in vitro* oxidation of Cys_{230} residue induced by PMS treatment (1:10 RhdA/PMS molar ratio), dramatically decreased RhdA functionality (Cereda et al. 2009).

To correlate RhdA biological function with the management of ROS, the oxidation behavior of the Cys_{230} residue in the RhdA pesulfurated (RhdA-SSH) and not persulfurated (RhdA-SH) forms was explored. The oxidation state of the RhdA-Cys_{230} sulfur residue, before and after PMS treatments,

was investigated using monobromobimane (mBBr), a thiol-sensitive probe with weak fluorescence (ε_{exc} 396 nm; ε_{em} 487nm). Considering that Cys_{230} is the only cysteine residue in RhdA, oxidation behavior of purified RhdA was studied using two different approaches based on the mBBr fluorescence. In both approaches, the RhdA was treated with equimolar PMS for 30 min and then reduced using 20 mM 2-mercaptoethanol (BME) before the mBBr labeling.

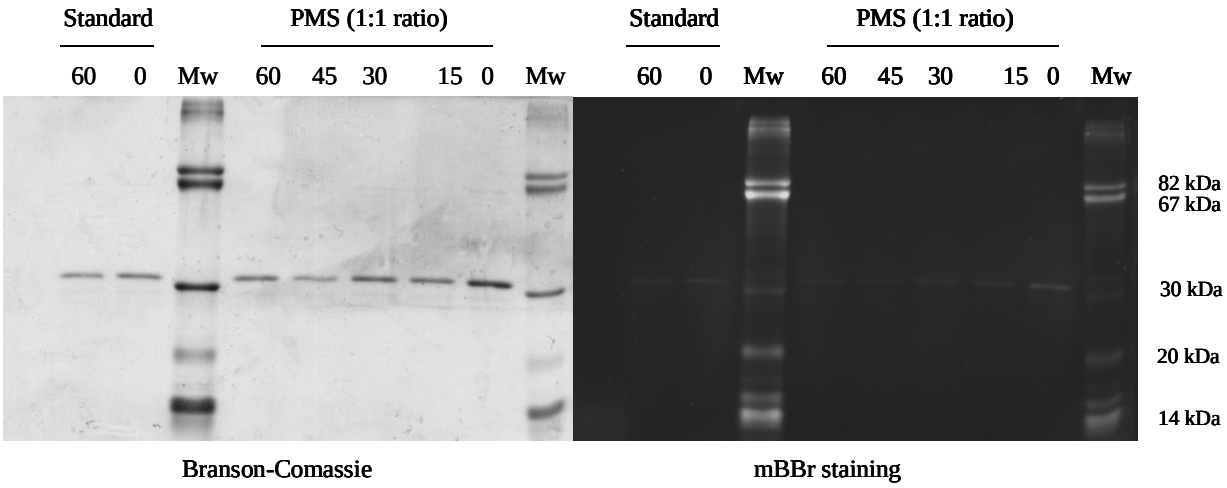

Figure SDS page RhdA Cys230 oxidation behavior. Recombinant purified RhdA-SH was derivatized with mBBr after incubation with PMS for variable amount of time as described in material and methods. 1 µg of derivatized protein was loaded on a 12% SDS-page gel under reducing conditions. Gel images were acquired under the UV light (mBBr staining) and after Branson-Comassie staining.

SDS-PAGE analyses highlighted a PMS incubation dependent decrease of RhdA fluorescence suggesting that PMS irreversibly oxidizes RhdA-Cys_{230} thiol lowering its ability to bind mBBr. Furthermore, the fluorescence density was quantified, using the software IMAGE master 1D®, showing that the relationship between the fluorescence decrease and the time of PMS incubation was proportional.

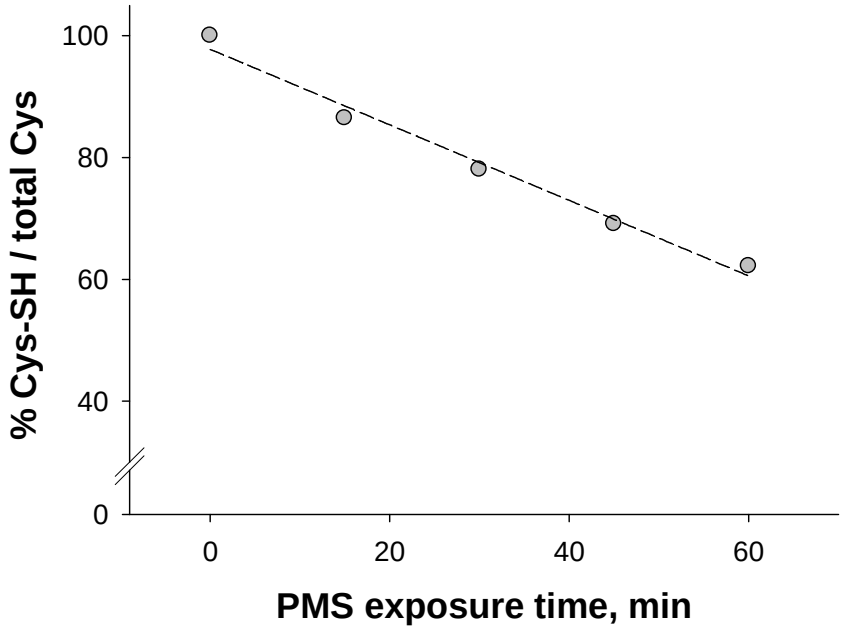

Figure semiquantification. The mBBr-derivatized RhdA-Cys_{230} residue were quantified by gel densitometry after different exposure to PMS. Results are presented as % thiolic cysteine (Cys-SH) under the total of the cysteine present. The straight line that interpolates the experimental points (grey dots) underline the time-dependent relationship between PMS exposure and Cys oxidations

Starting from these preliminary results, we settled up a protocol to measure directly, by using the spectrofluorimeter (L-150), the fluorescence of persulfurated (RhdA-SSH) and thiolic (RhdA-SH) RhdA/mBBr adducts. This latter method appears to be more sensitive and quantitative compared to the SDS-PAGE method because of the possibility to focus on the mBBr excitation and emission maxima (ε_{exc} 396 nm; ε_{em} 487nm). Combining this technique with TST assays, quantitative data on the oxidation behavior of the RhdA catalytic cysteine residue were gathered.

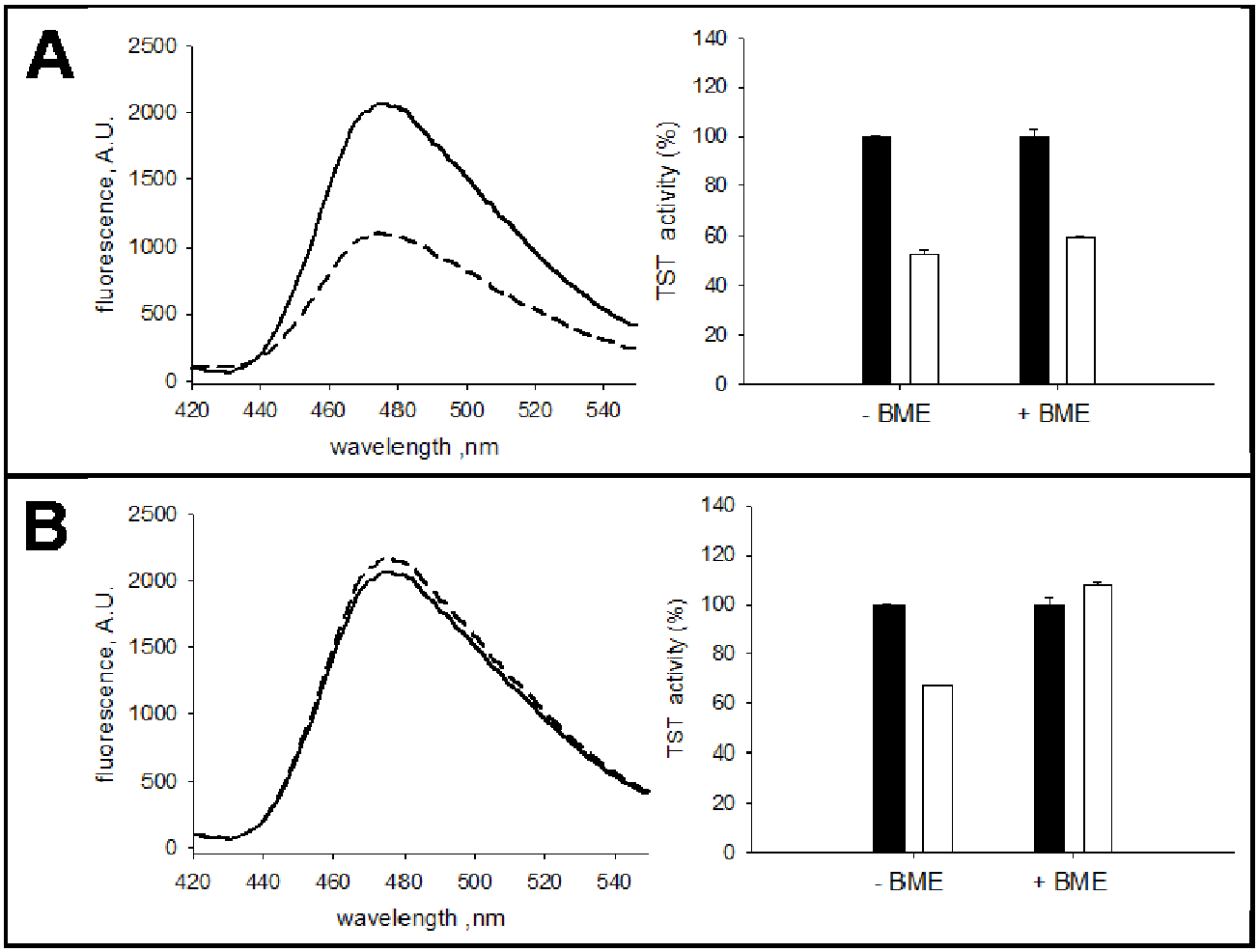

Figure fluorimetric measurements I. RhdA-SH (panel A) and RhdA-SSH (panel B)oxidation behaviors were studied by fluorimetric measurements. Various form of RhdA were derivatized with mBBr prior (solid lines) and after (dashed lines) 30-min PMS incubation and DTT reduction. Results were confirmed by TST activity prior and after 4 mM BME reduction of not-treated RhdA (black bars) and PMS-treated RhdA (with bars).

As shown in panel A either the drop of fluorescence and the inability of RhdA to recover its *in vitro* activity after treatment with BME indicates that RhdA catalytic Cys_{230} residue oxidation was irreversible if RhdA bears a thiol (Cys_{230}-SH). A different behavior was highlighted in panel B because of the presence of a persulfide sulfur on the Cys_{230} residue (Cys_{230}-S-SH) resulted in a reversible oxidation underlined by both the similar fluorescence values and the recovery of TST activity after BME treatment. These data correlates RhdA oxidation behavior with bovine rhodanese in which the derivatization of the catalytic cysteine thiol with a S_0 resulted in a protection against oxidative stress events (Horowitz et al., 1989) and may be explained by a strong oxidation of the exposed sulfur, that shift from the thiol form to presumably the sulfinic or the sulfonic forms. The presence, in the persulfurated form, of a cleavable disulfide bond can be the clue to understand the different *in vitro* reversibility behavior in the case of the persulfurated RhdA

because in this latter case the oxidation resides in the extra sulfur and can be further reduced by BME treatment.

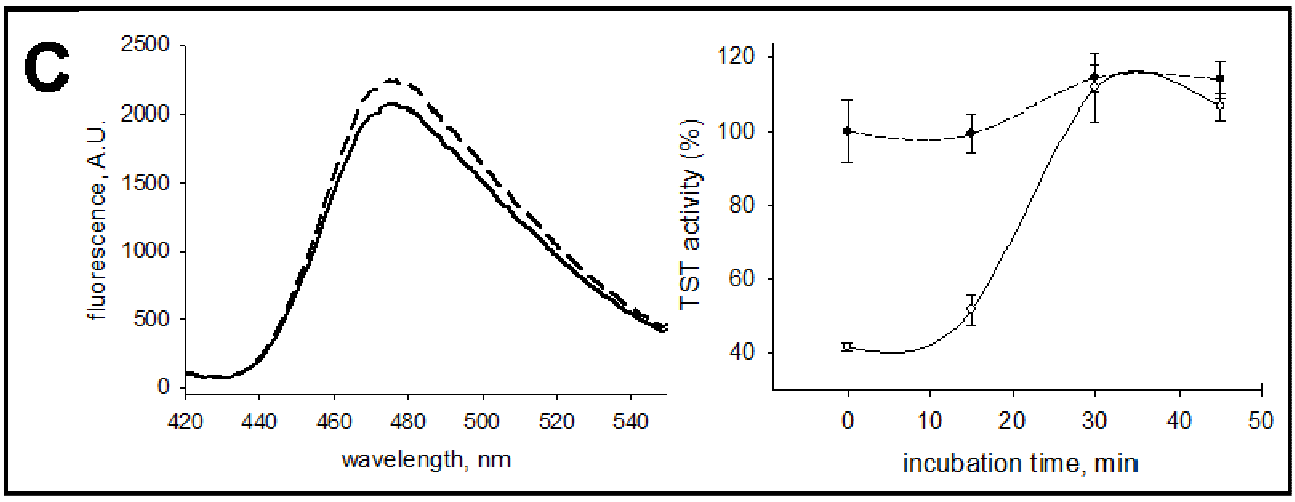

Figure fluorimetric measurements II. Fluorimetric measurements. RhdA-SH (panel C) oxidation behaviors after incubation with GSH was studied by fluorimetric measurements. RhdA-SH (solid line) was treated with GSH and derivatized mBBr and subjected to 30 min PMS incubation and DTT reduction (braked lines). RhdA interaction with GSH was then evidenced by TST activity.

The oxidation behavior of the RhdA-Cys_{230} residue in the presence of the biological relevant low-molecular-weight thiol glutathione (GSH; panel C) was studied. According to both the approaches (TST and mBBr assays), the presence of GSH resulted in a complete protection of the Cys_{230} residue to the oxidation as deducible by the recover of both the fluoresce and the TST activity (data not shown) after BME treatment. Furthermore as presented in panel C figure B the recovery of the TST activity, after incubation with glutathione, resulted to be not mediated by BME reducing treatment and time-dependent indicating that the binding between RhdA and GSH was reversible.

These latter experiments traces a direct *in vitro* interaction between RhdA and GSH , that together with GSSG represent the main intracellular redox buffer, and, together with the low level of soluble glutathione present in the MV474 strain, leads to the suggestion that this interaction may be the clue to explain RhdA biological function.

Chapter 5.4 Interaction of RhdA with glutathione species

The structural compatibility of a direct interaction between GSH and the RhdA active site region was firstly simulated by an *in silico* docking approach. RhdA structure model (1h4K.pdb), obtained by crystallographic measurements (Bordo et al., 2001), was used as a template to perform *in silico* prediction of the interaction of RhdA with either GSH or thiosulfate, the *in vitro* sulfane sulfur donor for sulfurtransferase activity.

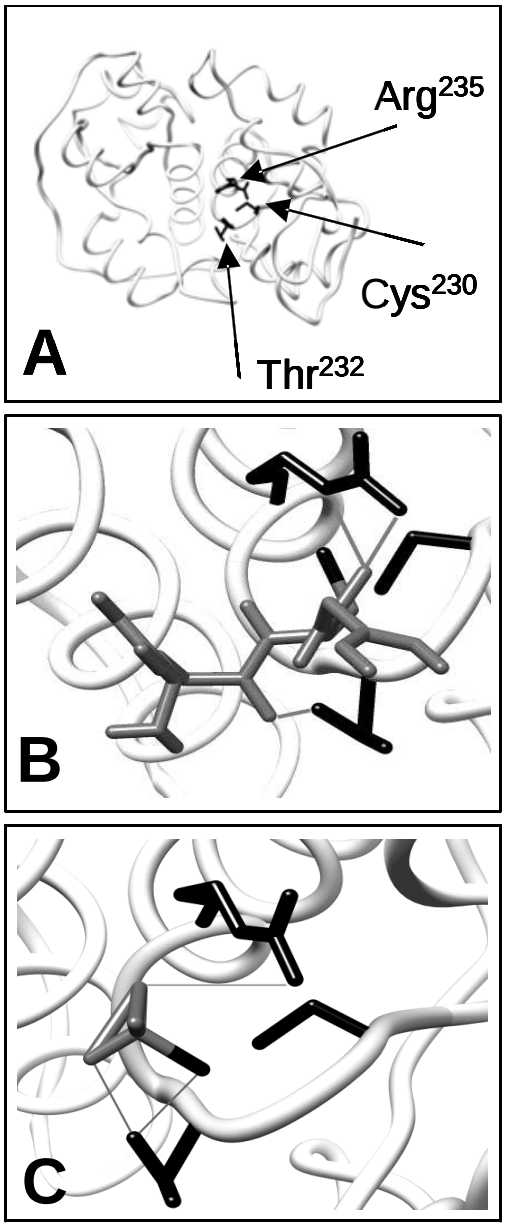

Figure docking. *In silico* docking of glutathione and thiosulfate to RhdA. Overall RhdA structure (A) and its active site region interacting with either reduced glutathione (B) and thiosulfate (C). In black, are highlighted amino acidic residues (Arg_{235}, Thr_{232} and Cys_{230}) involved in the interaction. Ligand backbone is displayed as dark grey sticks. *In silico* computed hydrogen bonds between ligands and amino acidic residues are displayed as light grey solid lines. Molecular docking has been performed using Argus 3.0 software and images are generated using UCSF chimera software (http://www.cgl.ucsf.edu/chimera/).

Targeting the binding on the RhdA active site region (Fig. Docking panel A highlighted in black), the position and orientation of both ligands into the RhdA active site indicated an involvement of the Cys_{230} thiol, being the estimated distance between the sulfur atoms 2.7 Å for GSH (Fig. Docking panel B) and 2.5 Å for thiosulfate (Fig. Docking panel C). Results of the docking simulated the involvement of Thr_{232} and Arg_{235} residue in the formation of 3 H-bonds that stabilize the complex with either GSH or thiosulfate. The docking of GSH and thiosulfate into the active site of RhdA gave rise to simulated complexes having dissociation free energy values of 5.29 (GSH) and 6.01 (thiosulfate) kcal mol^{-1} (22 and 25 kj mol^{-1}, respectively). Attempts to dock GSSG into the RhdA active site region did not generate relevantly scored complexes therefore indicating the inability of glutathione disulfide to enter in the active site of RhdA. In silico docking experiments indicated that the active site of RhdA appears properly structured to form a complex with GSH, and prompted us to investigate this interaction *in vitro*.

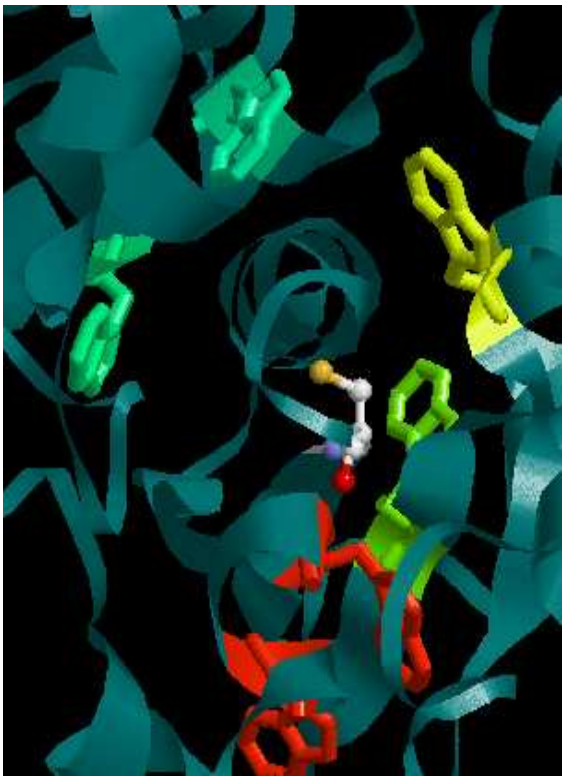

Figure tryptophan. The active site of RhdA is surrounded by a crown composed by 5 Trp residues

Taking advantage of the peculiar position of five tryptophan residues around the active site structure of RhdA (Bordo et al., 2001) (Fig. Tryptophan), *in vitro* interaction of RhdA with glutathione was investigated by monitoring intrinsic fluorescence changes (Forlani et al., 2005).

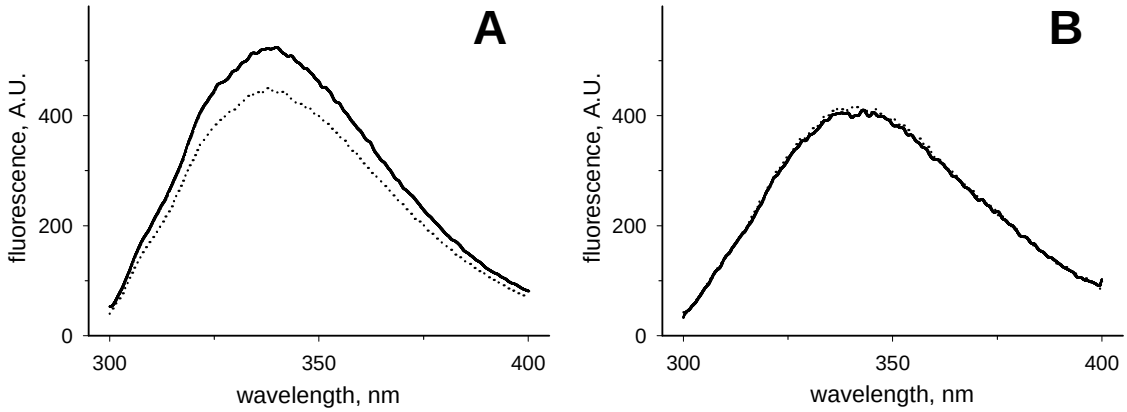

Figure GSH quenching. Effect of reduced glutathione on the intrinsic fluorescence of RhdA and RhdA-Cys^{230}Ala. Tryptophan fluorescence emission spectra (λ_{ex} = 280 nm; dotted lines) of RhdA in the presence of 50 µM GSH (A), and RhdA-Cys^{230}Ala in the presence of 50 µM GSH (B). Solid lines report spectra before the addition of GSH. In all cases, protein was 2 µM in 50 mM Tris-HCl, 100 mM NaCl (pH 7.4). Spectra were corrected for dilution.

As shown in the figure above (panel A), the intrinsic fluorescence of RhdA was quenched in the presence of GSH. Quenching of intrinsic fluorescence of RhdA was evident also when fluorescence measurement was preceded by a gel filtration step (data not shown) suggesting formation of a stable complex. The involvement of the active site Cys_{230} thiol of RhdA in the interaction, suggested by the *in silico* analysis, was proved using a site-directed mutant of RhdA in which the active-site cysteine was substituted by alanine (RhdA-Cys_{230}Ala) (Cartini et al., 2011). In this latter case no fluorescence change was observable in the presence of glutathione (panel B). Moreover, measurements of thermally induced changes of intrinsic fluorescence (Figure thermal) showed that first transition temperature of RhdA in the presence of GSH was higher than that monitored with RhdA alone, corroborating the formation of a fairly stable RhdA/GSH complex.

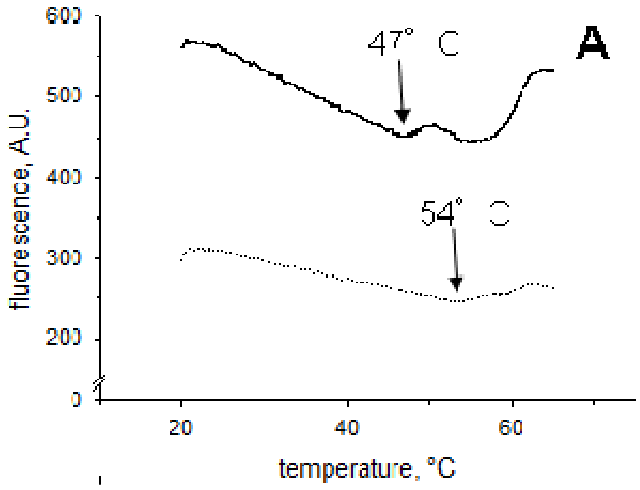

Figure thermal stability. Nature of the RhdA/GSH interaction. Conformation stability of the RhdA/GSH interaction by measurements of thermally-induced fluorescence changes. Fluorescence profiles of 2 µM RhdA (solid line) and RhdA/GSH complex (dotted line) in 50 mM Tris-HCl, 100 mM NaCl (pH 7.4). Tryptophan fluorescence has been monitored as a function of the temperature. Transition temperatures of the first conformational change are indicated.

Spectrophotometric, activity and MS-based approaches were used in order to get more insights about the nature of the complex between RhdA and GSH.

From *in silico* indications we can presume that the RhdA/GSH interaction cannot result in the formation of a disulfide bond because of the structural function of Cys_{230} residue, that forms H-bond with the surrounding residue in order to stabilize the active site 3D structure, and because Cys_{230} residue is deeply buried in the catalytic pocket. Furthermore the formation of a disulfide bond is often the result of a disulfide exchange reaction that has to be excluded because of the absence other cysteine residues in the protein and the simulated inability of RhdA to bind GSSG because of the position of RhdA Cys230 residue, that although is accessible to the solvent is however buried into the catalytic pocket.

A fairly stable RhdA/GSH complex was produced by incubating RhdA with 8-fold molar excess of reduced glutathione (molar ratio RhdA: GSH = 1:8) and by removing GSH excess *via* gel filtration (G-50 column). The stability of the complex, was confirmed by monitoring overnight its intrinsic fluorescence while the protein folding was controlled *via* TST assay (data not shown).

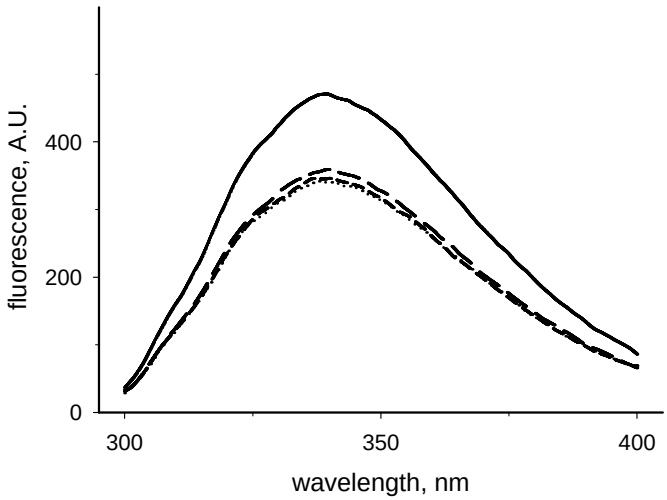

Figure TCEP. Nature of the RhdA/GSH interaction. Tryptophan fluorescence emission spectra (λ_{ex} = 280 nm) of 2 µM RhdA/GSH complex alone (dotted line) in 50 mM Tris-HCl, 100 mM NaCl_pH 7.4, in the presence of 0.8 mM Tris (2-carboxyethyl)phosphine (TCEP; long-dashed line), or in the presence of 0.2 mM DTT (short-dashed line). Solid line reports spectrum of 2 µM RhdA alone.

RhdA/GSH adduct instrinsic fluorescence spectra (Fig. TCEP) were acquired prior (solid line) and after (dashed line) the addition of the reducing agent tris(2-carboxyethyl)phosphine (TCEP) at a final concentration of 0.8 mM. TCEP treatment didn't result in any fluorescence recovery (dotted line), suggesting that GSH was not released in the solvent because there were no disulfide bridges to be broken. Taking into account that the Cys_{230} residue, the only residue in RhdA that can make a disulfide bond, could not be easily accessible to the reducing agent because it is buried inside the active site structure, the inability of RhdA to bind covalently GSH was verified by MS analyses using the whole protein as sample.

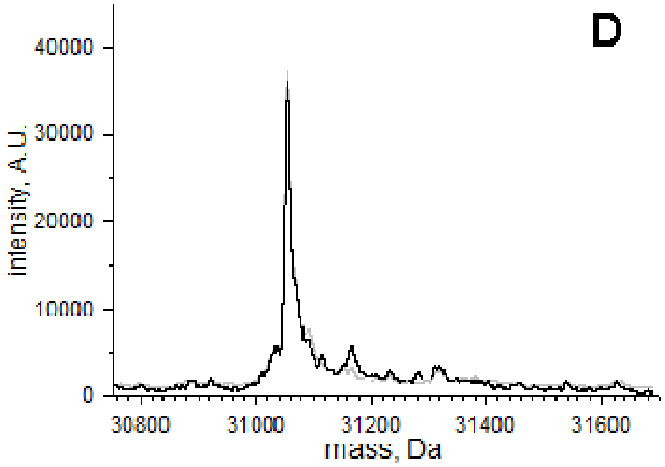

Figure MS. Nature of the RhdA/GSH interaction. LC/ESI Q-ToF analysis of RhdA/GSH complex. Molecular mass range of the deconvoluted ESI spectra of RhdA (grey line) and RhdA/GSH complex (black line). For RhdA/GSH complex, RhdA was incubated 20 min at 25 °C with 8-fold molar excess GSH and desalted by C4-chromatographic pipet tip.

The MS spectra of mixtures of RhdA and GSH did not show significant difference with respect to the spectra of RhdA alone (Figure MS). In both cases a main species at 31054.2 Da was identified, as expected from RhdA sequence (31054.0 Da).
Combining spectra results and MS analyses we can conclude that interaction of RhdA with GSH didn't imply the formation of a covalent complex.

To gain further information about the nature of the RhdA/GSH complex we studied the ability of RhdA to bind glutathione in different ionic condition.

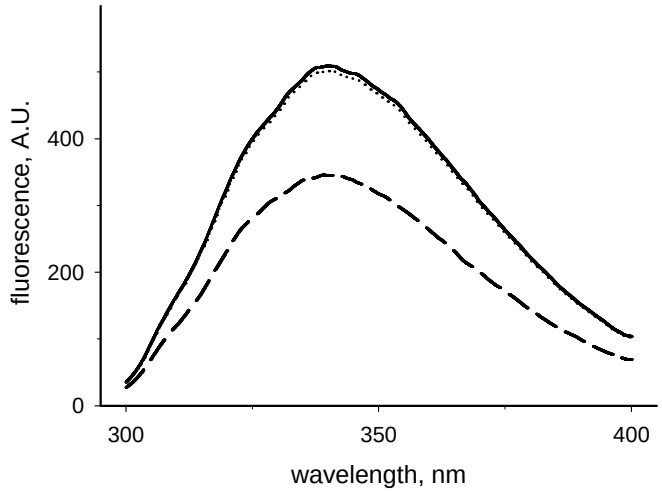

Figure NaCl. Nature of the RhdA/GSH interaction. Tryptophan fluorescence emission spectra (λ_{ex} = 280 nm) of 2 µM RhdA alone in high-saline concentrated buffer (50 mM Tris 1M NaCl pH 7.4) (solid line) or in the presence of GSH (dotted line). Spectrum of 2 µM RhdA in the presence 250 µM thiosulfate is reported as a positive control (dashed line)

As shown in figure NaCl, the increase of the ionic strength (from 0.1 M to 1 M NaCl) of the solvent prevented the quenching of RhdA intrinsic fluorescence by GSH indicating that the interaction did not occur. This result indicated that the complex is stabilized by electrostatic interactions which are weakened in the presence of an high ionic strength.

To deepen the interaction behavior of RhdA with glutathione, the study was extended to other species of glutathione.

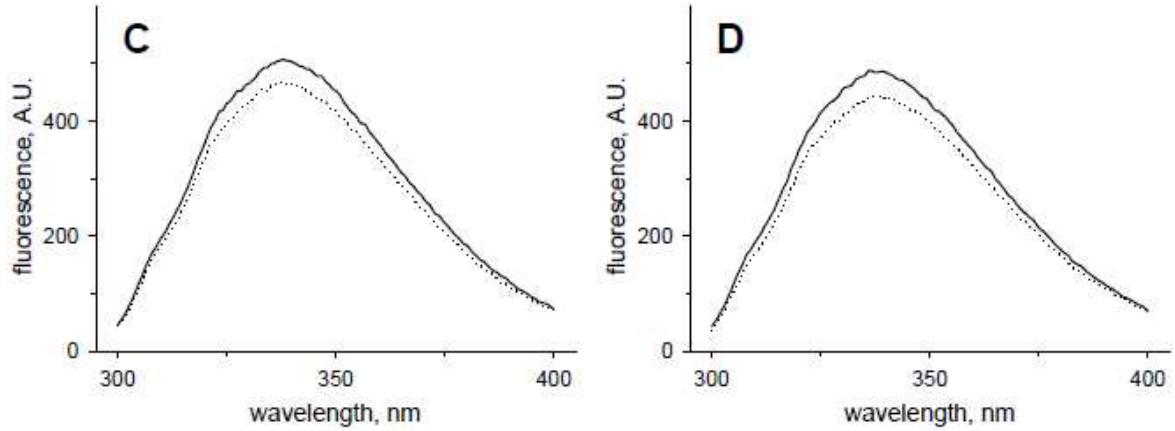

Figure glutathione quenching. Effect of glutathione disulfide (panel C) and glutathione thyil radical (panel D) on the intrinsic fluorescence of RhdA. Tryptophan fluorescence emission spectra (λ_{ex} = 280 nm; dotted lines) of RhdA in the presence of 100 µM GSSG (A), and 50 µM GS* (B). Solid lines report spectra before the addition of glutathione. In all cases, protein was 2 µM in 50 mM Tris-HCl, 100 mM NaCl (pH 7.4). Spectra were corrected for dilution

Fluorescence of RhdA was quenched in the presence of GSSG (panel C), although the fluorescence change recorded in this case was less pronounced than that of the ligand GSH. Noticeably, fluorimetric studies evidenced that RhdA interacts with glutathione-thiyl radical (GS*), an oxidized form of GSH (panel D).

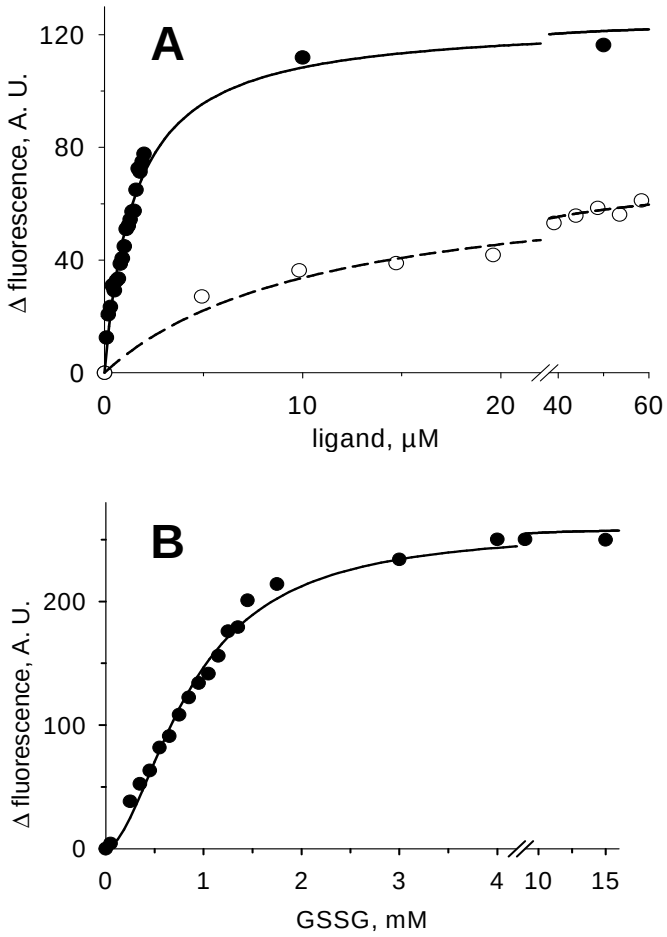

Figure glutathione quenching . Changes of the intrinsic fluorescence of RhdA upon titration with glutathione species. The indicated increasing amounts of GSH (A, full circles), GS• (A, empty circles), and GSSG (B, full circles) were successively added to 2 μM RhdA in 50 mM Tris-HCl, 100 mM NaCl (pH 7.4). Fluorescence intensity was measured at 340 nm (λ_{ex} = 280 nm), and was corrected for dilution.

Further fluorimetric analyses of the interaction of RhdA with GSH and GS* (figure glutathione quenching panel A) allowed the estimation of K_d figures of the RhdA/GSH, RhdA/GS* and RhdA/GSSG complexes that were 1.5±0.1μM, 11±2μM and 1.1 ± 0.1 mM, respectively. The binding of GSSG to RhdA appears to be very weak, as compared to that of GSH and GS* (figure glutathione quenching panel B). Considering that a K_d of 0.76 ± 0.01 μM was found by fluorimetric analysis of the binding of thiosulfate with RhdA (data not shown) the picture that emerged from the data makes GSH a "good" ligand for RhdA giving rise to a "stable" complex, according to the results of docking simulations (see above). Therefore the interactions of RhdA with glutathione species can be a possible key point to understand the mechanism by which RhdA could help maintaining glutathione cellular homeostasis.

Chapter 5.5 Glutathione-thiyl radical scavenging activity of RhdA.

Considering that thiyl radicals (RS^*) have been suggested to be important intermediate oxidants during biological conditions of oxidative stress (Wardman., 1995), we focused our study on the interaction of RhdA with the glutathione thiyl radical. GS* is generated by reaction of GSH with hydroxyl radical (OH*), and an "enzymatic" pathway (Starke et al., 2003) is needed to recover GS^* as GSSG, the substrate of glutathione reductase, in order to regenerate GSH.

In this process, a key step is considered the stabilization of a disulfide anion radical intermediate that facilitates the conversion of GS* to GSSG, and good players in the glutathione-thiyl radical scavenging activity are proteins (e.g. human glutaredoxin, *h*Grx1) bearing thiols with low pK_a (≈ 3.5). In RhdA, the only cysteine residue, Cys_{230}, is mandatory for the correct stabilization of the catalytic pocket structure (Bordo et al., 2001), and its presence in the cysteinate form is favoured by the strong electrostatic field of the catalytic pocket (Bordo et al., 2001). The electrostatic interactions with active-site residues (Ser_{236}, Arg_{235}, His_{234}, and Thr_{232}) influence the pK_a of the RhdA-Cys^{230} thiol that was predicted to be pK_a = 3.7 by the algorithm PROPKA.

We, therefore, reasoned that the peculiar property of the active site thiol of RhdA along with the interaction behaviour with glutathione (see above), could make RhdA a catalyst for GS^*-scavenging activity. To test this hypothesis, GSSG production *via* RhdA in the presence of a GS^*-generation system was studied.

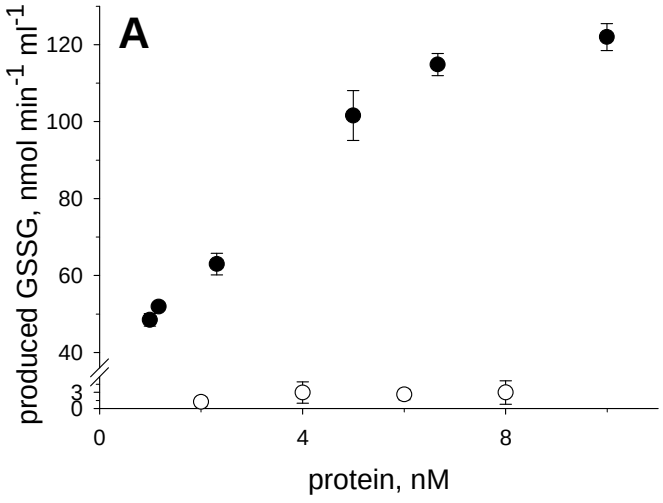

Figure $GS^\bullet$-scavenging activity of RhdA, RhdA concentration dependance. Initial rates of the RhdA-mediated production of glutathione disulphide (GSSG) in the presence of $GS^\bullet$ were spectrophotometrically (λ = 340 nm; ε = 6220 M^{-1} cm^{-1}) determinated by measuring the NADPH consumed in the glutathione oxido-reductase coupled reaction. Reactions were carried out in 50 mM sodium-phosphate buffer (pH 7.4) at 25 °C. Dependence of the reaction on different concentrations of RhdA (full circles) or RhdA-Cys_{230} (empty circles) is reported.

Rate of GSSG production was RhdA concentration dependent (black dots), and it was linear till 6-7 nM RhdA with a turnover of ~ 500 s^{-1}. At higher RhdA concentration the high reaction speed made it difficult to measure the initial velocity. The reaction was negligible when the site-directed mutant RhdA-Cys_{230}Ala was used (white dots), thus indicating that the RhdA-Cys_{230} residue is needed for the GS*-scavenging activity of RhdA.

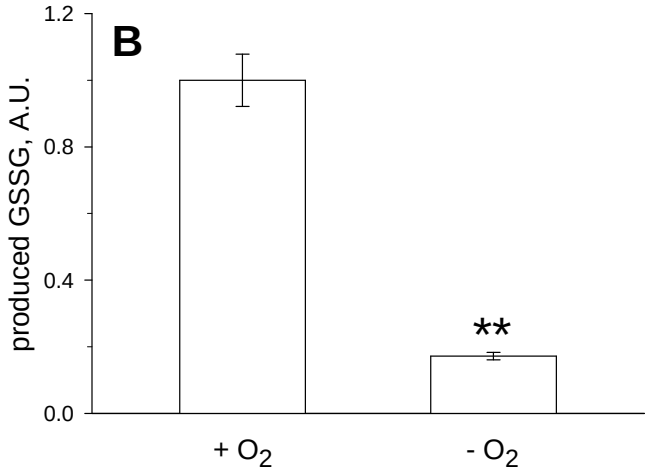

Figure $GS^{\bullet}$-scavenging activity of RhdA, RhdA concentration dependance. Initial rates of the RhdA-mediated production of glutathione disulphide (GSSG) in the presence of $GS^{\bullet}$ were spectrophotometrically (λ = 340 nm; ε = 6220 M^{-1} cm^{-1}) determinated by measuring the NADPH consumed in the glutathione oxido-reductase coupled reaction. Reactions were carried out in 50 mM sodium-phosphate buffer (pH 7.4) at 25 °C. $GS^{\bullet}$-scavenging activity of 16 nM RhdA in the absence (– O_2) of oxygen is reported relatively to that in standard conditions (+ O_2) taken as unitary. A. U., arbitrary units

The ability of RhdA to generate GSSG from GS^{*} was significantly diminished in conditions in which molecular oxygen was depleted, suggesting the participation of molecular oxygen in the RhdA-catalyzed reaction. Similar GS*-scavenging activity rates (data not shown) were obtained using the Fe(II)-ADP/H_2O_2 system (Starke et al., 2003) for GS*-generation.

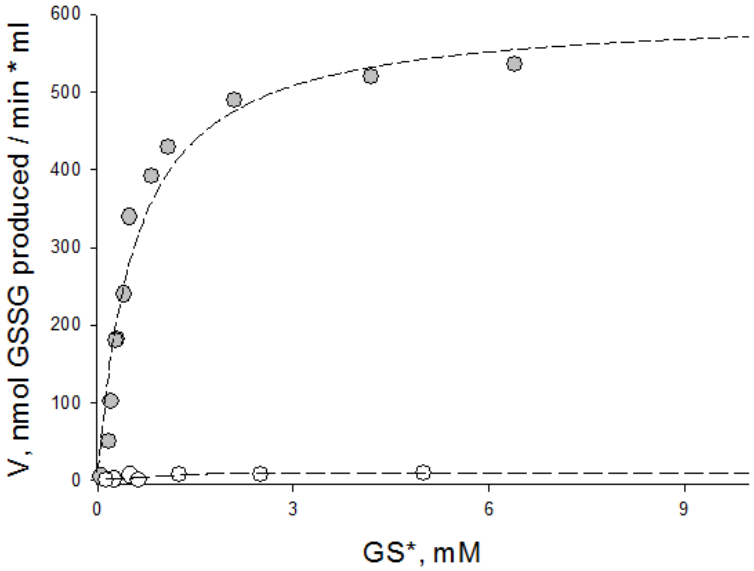

Figure $GS^{\bullet}$-scavenging activity of RhdA Michaelis-Menten behavior. Initial rates of the RhdA-mediated production of glutathione disulphide (GSSG) in the presence of $GS^{\bullet}$ were spectrophotometrically (λ = 340 nm; ε = 6220 M^{-1} cm^{-1}) determinated by measuring the NADPH consumed in the glutathione oxido-reductase coupled reaction. Reactions were carried out in 50 mM sodium-phosphate buffer (pH 7.4) at 25 °C. Michaelis-Menten of $GS^{\bullet}$-scavenging activity of RhdA (grey dots) and $RhdA_{C230A}$ (white dots). Best non-linear fit to experimental data is showed (dashed line).

To further elucidate the efficiency of RhdA in the $GS^{\bullet}$-scavenging activity, kinetic studies were performed, and, as shown in figure, the reaction appeared to follow a classical Michaelis-Menten kinetics. Calculations of apparent kinetic parameters gave the following figures:

K_m	0.56 ± 0.11 mM,
k_{cat}	629 ± 44 s^{-1}
k_{cat}/K_m	1.12 x 10^6 M^{-1} s^{-1}.

Control experiments showed that generation of GSSG by RhdA in the presence of GSH alone was negligible being k_{cat} figure about 0.01 s^{-1} .

Chapter 5.6 *In silico* prediction of the ability of *A. vinelandii* to synthesize conventional reductant cellular players

In *A. vinelandii* glutathione homeostasis is very important due to the lack of a complete biosynthetic pathway to produce others intracellular redox buffers like for example ascorbic acid biosynthetic

pathway that is blocked due to inability of *A. vinelandii* to synthesize for either D-sorbitol dehydrogenase (E.C. 1.1.99.21) or SDH (E.C 1.1.99.32) while L-sorbosone deH (C1DIZ2_AZOVD) is present. Glutathione seems to be the low molecular thiol devoted to the scavenging of reactive oxygen species (the intracellular concentration in standard growing condition is in the mM range**;** Fahey et al., 1987 and my work), for this reason backup strategies to protect glutathione from overoxidation, instead of synthesizing *de novo* GSH, have biological relevance.

CHAPTER 6:

Bacillus subtilis results

6.1 Putative RDPs are present in *Bacillus subtilis*.

B. subtilis strain 168 genome sequence was solved and published by Kunt and colleagues (Kunt et al., 1997) allowing us to perform sequence analyses studies in order to evidence the presence of putative RDPs. Starting from the catalytic domain sequences of the two most characterized RDPs (the mithocondrial bovine rhodanese and RhdA from *A. vinelandii*) we evidenced, using BLAST algorithm, the presence of 5 sequences coding for putative RDPs (YhqL, YrkF, YrkH, YbfQ, YtwF) Furthermore the presence of functional RDPs was stated by performing a TST activity assay on PS832 wild-type strain grown in standard conditions that results in 0.24 ± 0.02 U/mg.

Although their sequence homologies with most studied rhodaneses are weak, these proteins can be inscribed in rhodanese superfamily because of the predicted presence of the typical rhodanese domain module architecture (a catalytic cysteine in between an alpha helic and a beta strand).

A deeper analysis on these protein sequences allowed us to identify that all the rhodanese-like proteins of *B. subtilis* have a single rhodanese-like domain. Furthermore, the rhodanese-like domain is the only domain in three of them (YtwF, YqhL, YbfQ) or is fused to other functional domains in the other (in YrkF: fused to a putative tRNA processing unit; in YrkH: fused to a putative hydrolase). The *B. subtilis* RDPs present a weak sequence homology, and their genes are widespread in the genome. YrkF and YrkH that are localized in the same genome context. Among the *B. subtilis* RDPs the only one for which a putative activity was assigned is YrkH, that is annoted as a putative hydrolase. For this latter reason YrkH was excluded from the intial screaning. Noteworthy putative tandem domain RDPs (i.e RhdA) are not present in *B. subtilis* genome.

In order to understand if *B. subtilis* RDPs were involved in the protection against oxidative stress events we decided to investigate *in silico* the presence of transcriptional elements in their gene sequences in order to evidence the nature of their gene transcription regulators.

By using the BPROM software (http://linux1.softberry.com/) we found indications on RDPs gene transcription regulation (Figure regulators)

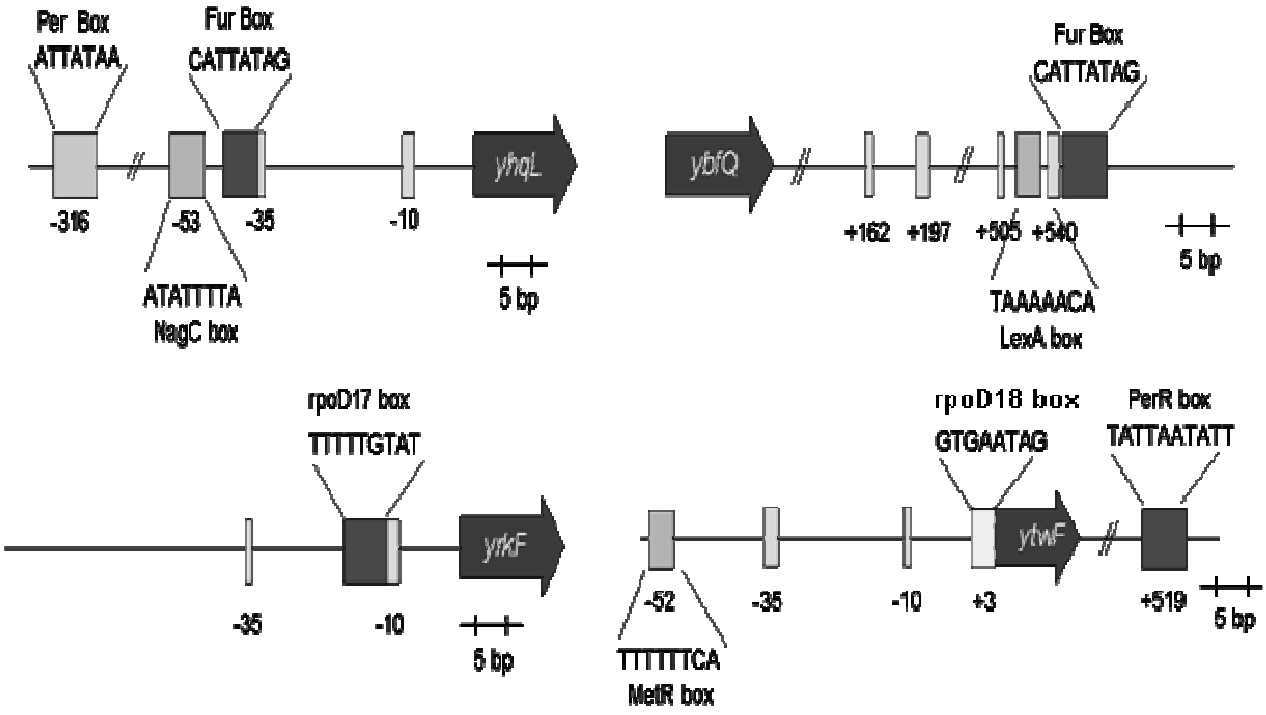

Figure regulators: Putative consensus sequence devoted to the regulation of *B.subtilis* RDPs

According to this sequence analysis, *yhqL* and *ybfQ* genes contain elements for Fur-type transcriptional regulators. In *B. subtilis* there are multiple Fur-like proteins implied either in metal uptake or in peroxide-induced oxidative stress response (Bsat et al., 1998). The most studied Fur-like transcriptional regulators are FurR, that regulates iron uptake, and PerR that is responsible for the peroxide-induced oxidative stress response system that present a fine inter-regulation (Fuanthong et al., 2002). Furthermore *yhqL* gene contains a putative NagC element. In literature NagC has been described as a regulator of *nagE* that codes for a protein involved in the transport of the N-acetilglucosammine (GlnN-Ac) (Plumbridge, 2001). Putative transcriptional regulatory sequences for rpoD17 and rpoD18 (Collado-Vides., 1993), members of the bacterial sigma70 regulator factor, have been identified in *yrkF* and *ytwF* genes, respectively. A putative MetR binding site was evidenced in the *ytwF* gene. MetR has been found in *streptococci* to be involved in the regulation of methionine and cysteine transport and metabolism (Kovaleva et al., 2007) indicating that this protein may serve as S_0 donor for methionine biosynthesis.

The identification of at least three RDP genes (*yhqL*, *ybfQ* and *ytwF*) by which the expression is putatively regulated by Fur homologs represents a solid indication of RDPs implication in protecting redox homeostasis in *B. subtilis* and therefore justify a deeper investigation.

6.2 Phenotype characterization of B. subtilis J1235 strain

The *B. subtilis* J1235strain, isogenic to the wild-type PS832 strain, in which genes coding for YtwF, YrkF, YbfQ and YhqL are inactivated, was kindly provided to me by Professor T. Larson and allowed me to characterize phenotype differences correlated to RDPs deficiency.

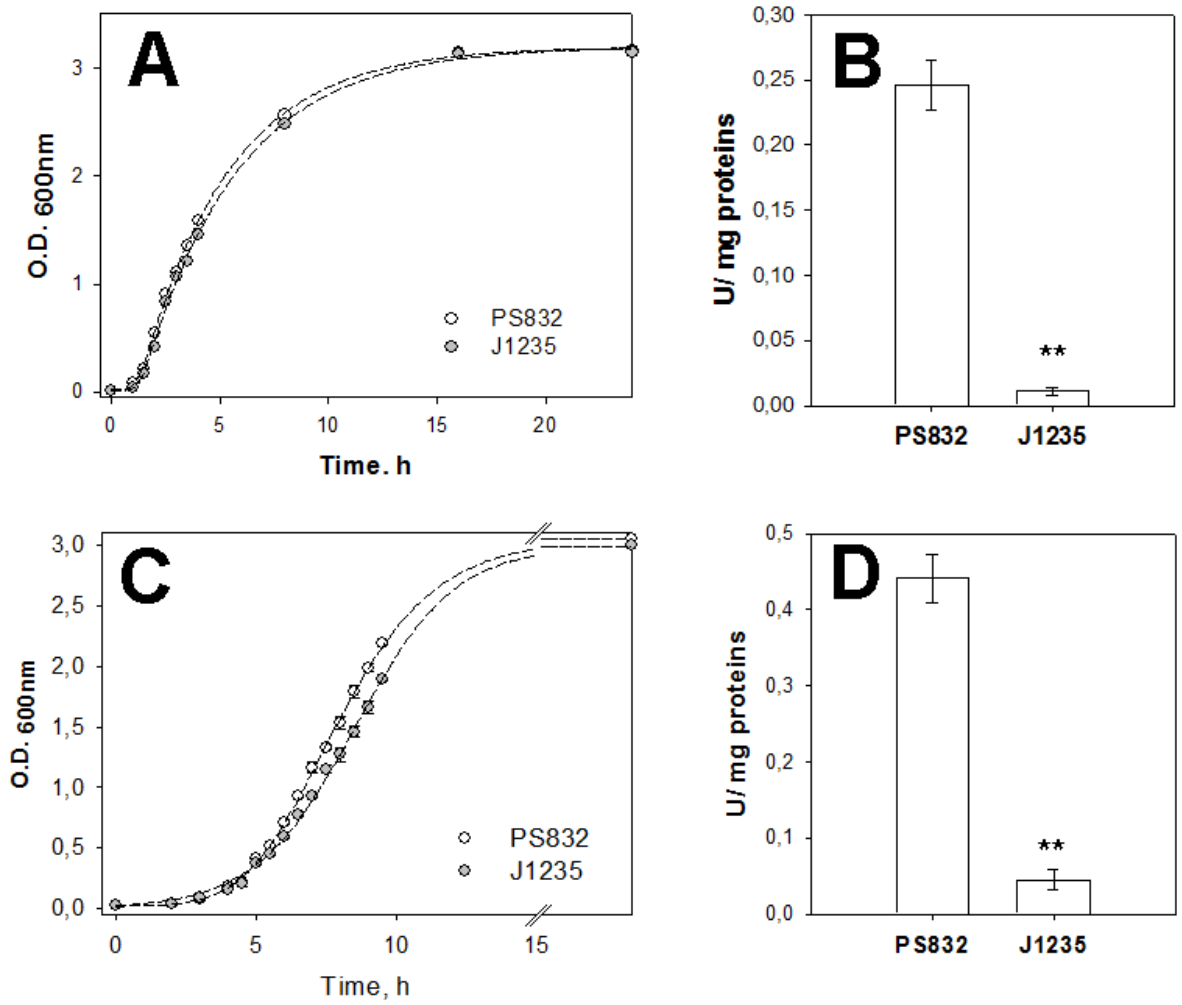

Figure growth. *B. subtilis* growth was monitored in LB (A) and Spizizen minimal media supplemented with sucrose 0.4% (C). TST activity was performed on total protein extract derived from cells collected after the growth in LB (B) and Spizizen minimal media (D). All the enzyme assay were performed in triplicate and are significant for $p < 0.01$ while growth curve were performed in duplicate.

In standard growth condition, LB medium, as shown in the panel A, the absence of the RDPs did not result in any growth change indicating that none of them is mandatory for the *B. subtilis* growth in standard conditions. The same analysis was performed in Spizizen minimal medium (panel C), a condition in which sugars (sucrose 0.4%) and metals, in particularly iron, are constraining. It resulted in a weak but evident growth deficiency in the J1235 strain. TST activity was depleted in the J1235 strain grown in both media (panel B and D), indicating that most of the TST activity in *B.*

subtilis is linked to one or more of the inactivated RDPs in the mutant strain. Furthermore, TST activity was 2-fold increased (p <0.05) in Spizizen minimal media (panel D) suggesting that the stressful condition induced by the growth in this medium leads to the activation of rhodanese activity.

The nature of the stress was unraveled using the aconitase assay as a marker for internal oxidative stress. The aconitase activity of either PS832 and J1235 strains was lower (p< 0.05.) in LB medium (panel A) compared to Spizizen minimal medium (panel B).

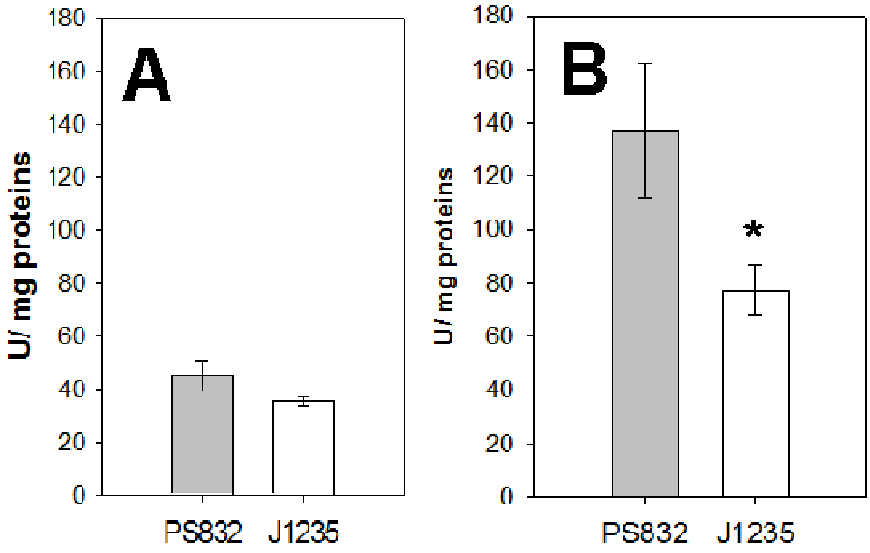

Figure aconitase assay. Aconitase activity assay was performed in crude extracts of B. subtilis PS832 strain (grey bars) or J1235 strain (white bars). Cells were grown until an O.D $_{600nm}$ =1 in LB media (A) or Spizizen minimal media (B) supplemented with sucrose 0.4%. Data are the mean of 3 biological replicates ± standard deviation. Result significance was calculated *via* t student p>0.05.

Moreover in LB media, aconitase activity values were comparable between the two strains (panel A), suggesting that in rich media the absence of RDPs does not result in an internal oxidative stress that indeed was present in the growth carried out in minimal media (panel B), in which the significant decrease (≈ 44%) of the aconitase activity suggests an internal oxidative stress problem that is raised by the inability to synthesize RDPs.

6.3 *B. subtilis* sensitivity to induced oxidative stress

To frame the relationship of RDPs with the oxidative stress response system, we compared the ability of *B. subtilis* PS832 and J1235 strains to survive after exposure to hydrogen peroxide (H_2O_2). The challenge was performed using two complementary methodologies: on one side we tested the ability of the *B. subtilis* strains to recover after short exposure (20 min) to high concentration of H_2O_2, while on the other side we tested their growth fitness after exposure to sublethal H_2O_2 doses.

It is known from proteomic studies that the oxidative stress response is fully activated after 30 min exposure to 58 µM H_2O_2 (Helmann et al., 2003). Treatments with high concentration of hydrogen peroxide led to a different fitness of J1235 strain compared to the wild-type PS832 strain (panel A). An increased mortality was observed for both strains **(**figure H_2O_2 sensitivity panel A), but J1235 mortality rate was more pronounced than that of PS832, indicating that the absence of RDPs increased sensitivity to oxidative stress damage.

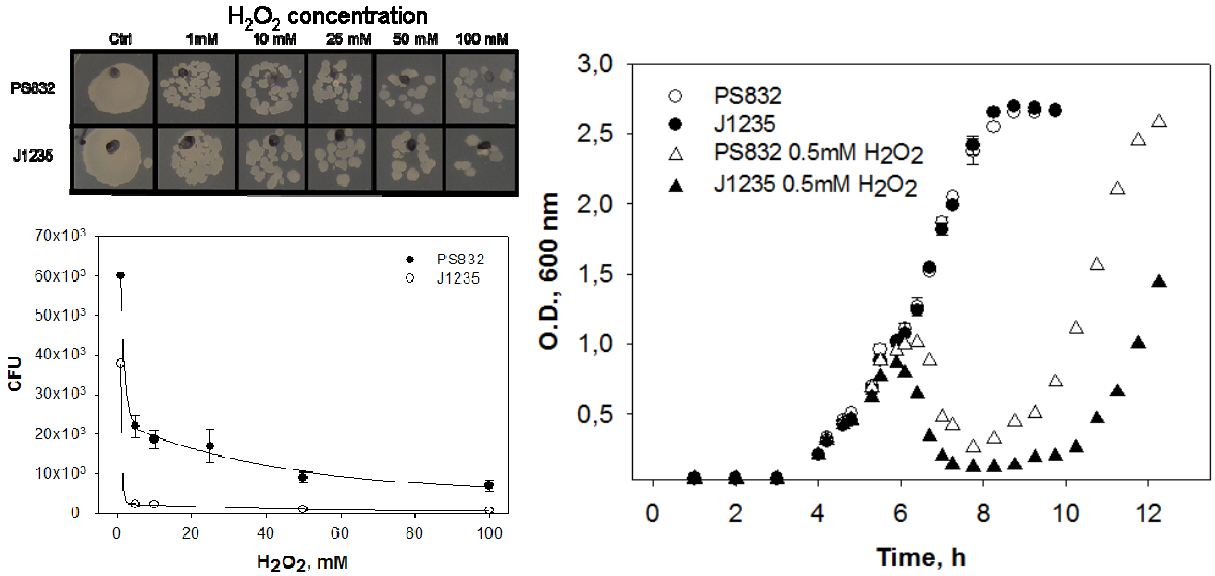

Figure H_2O_2 sensitivity: In figure is described the behavior of PS832 and J1235 B.subtilis strain after short incubation with high H_2O_2 concentration (panel A) or long incubation 0.5 mM H_2O_2 (panel B). In panel A survived cell were counted and expressed as CFU while in panel B the O.D. 600 nm was evaluated.

The increased sensitivity to oxidative stress, that is indeed present exposing J1235 to high H_2O_2 concentration, was not highlighted incubating J1235 strain to sublethal hydrogen peroxide concentrations (50-250 µM, data not shown). Significant growth differences were appreciable in the set of experiments in which *B. subtilis* strains were exposed to 500 µM H_2O_2 (panel B). At this latter concentration both PS832 and J1235 cellular density drastically decreased encountering a new lag phase from which PS832 strain arose faster than J1235 (PS832, white triangle; J1235, black triangle). *B. subtilis* is a spore-forming bacterium and the latter result opens to the hypothesis that the different sensitivity to oxidative stress observed in the J1235 strain may be also the effect of the decreased ability of the strain to sporulate.

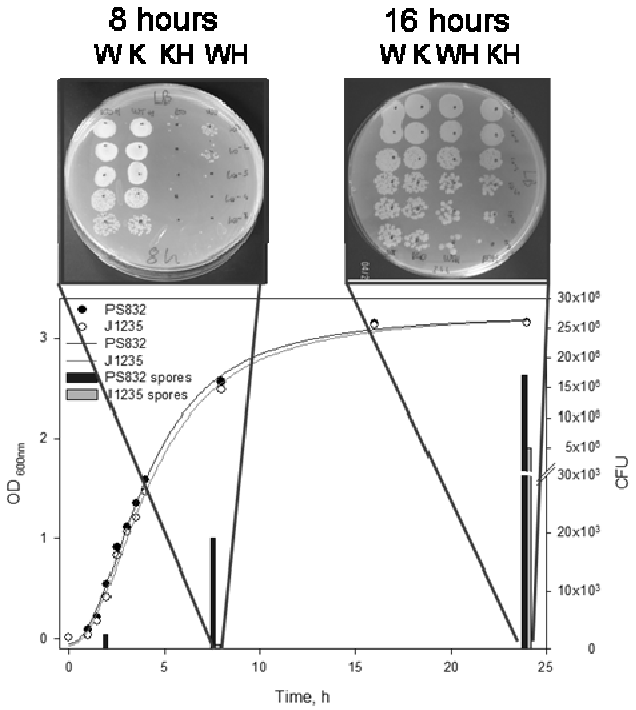

Figure sporulation. *B. subtilis* strains PS832 and J1235 were synchronized as described in material and methods and their growth was followed for 24 hours. Aliquot were taken after 2.5, 8 and 24 h serially diluted and plated overnight before and after thermal treatment. As bars are presented the number of counted spores

After colture synchronization, a procedure, described in material and methods, that allows the inoculation of vegetative cell avoiding spores contamination, *B. subtilis* strains were grown in LB medium and the formed spores were counted in middle exponential phase (2.5 h after the inoculation), in middle stationary phase (8h after the inoculation) and in late stationary phase (24 h after the inoculation). The spore number measured in the J1235 strain was 1000-fold less than that observed for the PS832 strain at the middle stationary phase, and a low difference was still present 24 h after the inoculation. Thereby, the absence of RDPs drastically decreases the *B. subtilis* ability to sporulate.

Gram-positive bacteria, especially *B. subtilis*, can be described as "specialized" bacteria meaning that they evolved specialized strategies instead of general strategies to recover from oxidative stress. The direct detoxification of hydrogen peroxide, for example, is under the control of three different catalases (KatA, KatB and KatX), while KatA and KatB are expressed in vegetative cells KatX is only expressed in spores indicating a specialized mechanism of protection (Casillas-Martinez et al., 1997). A major involvement of RDPs in protection against oxidative stress events that could occur either in spore or only in condition of severe stress can be hypothesized.

Catalase activity assays were performed on vegetative cells grown in Spizizen minimal medium until middle exponential phase (0.5 OD) and resulted in a higher activity in PS832 strain compared to the J1235 strain (fig catalase grey bars)

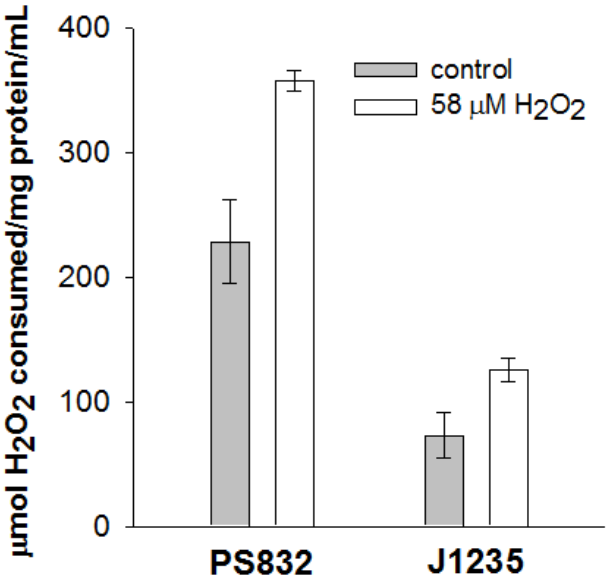

Figure catalase activity: Catalase activity assay was performed on PS832 and J1235 total extracts grown in spizizen minal medium with (white bars) and without (grey bars) the addition of 58 µM H_2O_2. Data are the mean of 3 biological replicates ± standard deviation.

Furthermore the catalase expression was artificially induced by incubating the cells for 30 min with 58 µM H_2O_2 , an hydrogen peroxide concentration in which the oxidative stress response system is shown to be activated by proteomics (Helmann et al., 2003). While catalase activity was significantly increased ($p < 0.05$) by H_2O_2 incubation in the wild-type strain no evident increase of the activity was highlighted in the RDPs mutant strain.

Although the decrease of catalase activity in J1235 strain does not seem to agree with the proposed involvement of RDP in protection against oxidative stress agents, a deeper investigation on *B. subtilis* KatA and KatB regulations is required. Vegetative catalase activity in *B. subtilis* is negatively regulated by the increased levels of organic hydroperoxides (Wang et al., 2004) in which the most representative are lipid hydroperoxides. Estimation of the lipid hydroperoxide content in the PS832 and J1235 *B. subtilis* strains highlighted that the absence of RDPs led to ≈48% increase of the lipid hydroperoxide content. Although experiments were conducted at different growth phases (the catalase assay was performed on cells grown until 0.5 OD while the lipids peroxides content was performed on cells grown until 1.0 OD) is it possible to compare the two data because

the trend was preserved at O.D 1.0 (data not shown) thus suggesting an explanation for the inhibition of the catalase activity observed in the mutant strain, .

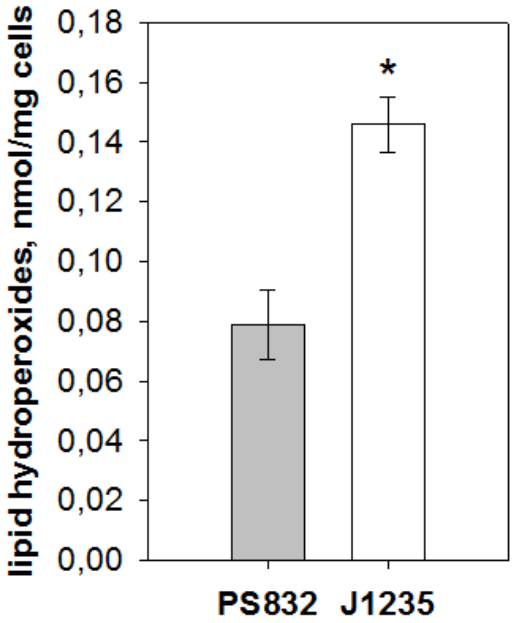

Figure lipid hydroperoxides: Lipid hydroperoxides were quantified in PS832 cells (grey bars) and J1235 cells (white bars) grown in Spizizen minimal medium until late exponential phase (O.D 600 nm =1) Data are the mean of 3 biological replicates ± standard defiance. Data significance analyses was estimated by Student test ($p<0.05$).

Accumulation of lipid hydroperoxides together with behavior of the aconitase activity could represent a link between the absence of RhdA in *A. vinelandii* and the absence of RDPs in *B. subtilis* leading to the hypothesis that at least one of the RDPs of *B. subtilis* shares the same physiological function with RhdA.

6.4 Low molecular weight thiols in *B. subtilis*

Differently from eukaryotes and most of the Gram-negative bacteria, the majority of the Gram-positive bacteria have evolved different strategies to maintain intracellular redox homeostasis that don't involve the synthesis of GSH (Fahey et al., 1978). The most thoroughly studied of these alternative compounds is mycothiol (MSH), produced by the high-(G+C)-content Gram-positive *Actinobacteria* (Rawat et al., 2007). In some low-(G+C) content Gram-positive bacteria coenzyme A (CoA) has proven to be a major thiol (Fahey et al., 1983). Thus CoA appears to function as a protective thiol in some Gram-positive bacteria like *A. aureus* (delCardayré et al., 1998) but has the disavantage that cannot serve as a reservoir of cysteine. Recent studies on *B. subtilis* redox sensitive thiol proteins, have uncovered an unknown low-molecular mass thiol in association with the transcription factor OhR (Nicely at al., 2007) that, in eukaryotic organisms, is regulated by

glutathionylation (Hermansson et al., 1990). This new molecule, named bacillithiol (BSH) shares the GlcNac and the cysteine moieties with MSH, but the sugar molecule changes (Newton et al., 2009) and its substituted by malic acid, and has proven to be the *B. subtilis* major low molecular weight thiol (Gaballa et al., 2010).

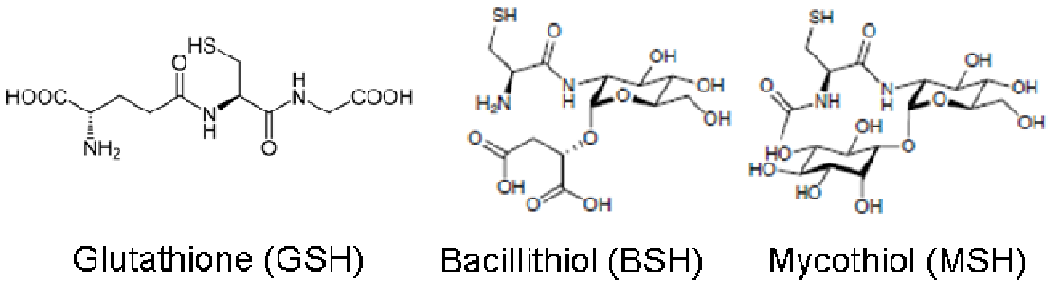

Figure structures: Chemical structure of reduced glutathione (GSH), Bacillithiol (BSH) and Mycothiol (MSH)

Low-molecular weight thiols were extracted as described in "material and methods" and, after monobromobimane derivatization, single compounds were resolved by C18 column chromatography. Bacillithiol levels were quantified in the PS832 and J1235 strains grown in Spizizen minimal medium until late exponential growth phase (O.D. 600 nm =1) and were measured as total, reduced (BSH), disulfide (BSSB), and protein-bound (BS-R) bacillithiol.

Bacillithiol pmol/ mg cells (wet weight)

Strain	BSH	BSSB	BS-R	Total	BSH/BSSB
PS832	315.36 ± 5.44	6.41 ± 0.02	141.98 ± 6.59	463.75 ± 12.01	49.22 ± 1.01
J1235	218.00 ± 29.52	11.25 ± 0.12	179.63 ± 12.86	408.87 ± 42.50	19.37 ± 2.42

Table total bacillithiol: Bacillithiol levels were quantified in PS832 strain and J1235 strain grown in spizizen minimum medium as described in material and methods. BSH, soluble reduced bacillithiol fraction. BSSB, soluble disulfide bacillithiol fraction; BS-R, bacillithiol bound to proteins. Total bacillithiol is calculated by the sum of BSH, BSSB and BS-R. Data are the mean of 3 biological replicates ± standard deviation.

The absence of RDPs resulted in a significant decrease of BSH (≈29%) and in an increase of BSSB. RPDs did not significantly alter the levels of bacillithiolated proteins suggesting that RDPs are not involved in bacillithiolation. Furthermore levels of total detected bacillithiol are lower in the J1235 strain compared to PS832 levels (≈14%). Although standard deviation values are high, due to the difficulties on the standardization of the extraction methods, quantifications of total bacillithiol in the J1235 strain were systematically lower compared to the PS832 strain supporting the statistical value of the data acquired. Analyses of the bacillithiol levels further confirmed that the absence of

RDPs led to a misregulation of the cellular redox balance because of the dramatic drop of the BSH/BSSB ratio.

6.5 *B. subtilis* YhqL as a putative *A. vinelandii* RhdA ortholog

The preliminary characterization of the J1235 phenotype highlighted changes that agrees with *A. vinelandii* MV474 phenotype. In particular in both system the absence of RDPs/RhdA led to the misregultation of the redox homeostasys evidenced by: the decrease of the most representative low-molecular weight thiols (glutathione for *A. vinelandii*; bacillithiol for *B. subtilis*), the decrease of the aconitase activity (Cereda et al., 2009 for *A. vinelandii)* and the increase of lipid hydroperoxides.

Although the phenotype alterations caused by the absence of RhdA in *A. vinelandii* were studied more exhaustively, it is legitimate to hypothesize that at least one of the *B. subtilis* RDPs could be the *B.subtilis* ortholog of RhdA.

Indications could arise from studying the primary sequence of the *B. subtilis* RDPs. Taking in consideration that:

a) The active site structure of the RhdA ortholog in *B. subtilis* has to be structurally different, because of the binding with bacillithiol, that has a 3D structure completely different from glutathione.

b) The specialization of *B. subtilis* lead to think that the RhdA ortholog cellular localization has to be near the membrane in order to dissipate the OH* produced by cellular respiration.

c) *B. subtilis* RhdA ortholog expression has to be putative regulated by transcription factors involved in the management of bacillithiol, or has to be directly regulated by the oxidative stress response system machinery.

Among the RDPs of *B. subtilis* YqhL seems to respond to these prerequisites. In the N-terminal extremity of its sequence is present a long hydrophobic region (2-26) that agrees with a membrane domain that let to suppose that the protein is localized at the membrane level. Furthermore among the putative regulatory sequences found in *yhqL* we can evidence the presence of FurR element at -35 bp**,** NagC element at -51 bp, and a PerR element at -316 bp.

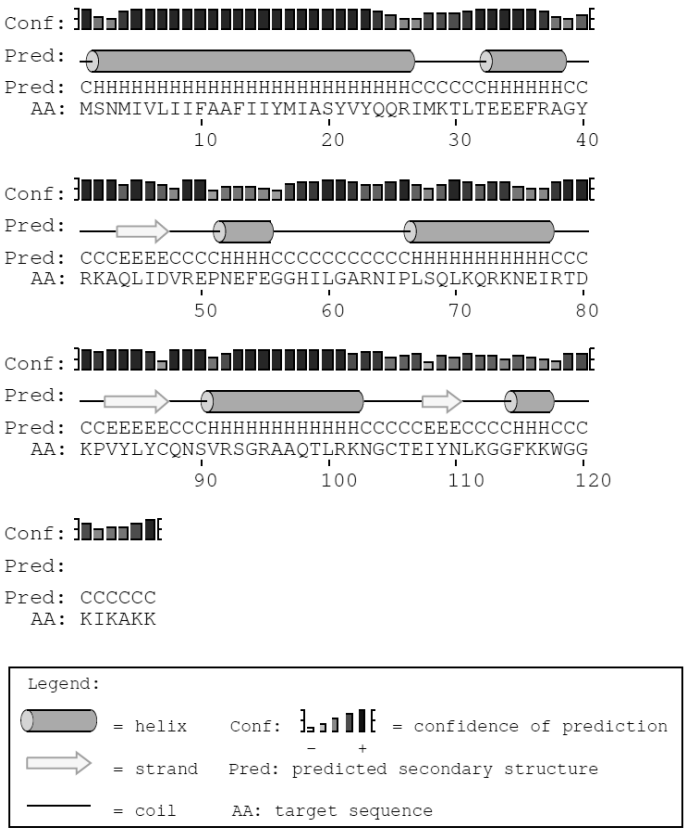

Figure YqhL: Secondary structure prediction of YqhL

Starting from these *in silico* evidences we performed the quantification of the lipid hydroperoxides and we monitored the levels of bacillithiol in the JD0206 *B. subtilis* strain in which *yqhL* gene was inactivated by insertion.

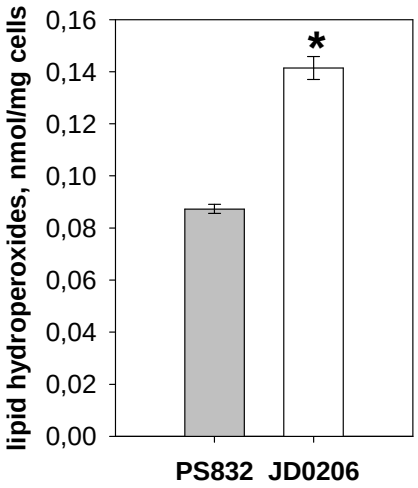

Figure lipid hydroperoxides: Lipid hydroperoxides were quantified in in PS832 cells (grey bars) and JD0206 (white bars) grown in Spizizen minimal media until late exponential phase (O.D 600 nm =1) Data are the mean of 3 biological replicates ± standard defiance. Data significance analyses was estimated by Student test ($p<0.05$).

The preliminary data indicates that the absence of YhqL lead to the accumulation of lipid hydroperoxides and to the misregulation of the BSH/BSSB ratio to levels that agrees with the one founded for J1235 strain supporting the idea that this RDP could be the RhdA functional analog in *B. subtilis*.

bacillithiol pmol/ mg cells (wet weight)

Strain	BSH	BSSB	BS-R	Total	BSH/BSSB
JD0206	202.88	9.27	221.25	433.41	21.88
PS832	315.36 ± 5.44	6.41 ± 0.02	141.98 ± 6.59	463.75 ± 12.01	49.22 ± 1.01

Table bacillithiol in JD0206 strain: Bacillithiol levels were quantified in PS832 strain and JD0206 strain grown in spizizen minimum media as described in material and methods. BSH soluble reduced bacillithiol fraction, BSSB soluble disulfide bacillithiol fraction, BS-R bacillithiol bounded to protein. With Total bacillithiol is intended the sum of BSH, BSSB and BS-R. Data are the mean of 3 biological replicates ± standard deviation.

CHAPTER 7:

General discussion

The redundancy of mechanisms devoted to control cell redox homeostasis and formation of radical species allows the growing of bacteria in stressful conditions. The major players in the oxidative stress control systems are well studied (catalases and peroxidase for hydrogen peroxide; superoxide dismutases and for superoxide anion), but new enzymes are emerging players for direct or indirect control of reactive oxygen species. To search "new players" in these processes, I focused my attention on proteins belonging to the rhodanese-like superfamily (RDPs PFAM accession number: PF00581). In particular, I choose two aerobic bacterial models in which these proteins are abundant: the Gram-negative *A.vinelandii* and the Gram-positive *Bacillus subtilis.* In my work I assessed that both the lack of the RDP RhdA in *Azotobacter vinelandii* and the lack of RDPs in *Bacillus subtilis* led to the *in vivo* perturbation of the redox homeostasis, shifting the redox balance to a more oxidized state. When both mutant bacteria were grown in their minimum medium, decreased levels of reduced low molecular weight thiols (GSH for *A. vinelandii* and BSH for *B. subtilis*), altered ratio of reduced/disulfide low molecular weight thiols and decrease of the aconitase activity have been found. In *A. vinelandii,* also in standard grow conditions, the absence of RhdA induces the activation of the oxidative stress response system, evidenced by the higher expression and accumulation of AhpC, a member of the OxyR regulon (that in Gram negative bacteria is devoted to the control of the hydrogen peroxide dependent oxidative stress response system). Furthermore, in induced oxidative stress growth conditions, in both *B.subtilis* and *A.vinelandii* the thiosulfate-cyanide sulfurtransferase activity (marker of RDPs presence) was increased, and in *A.vinelandii rhdA* overexpression was evidenced. These results indicated an *in vivo* correlation between RDPs and the control of cell redox homeostasis, and they open the question about the mechanisms by which RDPs are involved in this process.

In vitro experiments showed that *A. vinelandii* RhdA was sensitive to the oxidative stress induced by (the mixed radical generator) phenazine methosulfate (PMS) and that, in order to maintain its sulfurtransferase activity, the catalytic cysteine has to be "protected" by either an extra sulfur (forming a persulfide) or a molecule of GSH (forming an RhdA/GSH adduct).

Moreover, the evidenced interaction with GSH prompted us to investigate on the direction of a coupled RhdA-glutathione process, being glutathione the most abundant low molecular weight thiol in *A. vinelandii* (Fahey et al., 1987).

The finding that lipid hydroperoxides, the oxidized lipid species that result from the accumulation of hydroxyl radicals, and are mainly produced by the cellular respiration, in the RhdA null mutant was accumulate, was the reason why I focused the second part of my study on a possible relationship between *A. vinelandii* RhdA and the protection of the cellular respiration machinery from damages induced by the accumulation of hydroxyl radicals.

The drop of total glutathione level, evidenced in the *rhdA* null mutant MV474 *A. vinelandii* strain, indicated that the recycling of GSH was impaired in the absence of the RhdA, suggesting that in MV474 glutathione was in an oxidized form that could not be recycled in the canonical glutathione recovery pathway that implies the final formation of glutathione disulfide (GSSG) and the action of the NADPH dependent enzyme glutathione reductase (GR) to regenerate two GSH molecule.

Considering that the peculiarity of GSH is that it can spontaneously interact, *via* one electron reaction, with hydroxyl radicals leading to the production of water and glutathione thyil radical (GS* Quintiliani et al., 1977), and that the kinetics of the reaction at physiologic pH value (k=1.3 $x10^{10}$ $M^{-1}s^{-1}$) makes GSH an *in vivo* scavenger of hydroxyl radicals (Quintiliani et al., 1977), interaction of RhdA with GS* was investigated. The fate of thiyl radicals in the cell, and in particular the fate of GS*, has been deeply studied, and the kinetic parameters of the principals chemical reactions in which GS* is involved (in the cellular environment) have been calculated and reviewed by Wardman and colleagues (Wardman et al., 1995). Once it is formed, GS* can undergo to three different reactions:

A. GS* can interact with GS^- leading to the production of $GSSG^{-}$* ($k_{f1a} = 6x10^8\ M^{-1}s^{-1}$) ,that can further react with molecular oxygen promoting the production of GSSG and a superoxide anion ($k_{f2a} = 5x10^9\ M^{-1}s^{-1}$). (Wardman et al., 1995)
B. GS* can undergo to conjugative reaction with O_2 leading to the production of glutathione thiylperoxyl radical (GSOO*) ($k_{f1b} = 2x10^9\ M^{-1}s^{-1}$), which destiny is still a matter of controversy, although has been hypothesized that this radical could either rearrange to form sulfonyl radical or transfer an oxygen atom to thiol to give a sulfinyl radical and a sulfenic acid. (Wardman et al., 1995)
C. GS* can undergo to chemical rearrangement producing other reactive species having the radical centered in the α-carbon or β-carbon following the 8:3:1 ratio (S; β-C; α-C centered respectively). Carbon centered glutathione radicals are considered as "sticky" species and their further interaction with GS^- can not occur. (Hofstetter et al., 2010)

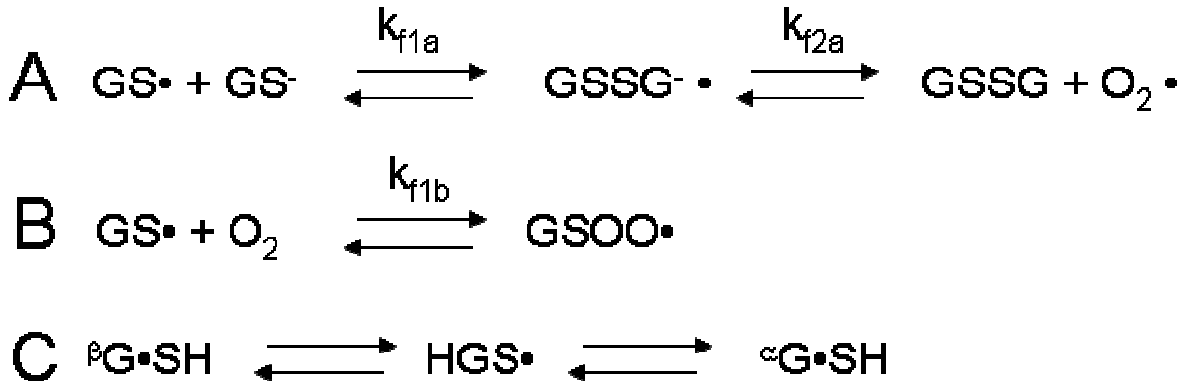

Figure fate of GS*. The scheme depicts the fate of the intracellular GS* that can form conjugates with either glutathione in the thiolate form (A) or with the molecular oxygen (B). Furthermore GS* can undergo to chemical rearrangements having the radical centred on the α or β carbon (C). k_{f1a} and k_{f1b} are the kinetic constants leading to the formation of GSSG-* and GSSG respectively while k_{2fa} is the kinetic constant of the GSOO* formation.

Considering the kinetics constant of the reactions A and B (figure fate of GS*), it clearly results that, in ideal conditions, GS* preferentially conjugates with molecular oxygen instead of thiols, being $k_{f1b} > k_{f1a}$. A different behavior is found in physiological conditions, because, taking in account a cellular oxygen concentration of 0.2 mM and a GS^- concentration around 0.025 mM (Wardmann et al., 1995), the two competitive reactions presents lower and comparable kinetics constant leading to the conclusion that none of the reactions is favored. In this study, I found that RhdA is able to bind GS*, leading to the production of GSSG, and, although intermediates in the catalytic mechanism of $GS^{\bullet}$-scavenging by RhdA were not detected, some considerations make this activity physiologically relevant. Firstly, the measured affinity for RhdA of both GSH and GSSG revealed a K_d value for RhdA/GSH complex about 700-fold lower than that found for RhdA/GSSG complex suggesting that the binding of GSH to RhdA easily occurs, thus favoring formation of the low-affinity leaving group GSSG. The measured high affinity of RhdA for GSH (K_d = 1.5±0.1μM), along with the depicted orientation and proximity of GSH thiol and RhdA-Cys_{230} thiol, predicted by the *in silico* model, might explain the catalytic efficiency (k_{cat}/K_m =1.12 x 10^6 M^{-1} s^{-1}) of RhdA in producing GSSG starting from GS* thus favoring the formation of thiol conjugate (reaction A figure fate of GS*). The reasons of this favored catalysis can be explained by the followings: RhdA stabilizes an intermediate with GS* (K_d = 11±2 μM), thus counteracting its conjugation with oxygen or other chemical rearrangements, while the RhdA, catalyzed formation of GSSG-*, does contribute to the increase of the overall k_{f1a} constant.

Starting from these considerations, the presence of RhdA in the *A. vinelandii* cellular system helps the efficient reshuffling of GSH, because, considering the RhdA K_{cat} number (629 s^{-1}) the production of GSSG is favored thus allowing a fast GSH recovery instead of the production of GSOO*. The RhdA ability to fasten the GS* conjugation with GSH might explain the loss of glutathione evidenced *in vivo* when RhdA was absent (MV474 *A. vinelandii* strain).

This idea is further supported by considering that:

a) only the reduced glutathione in thiolate form (GS^-) can react with GS* and that its cytosolic concentration is ~2% of the total GSH (Wardmann et al., 1995), we can calculate that in *A. vinelandii* the intracellular GS^- concentration is ~25 µM.

b) *In silico* prediction of the pK_a of RhdA catalytic cysteine residue is 3.7, that is in the range of the acid cysteine residue of hGrx1, the only protein for which the *in vitro* GS*-scavenging activity has been quantified (Starke et al., 2003).

Although intermediates in the catalytic mechanism of GS*-scavenging by RhdA have been not detected in this work, we can suggest that RhdA ability to catalyze GSSG production, starting from GSH and GS*, could reside in the ability of the acid cysteine residue to promote the formation of GS^- by taking the hydrogen from GSH.

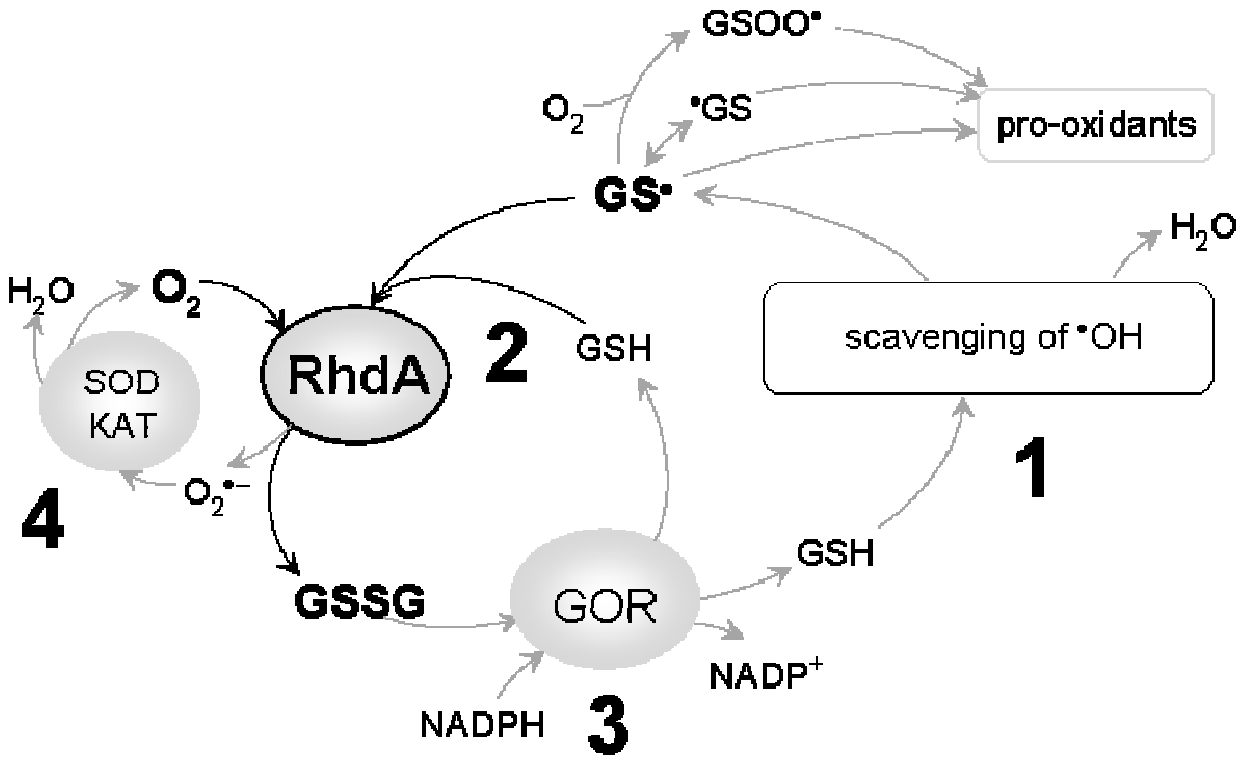

Figure RhdA mediated GS* scavenging. The scheme depicts the possible interplays of RhdA-catalyzed GS•-scavenging (thick lines) with other players (grey lines) involved in GSH homeostasis. The oxygen-dependent GS•-scavenging activity of RhdA would allow the dissipation of GS• as disulfide glutathione (GSSG). The superoxide anion can be removed by the most recognized players (e.g. superoxide dismutase, SOD, and catalase, KAT) in superoxide scavenging machinery, and GSH can be recovered from GSSG by glutathione reductase activity (GR).

The above scheme represents the working hypothesis of the mechanistic interplay of RhdA in the scavenging of hydroxyl radicals . The first reaction that occurs is the scavenge of hydroxyl radical, performed by GSH, with the formation of water on GS* (RhdA mediated GS* scavenging point 1). The presence of RhdA allows the preferential formation of thiol conjugates with GS^-, instead of the one with oxygen, catalyzing the formation of the GSG^-* intermediated, that, interacting with molecular oxygen, spontaneously decades to glutathione disulfide leading to the production of a superoxide anion (RhdA mediated GS* scavenging point 2). The produced GSSG can be recovered as two GSH, with the consumption of NADPH, by the glutathione reductase (RhdA mediated GS* scavenging point 3) while, the radical, that now resides on superoxide anion, can be further scavenged by superoxide dismutases (SODs) and than catalases (KATs), in order to produce a water molecule (RhdA mediated GS* scavenging point 4).

Our model supports the general accepted mechanism in which the superoxide anion is considered an "intracellular radical sink" (Winterbourn., 1993), but, as reported by Wardman and colleagues

(Wardman et al., 1995), the kinetics of superoxide pathway for radicals scavenging in cells has to consider the role of ascorbate. Noticeably, *in silico* analyses indicate that the ascorbate cycle is not functional in *A. vinelandii*, due to its inability to synthesize both D-sorbitol dehydrogenase (E.C. 1.1.99.21) and SDH (E.C 1.1.99.32), supporting the biological relevance to the kinetic mechanisms before discussed.

As for the *B. subtilis* system, the data here presented indicate that RDPs absence leads to similar phenotypic features (accumulation of lipids hydroperoxides and decrease of the reduced bacillithiol pool) to that evidenced for RhdA deficiency in *A. vinelandii* . Furthermore, my *in silico* studies on the transcription factors that regulate the expression of *B. subtilis* RDPs indicated that, at least 3 of these proteins are under the control of FurR, which regulates the intake of iron that is important for generating ROS and in particular hydroxyl radicals. These informations suggest the presence of RhdA ortholog(s) in *B. subtilis*, and the different structure between GSH and BSH can be the key to explain the amino acidic differences RhdA and *B. subtilis* RDPs.

Among the RDPs single *B. subtilis* mutant strains studied in this work, the deletion of YhqL (strain JD0206) leads to similar phenotypic characteristics of the quadruple mutant strain (strain J1235), making this protein a good candidate for being the RhdA orthologs in the *B. subtilis* system. Noticeably, YhqL contains a long hydrophobic N-terminal domain that suggests membrane localization, and a likely involvement in the respiration system thus making YhqL a possible RhdA orthologous in *B. subtilis.* A deeper study, involving both YhqL and BSH purification, is in progress.

In conclusion this work provided evidence that RhdA of *A. vinelandii*, and at least one of the RDPs of *B. subtilis,* are important enzymes for the regulation of the intracellular redox homeostasis. RhdA action is focused on protecting the cell against the accumulation of hydroxyl radical, that can be endogenously produced by the cellular respiration system. Finally I found evidence that at least one of the RDPs in the *B. subtilis* system might be the RhdA orthologous.

The production of hydroxyl radicals, *via* Fenton reaction, is a key process of the eukaryotic cells' response to pathogen bacteria. The link between RDPs and the protection against hydroxyl radicals makes these proteins a potential target of applicative studies focused on pathogen eradication.

CHAPTER 8:

Literature cited in this work

Abdolrasulnia, R. and J. L. Wood. 1979. Transfer of persulfide sulfur from thiocystine to rhodanese. *Biochim.Biophys.Acta* **567**:135-143.

Adams H, Teertstra W, Koster M, Tommassen J. 2002. PspE (phage-shock protein E) of Escherichia coli is a rhodanese. *FEBS Lett.* **518**(1-3):173-6.

Alonso-Moraga A, Bocanegra A, Torres JM, López-Barea J, Pueyo C. 1987. Glutathione status and sensitivity to GSH-reacting compounds of Escherichia coli strains deficient in glutathione metabolism and/or catalase activity. *Mol Cell Biochem.* **73**(1):61-8.

Alphey MS, Williams RA, Mottram JC, Coombs GH, Hunter WN. 2003. The crystal structure of Leishmania major 3-mercaptopyruvate sulfurtransferase. A three-domain architecture with a serine protease-like triad at the active site. *J Biol Chem.* **278**(48):48219-27.

Beinert, H. 2000. A tribute to sulfur. *Eur.J.Biochem* 267:5657-5664.

Bishop PE and Brill WJ. 1977. Genetic analysis of *Azotobacter vinelandii* mutant strain enable to fix nitrogen, *Journal of Bacteriology* **130**: 954-956.

Bligh EG, Dyer WJ. 1959. A rapid method of total lipid extraction and purification. *Can J Biochem Physiol.* **37**(8):911-7

Bordo D, Deriu D, Colnaghi R, Carpen A, Pagani S, Bolognesi M. 2000. The crystal structure of a sulfurtransferase from Azotobacter vinelandii highlights the evolutionary relationship between the rhodanese and phosphatase enzyme families. *J Mol Biol.* **298**(4):691-704.

Bordo D, Forlani F, Spallarossa A, Colnaghi R, Carpen A, Bolognesi M, Pagani S. 2001. A persulfurated cysteine promotes active site reactivity in Azotobacter vinelandii Rhodanese. *Biol Chem.* **382**(8):1245-52.

Bordo, D. and P. Bork. 2002. The rhodanese/Cdc25 phosphatase superfamily: Sequence-structure function relations. *EMBO* Rep. **3**:741-746

Brosnan JT, Brosnan ME. 2006. The sulfur-containing amino acids: an overview. *J Nutr.* **136**(6 Suppl):1636S-1640S.

Brown WH. 2000. Introduction to organic chemistry: 2nd edition. *Harcourt Brace and Company.*.

Bsat N, Chen L, Helmann JD. 1996. Mutation of the Bacillus subtilis alkyl hydroperoxide reductase (ahpCF) operon reveals compensatory interactions among hydrogen peroxide stress genes. *J Bacteriol.* **178**(22):6579-86.

Bsat, N., A. Herbig, L. Casillas-Martinez, P. Setlow, and J. D. Helmann. 1998. *Bacillus subtilis* contains multiple Fur homologues: identification of the iron uptake (Fur) and peroxide regulon (PerR) repressors. *Mol. Microbiol.* **29:**1 89–198.

Carlioz A, Touati D. 1986. Isolation of superoxide dismutase mutants in Escherichia coli: is superoxide dismutase necessary for aerobic life?. *EMBO J*. **5**(3):623-30.

Cartini F, Remelli W, Dos Santos PC, Papenbrock J, Pagani S, Forlani F. 2011. Mobilization of sulfane sulfur from cysteine desulfurases to the Azotobacter vinelandii sulfurtransferase RhdA. *Amino Acids.* **41**(1):141-50.

Casillas-Martinez L, Setlow P. 1997. Alkyl hydroperoxide reductase, catalase, MrgA, and superoxide dismutase are not involved in resistance of Bacillus subtilis spores to heat or oxidizing agents. *J Bacteriol*. **179**(23):7420-5.

Cereda A, Carpen A, Picariello G, Tedeschi G, Pagani S. 2009. The lack of rhodanese RhdA affects the sensitivity of Azotobacter vinelandii to oxidative events. *Biochem J.* **418**(1):135-43.

Cereda A, Forlani F, Iametti S, Bernhardt R, Ferranti P, Picariello G, Pagani S and Bonomi F. 2003. Molecular recognition between Azotobacter vinelandii rhodanese and a sulfur acceptor protein. *Biol. Chem.* **384**: 1473-1481.

Cereda A., Carpen A., Picariello G., Tedeschi G, and Pagani S., (2009) The lack of rhodanese RhdA affects the sensitivity of Azotobacter vinelandii to oxidative events, *Biochem. J. 418:* 135-143

Christman MF, Morgan RW, Jacobson FS, Ames BN. 1985. Positive control of a regulon for defenses against oxidative stress and some heat-shock proteins in Salmonella typhimurium. *Cell*. **41**(3):753-62.

Collado-Vides J. 1993. A linguistic representation of the regulation of transcription initiation. II. Distinctive features of sigma 70 promoters and their regulatory binding sites. *Biosystems.* **29**(2-3):105-28.

Collins HL., 2003. The role of Iron in infections with intracellular bacteria. *Immunology Letters.* **85**:193-195.

Colnaghi R, Pagani S, Kennedy C and Drummond M. Cloning, sequence analysis and overexpression of the rhodanese gene of *Azotobacter vinelandii*. *European Journal of Biochemistry* 236: 240-248, (1996).

Cooper, A. J. 1983. Biochemistry of sulfur-containing amino acids. *Annu.Rev.Biochem* **52:**187-222:187-222.

Cupp-Vickery, J. R., H. Urbina, and L. E. Vickery. 2003. Crystal structure of IscS, a cysteine desulfurase from *Escherichia coli*. *J.Mol Biol.* **330**:1049-1059

delCardayre SB, Davies JE. 1998. Staphylococcus aureus coenzyme A disulfide reductase, a new subfamily of pyridine nucleotide-disulfide oxidoreductase. Sequence, expression, and analysis of cdr. *J Biol Chem.* **273**(10):5752-7.

Ding H, Demple B. 1997. In vivo kinetics of a redox-regulated transcriptional switch. *Proc Natl Acad Sci U S A.* **94**(16):8445-9.

Doke N, Miura Y, Sanchez LM, Park HJ, Noritake T, Yoshioka H, Kawakita K. 1996. The oxidative burst protects plants against pathogen attack: mechanism and role as an emergency signal for plant bio-defence--a review. *Gene.* **179**(1):45-51.

Fahey RC, Brown WC, Adams WB, Worsham MB. 1978. Occurrence of glutathione in bacteria. *J Bacteriol.* **133**(3):1126-9.

Fauman EB, Cogswell JP, Lovejoy B, Rocque WJ, Holmes W, Montana VG, Piwnica-Worms H, Rink MJ, Saper MA. 1998. Crystal structure of the catalytic domain of the human cell cycle control phosphatase, Cdc25A. *Cell.* **93**(4):617-25.

Fauman, E. B., J. P. Cogswell, B. Lovejoy, W. J. Rocque, W. Holmes, V. G. Montana, H. Piwnica-Worms, M. J. Rink, and M. A. Saper. 1998. Crystal structure of the catalytic domain ofthe human cell cycle control phosphatase, Cdc25A. *Cell* **93**:617-625.

Flint DH, Tuminello JF, Emptage MH. 1993. The inactivation of Fe-S cluster containing hydro-lyases by superoxide. *J Biol Chem*. **268**(30):22369-76.

Forlani F, Carpen A, Pagani S. 2003. Evidence that elongation of the catalytic loop of the Azotobacter vinelandii rhodanese changed selectivity from sulphur- to phosphate-containing substrates. *Prot. Eng.* **16**: 1-5.

Forlani F, Cereda A, Freuer A, Nimtz M, Leimkühler S, Pagani S. 2005. The cysteine-desulfurase IscS promotes the production of the rhodanese RhdA in the persulfurated form. *FEBS Lett*. **579**: 6786-6790.

Frazzon, J., J. R. Fick, and D. R. Dean. 2002. Biosynthesis of iron-sulphur clusters is a complex and highly conserved process. *Biochem.Soc.Trans*. **30**:680-685.

Fuanthong M., Herbig A.F., Bsat N., and Helmann J.D. 2002. Regulation of the *Bacillus subtilis fur* and *perR* Genes by PerR: Not All Members of the PerR Regulon Are Peroxide Inducible. *J. Bacteriol*. **184** (12): 3276-328

Gaballa A, Newton GL, Antelmann H, Parsonage D, Upton H, Rawat M, Claiborne A, Fahey RC, Helmann JD. 2010. Biosynthesis and functions of bacillithiol, a major low-molecular-weight thiol in Bacilli. *Proc Natl Acad Sci U S A.* **107**(14):6482-6.

Gliubich F, Gazerro M, Zanotti G, Delbono S, Bombieri G, Berni R. 1996. Active site structural features for chemically modified forms of rhodanese. *J Biol Chem.* **271**(35):21054-61.

Griffiths G, Leverentz M, Silkowski H, Gill N, Sánchez-Serrano JJ. 2000. Lipid hydroperoxide levels in plant tissues. *J Exp Bot.***51**(349):1363-70.

Haddock BA, Jones CW. 1977. Bacterial Respiration. *Bacteriol Rev.* **41**(1):47-99.

Halliwell B., Gutteridge J. M.C., Oxygen toxicity, Oxigen Radicals, transition metals and desease; *Biochem. J. 219:* 1-14 (1984)

Hassan HM, Fridovich I. 1977. Regulation of the synthesis of superoxide dismutase in Escherichia coli. Induction by methyl viologen. *J Biol Chem.* **252**(21):7667-72

Helmann JD, Wu MF, Gaballa A, Kobel PA, Morshedi MM, Fawcett P, Paddon C. 2003 The global transcriptional response of Bacillus subtilis to peroxide stress is coordinated by three transcription factors. *J Bacteriol.*; 185(1):243-53.

Henle ES, Han Z, Tang N, Rai P, Luo Y, Linn S. 1999. Sequence-specific DNA cleavage by Fe2+-mediated fenton reactions has possible biological implications. *J Biol Chem*. **274**(2):962-71.

Hildebrandt TM, Grieshaber MK. 2008. Three enzymatic activities catalyze the oxidation of sulfide to thiosulfate in mammalian and invertebrate mitochondria. *FEBS J.* **275**(13):3352-61.

Hillar A, Peters B, Pauls R, Loboda A, Zhang H, Mauk AG, Loewen PC. 2000. Modulation of the activities of catalase-peroxidase HPI of Escherichia coli by site-directed mutagenesis. *Biochemistry*. **39**(19):5868-75.

Hofstetter D, Nauser T, Koppenol WH. 2010. Hydrogen Exchange Equilibria in Glutathione Radicals: Rate Constants. *Chem Res Toxicol.* Sep 30. [Epub ahead of print]

Holtzhauer M. 2006. Basic methods for the biochemical lab: First English edition. *Springer Berlin Heidelberg*, New York

Horowitz PM, Bowman S. 1989. Oxidative inactivation of rhodanese by hydrogen peroxide produces states that show differential reactivation. *J Biol Chem*. **264**(6):3311-6.

Huang YF, Huang YH. 2009. Behavioral evidence of the dominant radicals and intermediates involved in bisphenol A degradation using an efficient Co2+/PMS oxidation process. *J Hazard Mater*. **167**(1-3):418-26.

Iciek, M. and L. Wlodek. 2001. Biosynthesis and biological properties of compounds containing highly reactive, reduced sulfane sulfur. *Pol.J.Pharmacol*. **53**:215-225

Jacobson, M. R., V. L. Cash, M. C. Weiss, N. F. Laird, W. E. Newton, and D. R. Dean. 1989. Biochemical and genetic analysis of the *nifUSVWZM* cluster from *Azotobacter vinelandii. Mol.Gen.Genet*. **219**:49-57.

Jang S, Imlay JA. 2007. Micromolar intracellular hydrogen peroxide disrupts metabolism by damaging iron-sulfur enzymes. *J Biol Chem*. **282**(2):929-37.

Jung CH, Thomas JA. 1996. S-glutathiolated hepatocyte proteins and insulin disulfides as substrates for reduction by glutaredoxin, thioredoxin, protein disulfide isomerase, and glutathione. *Arch Biochem Biophys.* **335**(1):61-72.

Kambampati R, Lauhon CT. 2000. Evidence for the transfer of sulfane sulfur from IscS to ThiI during the in vitro biosynthesis of 4-thiouridine in Escherichia coli tRNA. *J. Biol. Chem.* **275**(15):10727-30

Keyer K, Imlay JA. 1996. Superoxide accelerates DNA damage by elevating free-iron levels. *Proc Natl Acad Sci U S A*. **93**(24):13635-40.

Kim SO, Merchant K, Nudelman R, Beyer WF Jr, Keng T, DeAngelo J, Hausladen A, Stamler JS. 2002. OxyR: a molecular code for redox-related signaling. *Cell.* **109**(3):383-96.

Klatt P, Lamas S. 2000. Regulation of protein function by S-glutathiolation in response to oxidative and nitrosative stress. *Eur J Biochem.* **267**(16):4928-44.

Klodmann, J., Sunderhaus, S., Nimtz, M., Jänsch, L., Braun, H.P., 2010. Internal architecture of mitochondrial complex I from Arabidopsis thaliana. *Plant Cell* **22**, 797-810

Korshunov S, Imlay JA. 2006. Detection and quantification of superoxide formed within the periplasm of Escherichia coli. *J Bacteriol.* **188**(17):6326-34.

Kosower NS, Kosower EM. 1978. The glutathione status of cells. *Int Rev Cytol*. **54**:109-60.

Kovaleva GY., Gelfand MS. 2007. Transcriptional regulation of the methionine and cysteine transport and metabolism in streptococci. *FEMS Microbiol Lett.* 276(2):207-15.

Kunst F., Ogasawara N., Moszer I., Albertini A.M., Alloni G., Azevedo V., Bertero M.G., Bessieres P., Bolotin A., Borchert S., Borriss R., Boursier L., Brans A., Braun M., Brignell S.C., Bron S., Brouillet S., Bruschi C.V. Danchin A. (1997) ;The complete genome sequence of the Gram-positive bacterium *Bacillus subtilis*; *Nature* 390:249-256

Lauhon, C. T. and R. Kambampati. 2000. The *iscS* gene in *Escherichia coli* is required for the biosynthesis of 4-thiouridine, thiamin, and NAD. *J.Biol.Chem.* **275**:20096-20103.

Leammli U.K., 1970. Cleavage of structural proteins during the assembly of the head of bacteriophage T4. *Nature*. **227**. 680-685

Lee JW, Helmann JD. 2006. The PerR transcription factor senses H2O2 by metal-catalysed histidine oxidation. *Nature*. **440**(7082):363-7.

Ligeza A,Tikhonov AN, Hyde JS, SubczynskiWK. 1998. Oxygen permeability of thylakoid membranes: electron paramagnetic resonance spin labeling study.*Biochim. Biophys. Acta* **1365**:453–63

Livak K.J., Schmittgen T.D. (2001). Analysis of Relative Gene Expression Data Using Real-Time Quantitative PCR and the $2^{-\Delta\Delta C}{}_T$ Method. *Methods* 25, 402–408.

Loewen PC. 1979. Levels of glutathione in Escherichia coli. *Can J Biochem*. **57**(2):107-11.

Luo G and Horowitz PM. 1994. The sulfurtransferase activity and structure of rhodanese are affected by site-directed replacement of Arg-186 or Lys-249. *J. Biol. Chem.* **269:** 8220-8225.

Lynch RE, Fridovich I. 1978. Permeation of the erythrocyte stroma by superoxide radical. *J Biol Chem.* **253**(13):4697-9.

Massey V, Strickland S, Mayhew SG, Howell LG, Engel PC, Matthews RG, Schuman M, Sullivan PA. 1969. The production of superoxide anion radicals in the reaction of reduced flavins and flavoproteins with molecular oxygen. *Biochem Biophys Res Commun*. **36**(6):891-7**.**

Matthies A, Rajagopalan KV, Mendel RR, Leimkühler S. 2004. Evidence for the physiological role of a rhodanese-like protein for the biosynthesis of the molybdenum cofactor in humans. *Proc Natl Acad Sci U S A.* **101**(16):5946-51.

Mihara, H. and N. Esaki. 2002. Bacterial cysteine desulfurases: their function and mechanisms. *Appl.Microbiol.Biotechnol*. **60**:12-23.

Miranda-Vizuete A, Rodríguez-Ariza A, Toribio F, Holmgren A, López-Barea J, Pueyo C. 1996. The levels of ribonucleotide reductase, thioredoxin, glutaredoxin 1, and GSH are balanced in Escherichia coli K12. *J Biol Chem.* **271**(32):19099-103.

Mueller EG. 2006. Trafficking in persulfides: delivering sulfur in biosynthetic pathways. *Nature Chem. Biol.* **4**: 185-194.

Muller A; Krebs B., 1984. Sulfur: Its Significance for Chemistry, for the *Geo-*, *Bio-*, *and Cosmosphere and Technology*. Elsevier Science Publishers, Amsterdam, New York.

Murphy P, Dowds BC, McConnell DJ, Devine KM. 1987. Oxidative stress and growth temperature in Bacillus subtilis. *J Bacteriol.*, **169(12)**:5766-70.

Nachin L, Loiseau L, Expert D, Barras F. SufC: an unorthodox cytoplasmic ABC/ATPase required for [Fe-S] biogenesis under oxidative stress. *The EMBO Journal* 22: 427-437, (2003)

Nagahara N, Ito T, Minami M. 1999. Mercaptopyruvate sulfurtransferase as a defense against cyanide toxication: molecular properties and mode of detoxification. *Histol Histopathol.* **14**(4):1277-86.

Nagahara N, Katayama A. 2005. Post-translational regulation of mercaptopyruvate sulfurtransferase via a low redox potential cysteine-sulfenate in the maintenance of redox homeostasis. *J Biol Chem.* **280**(41):34569-76.

Nagahara N, Nishino T. 1996. Role of amino acid residues in the active site of rat liver mercaptopyruvate sulfurtransferase. CDNA cloning, overexpression, and site-directed mutagenesis. *J Biol Chem.* **271**(44):27395-401.

Nagahara N, Okazaki T, Nishino T. 1995. Cytosolic mercaptopyruvate sulfurtransferase is evolutionarily related to mitochondrial rhodanese. Striking similarity in active site amino acid sequence and the increase in the mercaptopyruvate sulfurtransferase activity of rhodanese by site-directed mutagenesis. *J Biol Chem.* 1995 **270**(27):16230-5.

Nandi DL, Horowitz PM, Westley J. 2000. Rhodanese as a thioredoxin oxidase. *Int J Biochem Cell Biol.* **32**(4):465-73.

Nandi DL, Westley J. 1998. Reduced thioredoxin as a sulfur-acceptor substrate for rhodanese. *Int J Biochem Cell Biol.* **30**(9):973-7.

Newton GL, Arnold K, Price MS, Sherrill C, Delcardayre SB, Aharonowitz Y, Cohen G, Davies J, Fahey RC, Davis C. 1996. Distribution of thiols in microorganisms: mycothiol is a major thiol in most actinomycetes. *J Bacteriol.* **178**(7):1990-5.

Newton GL, Bewley CA, Dwyer TJ, Horn R, Aharonowitz Y, Cohen G, Davies J, Faulkner DJ, Fahey RC. 1995. The structure of U17 isolated from Streptomyces clavuligerus and its properties as an antioxidant thiol. *Eur J Biochem*. **230**(2):821-5

Newton GL, Rawat M, La Clair JJ, Jothivasan VK, Budiarto T, Hamilton CJ, Claiborne A, Helmann JD, Fahey RC. 2009. Bacillithiol is an antioxidant thiol produced in Bacilli. *Nat Chem Biol*. **5**(9):625-7.

Newton J. W., Wilson P. W. and Burris R.H., 1953. Direct determination in of ammonia as an intermediate of nitrogen fixation by Azotobacter *J. Biol. Chem* **204**, 445-451

Nishida M, Kong KH, Inoue H, Takahashi K. 1994. Molecular cloning and site-directed mutagenesis of glutathione S-transferase from Escherichia coli. The conserved tyrosyl residue near the N terminus is not essential for catalysis. *J Biol Chem.* **269**(51):32536-41.

Pagani S, Forlani F, Carpen A, Bordo D and Colnaghi R. 2000. Mutagenic analysis of Thr-232 in rhodanese from Azotobacter vinelandii highlighted the differences of this prokaryotic enzyme from the known sulfurtransferases. *FEBS Lett.* **472**: 307-311.

Palenchar PM, Buck CJ, Cheng H, Larson TJ, Mueller EG. 2000. Evidence that ThiI, an enzyme shared between thiamin and 4-thiouridine biosynthesis, may be a sulfurtransferase that proceeds through a persulfide intermediate. *J Biol Chem.* **275**(12):8283-6.

Papenbrock J, Schmidt A. 2000. Characterization of two sulfurtransferase isozymes from Arabidopsis thaliana. *Eur J Biochem.* **267**(17):5571-9.

Park S, Imlay JA. 2003. High levels of intracellular cysteine promote oxidative DNA damage by driving the fenton reaction. *J Bacteriol.* **185**(6):1942-50

Parsonage D, Youngblood DS, Sarma GN, Wood ZA, Karplus PA, Poole LB. 2005. Analysis of the link between enzymatic activity and oligomeric state in AhpC, a bacterial peroxiredoxin. *Biochemistry*. **44**(31):10583-92.

Perito B, Allocati N, Casalone E, Masulli M, Dragani B, Polsinelli M, Aceto A, Di Ilio C. 1996. Molecular cloning and overexpression of a glutathione transferase gene from Proteus mirabilis. *Biochem J.* **318** (Pt 1):157-62.

Ploegman JH, Drent G, Kalk KH, Hol WG. 1978. Structure of bovine liver rhodanese. I. Structure determination at 2.5 A resolution and a comparison of the conformation and sequence of its two domains. *J Mol Biol.* **123**(4):557-94.

Ploegman JH, Drent G, Kalk KH, Hol WG. 1979. The structure of bovine liver rhodanese. II. The active site in the sulfur-substituted and the sulfur-free enzyme. *J Mol Biol.* **127**(2):149-62.

Plumbridge J., 2001. DNA binding sites for the Mlc and NagC proteins: regulation of *nagE*, encoding the *N*-acetylglucosamine-specific transporter in Escherichia coli. *Nucleic Acids Res*; 29(2): 506–514.

Pohl S, Tu WY, Aldridge PD, Gillespie C, Hahne H, Mäder U, Read TD, Harwood CR. 2011. Combined proteomic and transcriptomic analysis of the response of Bacillus anthracis to oxidative stress. *Proteomics*. **11**(15):3036-55.

Pomposiello PJ, Bennik MH, Demple B. 2001. Genome-wide transcriptional profiling of the Escherichia coli responses to superoxide stress and sodium salicylate. *J Bacteriol.* **183**(13):3890-902.

Quintiliani M, Badiello R, Tamba M, Esfandi A, Gorin G. 1977. Radiolysis of glutathione in oxygen-containing solutions of pH7. *Int J Radiat Biol Relat Stud Phys Chem Med.* **32**(2):195-202.

Ray WK, Zeng G, Potters MB, Mansuri AM, Larson TJ. 2000. Characterization of a 12-kilodalton rhodanese encoded by glpE of Escherichia coli and its interaction with thioredoxin. *J Bacteriol.* **182**(8):2277-84.

Reynolds RA, Yem AW, Wolfe CL, Deibel MR Jr, Chidester CG and Watenpaugh KD. 1999. Crystal structure of the catalytic subunit of Cdc25B required for G2/M phase transition of the cell cycle. *J. Mol. Biol.* **293**: 559–568.

Roy, A. B. and P. A. Trudinger. 1970. The chemistry of some sulfur compounds, p. 7-42. *In* The Biochemistry of Inorganic Compounds of Sulfur. Cambridge University Press.

Saas J, Ziegelbauer K, von Haeseler A, Fast B, Boshart M. 2000. A developmentally regulated aconitase related to iron-regulatory protein-1 is localized in the cytoplasm and in the mitochondrion of Trypanosoma brucei. *J Biol Chem.* **275**(4):2745-55.

Sakuda S, Zhou ZY, Yamada Y. 1994. Structure of a novel disulfide of 2-(N-acetylcysteinyl)amido-2-deoxy-alpha-D-glucopyranosyl-myo-inositol produced by Streptomyces sp.. *Biosci Biotechnol Biochem.* **58**(7):1347-8.

Sambrock J, Fritsch EF and Maniatis T. Molecular cloning: a laboratory manual, *Cold Spring Harbour Laboratory Press*, 2nd edition ed., (1989).

Schafer FQ, Buettner GR. 2001. Redox environment of the cell as viewed through the redox state of the glutathione disulfide/glutathione couple. *Free Radic Biol Med.* **30**(11):1191-212.

Seaver LC, Imlay JA. 2001. Hydrogen peroxide fluxes and compartmentalization inside growing Escherichia coli. *J Bacteriol.* **183**(24):7182-9.

Segal AW, Abo A. 1993. The biochemical basis of the NADPH oxidase of phagocytes. *Trends Biochem Sci.* **18**(2):43-7.

Sipe HJ Jr, Corbett JT, Mason RP. 1997. In vitro free radical metabolism of phenolphthalein by peroxidases. *Drug Metab Dispos.* **25**(4):468-80.

Smirnova GV, Muzyka NG, Glukhovchenko MN, Oktyabrsky ON. 2000. Effects of menadione and hydrogen peroxide on glutathione status in growing Escherichia coli. *Free Radic Biol Med.* **28**(7):1009-16.

Sorbo BH; Lagerkvist, Ulf; Pesola, Rainer; Virtanen, Artturi I.; Sörensen, Nils Andreas (1953). "Crystalline rhodanese. II. The enzyme catalyzed reaction". *Acta Chem. Scand.* **7**: 1137–1145.

Spallarossa A, Donahue JL, Larson TJ, Bolognesi M, Bordo D. 2001. Escherichia coli GlpE is a prototype sulfurtransferase for the single-domain rhodanese homology superfamily. *Structure* **9**(11):1117-25.

Spallarossa A, Forlani F, Carpen A, Armirotti A, Pagani S, Bolognesi M, Bordo D. 2004. The "rhodanese" fold and catalytic mechanism of 3-mercaptopyruvate sulfurtransferases: crystal structure of SseA from Escherichia coli. *J Mol Biol.* **335**(2):583-93.

Spies, H. S. C., and D. J. Steenkamp. 1994. Thiols of intracellular pathogens. Identification of ovothiol A in *Leishmania donovani* and structural analysis of a novel thiol from *Mycobacterium bovis*. *Eur. J. Biochem*. **224**:203–213.

Starke DW, Chock PB, Mieyal JJ. 2003. Glutathione-thiyl radical scavenging and transferase properties of human glutaredoxin (thioltransferase). Potential role in redox signal transduction. *J Biol Chem.* **278**(17):14607-13.

Studier FW, Rosenberg AH, Dunn JJ and Dubendorff JW.1990. Use of T7 RNA polymerase to direct expression of cloned genes. *Methods Enzymology* **185**: 60-89.

Sundaram, S. G. and J. A. Milner. 1996. Diallyl disulfide inhibits the proliferation of human tumor cells in culture. *Biochim.Biophys.Acta* **1315**:15-20.

Szczepkowski, T. W. and J. L. Wood. 1967. The cystathionase-rhodanese system. *Biochim.Biophys.Acta* **139**:469-478.

Toohey, J. I. 1989. Sulphane sulphur in biological systems: a possible regulatory role. *Biochem J*. **264**:625-632.

Vennesland, B., P. A. Castric, E. E. Conn, L. P. Solomonson, M. Volini, and J. Westley. 1982. Cyanide metabolism. *Fed.Proc.* **41**:2639-2648

Vuilleumier S. 1997. Bacterial glutathione S-transferases: what are they good for?. *J Bacteriol.* **179**(5):1431-41.

Wang G, Conover RC, Benoit S, Olczak AA, Olson JW, Johnson MK, Maier RJ. 2004. Role of a bacterial organic hydroperoxide detoxification system in preventing catalase inactivation. *J Biol Chem.* 279(50):51908-14. Epub 2004 Sep 28.

Wang Ge, Conover R., Benoit S, Olczak A., Olson J. W., Johnson M. K., Maier R. J.; Role of Bacteria Organic Hydroperoxides Detoxification System in preventing Catalase Inactivation; *The Journal of Biological Chemistry 279*: 50; 51908-51914 (2004)

Wardman P, von Sonntag C. 1995. Kinetic factors that control the fate of thiyl radicals in cells. *Methods Enzymol.* **251**:31-45

Wardman P. 1995. Reactions of thiyl radicals. In: Packer L, Cadenas E (eds) Biothiols in Health and Disease. Marcel Dekker Inc., New York, pp 1-19

Westley J, Adler H, Westley L, Nishida C. 1983. The sulfurtransferases. *Fundam Appl Toxicol.* **3**(5):377-82.

Westley J. 1981. Thiosulfate: cyanide sulfurtransferase (rhodanese). *Methods Enzymol.* **77**:285-91.

Wientjes FB, Segal AW. 1995. NADPH oxidase and the respiratory burst. *Semin Cell Biol.* 1995 **6**(6):357-65.

Williams RA, Kelly SM, Mottram JC, Coombs GH. 2003. 3-Mercaptopyruvate sulfurtransferase of Leishmania contains an unusual C-terminal extension and is involved in thioredoxin and antioxidant metabolism. *J Biol Chem.* **278(**3):1480-6.

Winterbourn CC. 1993. Superoxide as an intracellular radical sink. *Free Radic Biol Med.* **14**(1):85-90.

Wolfe MD, Ahmed F, Lacourciere GM, Lauhon CT, Stadtman TC, Larson TJ. 2004. Functional diversity of the rhodanese homology domain: the Escherichia coli ybbB gene

encodes a selenophosphate-dependent tRNA 2-selenouridine synthase. *J Biol Chem.* **279**(3):1801-9.

Wolff S.P.. 1994**.** Ferrous ion oxidation in presence of ferric ion indicator xylenol orange for measurement of hydroperoxides. *Methods Enzymol.* 233 182-189.

Zheng M, Aslund F, Storz G. 1998. Activation of the OxyR transcription factor by reversible disulfide bond formation. *Science*., **279**(5357):1718-21.

Zheng, L., R. H. White, V. L. Cash, and D. R. Dean. 1994. Mechanism for the desulfurization of L-cysteine catalyzed by the *nifS* gene product. *Biochemistry* **33**:4714-4720

Zheng, L., R. H. White, V. L. Cash, R. F. Jack, and D. R. Dean. 1993. Cysteine desulfurase activity indicates a role for NIFS in metallocluster biosynthesis. Proc.Natl.Acad.Sci.U.S.A. **90**:2754-2758.

Zheng, L., V. L. Cash, D. H. Flint, and D. R. Dean. 1998. Assembly of iron-sulfur clusters. Identification of an *iscSUA-hscBA-fdx* gene cluster from *Azotobacter vinelandii*. *J.Biol.Chem.* **273**:13264-13272.

CHAPTER 9:

Scientific production

During my three year PhD program I actively partecipate to the following scientific productions:

Biol Chem. 2010 Jul;391(7):777-84.

The rhodanese RhdA helps Azotobacter vinelandii in maintaining cellular redox balance.

Remelli W, Cereda A, Papenbrock J, Forlani F, Pagani S.

Dipartimento di Scienze Molecolari Agroalimentari, Università degli Studi di Milano, I-20133 Milano, Italy.

Abstract

The tandem domain rhodanese-homology protein RhdA of Azotobacter vinelandii shows an active-site loop structure that confers structural peculiarity in the environment of its catalytic cysteine residue. The in vivo effects of the lack of RhdA were investigated using an A. vinelandii mutant strain (MV474) in which the rhdA gene was disrupted by deletion. Here, by combining analytical measurements and transcript profiles, we show that deletion of the rhdA gene generates an oxidative stress condition to which A. vinelandii responds by activating defensive mechanisms. In conditions of growth in the presence of the superoxide generator phenazine methosulfate, a stressor-dependent induction of rhdA gene expression was observed, thus highlighting that RhdA is important for A. vinelandii to sustain oxidative stress. The potential of RhdA to buffer general levels of oxidants in A. vinelandii cells via redox reactions involving its cysteine thiol is discussed.

Amino Acids. 2011 Jun;41(1):141-50

Mobilization of sulfane sulfur from cysteine desulfurases to the Azotobacter vinelandii sulfurtransferase RhdA.

Cartini F, Remelli W, Dos Santos PC, Papenbrock J, Pagani S, Forlani F.

Dipartimento di Scienze Molecolari Agroalimentari, Università degli Studi di Milano, I-20133 Milano, Italy.

Abstract

Mobilization of the L-cysteine sulfur for the persulfuration of the rhodanese of Azotobacter vinelandii, RhdA, can be mediated by the A. vinelandii cysteine desulfurases, IscS and NifS. The amount of cysteine was higher in mutant strains lacking rhdA (MV474) than in wild type. The diazotrophic growth of MV474 was impaired. Taking into account the functional results about rhodanese-like proteins and RhdA itself, it is suggested that RhdA-dependent modulation of L-cysteine levels must deal with a redox-related process.

Environ Microbiol. 2011 Dec 19. doi: 10.1111/j.1462-2920.2011.02678.x.

Altered expression level of Escherichia coli proteins in response to treatment with the antifouling agent zosteric acid sodium salt.

Villa F, Remelli W, Forlani F, Vitali A, Cappitelli F.

Dipartimento di Scienze e Tecnologie Alimentari e Microbiologiche, Università degli Studi di Milano, via Celoria 2, 20133 Milano, Italy Dipartimento di Scienze Molecolari Agroalimentari, Università degli Studi di Milano, via Celoria 2, 20133 Milano, Italy Istituto di Chimica del Riconoscimento Molecolare, Consiglio Nazionale delle Ricerche, c/o Istituto Biochimica e Biochimica Clinica, Università Cattolica, L.go F. Vito, 1, 00168 Roma, Italy.

Abstract

Zosteric acid sodium salt is a powerful antifouling agent. However, the mode of its antifouling action has not yet been fully elucidated. Whole cell proteome of Escherichia coli was analysed to study the different protein patterns expressed by the surface-exposed planktonic cells without and with sublethal concentrations of the zosteric acid sodium salt. Proteomic analysis revealed that at least 27 proteins showed a significant (19 upregulated and 8 downregulated, P<0.001) altered expression level in response to the antifoulant. The proteomic signatures of zosteric acid sodium salt-treated cells are characterized by stress-associated (e.g. AhpC, OsmC, SodB, GroES, IscU, DnaK), motility-related (FliC), quorum-sensing-associated (LuxS) and metabolism/biosynthesis-related (e.g. PptA, AroA, FabD, FabB, GapA) proteins. Consistent with the overexpression of LuxS enzyme, the antifouling agent increased autoinducer-2 (AI-2) concentration by twofold. Moreover, treated cells experienced a statistically significant 23%), tryptophanase but modest increase of reactive oxygen species + (1.2-fold) and indole (1.2-fold) synthesis. Overall, our data suggest that zosteric acid sodium salt acts as environmental cue leading to coli cells, which favours the expression of various global stress on *E. coli* protective proteins, the AI-2 production and the synthesis of flagella, to escape from adverse conditions.

Furthermore I participate to the following national and international meetings producing both abstracts and posters/oral speaches:

11th International Congress on Amino Acids, Peptides and Proteins
Vienna, Austria August 3–7, 2009

Searching for a functional role of the Azotobacter vinelandii sulfurtransferase RhdA: from sulfur delivery protein to ‘‘antioxidant’’ protein

Fabio Forlani, Angelo Cereda, William Remelli, and Silvia Pagani
Dipartimento di Scienze Molecolari Agroalimentari, Universita` di Milano, Via Celoria 2, 20133 Milano, Italy

Abstract

The ubiquitous rhodanese-domain proteins *in vitro* catalyse the transfer of a sulfur atom from a suitable sulfur donor (thiosulfate for rhodaneses, 3-mercaptopyruvate for 3-mercaptopyruvate sulfurtransferases) to cyanide, with concomitant formation of thiocyanate. The wide distribution of these proteins (PFAM acc. no.: PF00581), along with the presence of paralogs in the majority of organisms, corroborate the hypothesis that they evolved distinct physiological functions. In *Azotobacter vinelandii* the tandem-domain rhodanese RhdA contains an active-site motif (HCQTHHR) that supports the stabilization of the persulfurated form (RhdA-SSH). The *A. vinelandii* cysteine desulfurases, IscS and NifS, can *in vitro* mediate the production of RhdA-SSH, in the presence of free L-cysteine as substrate, thus making interesting investigations on the role of the sulfane sulfur bound to RhdA-SSH in driving its *in vivo* functions. Moreover, the picture that has emerged from the phenotypic characterization of an *A. vinelandii* RhdA null mutant strain indicated that RhdA might trigger protection to oxidative events since the lack of RhdA led to an increased amount of reactive oxygen species (ROS), and growth impairment in the presence of a chemical oxidant (phenazine methosulfate).

54th National congress SIB
Catania, Italy, September 23-27, 2009

Effects of the lack of rhodanese RhdA in Azotobacter vinelandii

William Remelli[1], Jutta Papenbrock[2], Silvia Pagani[1], and Fabio Forlani[1]
[1]DISMA, Università degli Studi di Milano, Milano, Italy.
[2]Institut für Botanik, Liebniz Universität, Hannover, Germany

Abstract

The rhodanese-like proteins *in vitro* catalyse the transfer of a sulfur atom from thiosulfate to cyanide, with formation of thiocyanate, but the wide distribution of these proteins corroborates the hypothesis that they evolved distinct physiological functions. Among the rhodanese-like proteins of *Azotobacter vinelandii*, RhdA contains an active-site motif not common found in other rhodaneses. Phenotypical characterisation of an *A. vinelandii* mutant strain in which *rhdA* was deleted evidenced inactivation of enzymes containing labile Fe-S. In the present work, further characterization of the mutant strain revealed that glutathione was significantly lower in the mutant compared to that of the wild-type strain, in line with the increased general levels of reactive oxygen species found in the mutant strain. Moreover, we found that the expression of *ahpC*, a member of the OxyR regulon, was significantly induced in the mutant strain. These results provided experimental evidence that an internal oxidative stress problem occurred in *A. vinelandii* cells lacking RhdA, thus corroborating the hypothesis that RhdA has a role in maintaining cellular redox balance.

Annual meeting SIB- LLP 2010
Varese, Italy, May 28, 2010

In vitro oxidation of the RhdA catalytic residue (Cys_{230})

William Remelli, Nicoletta Guerrieri, Fabio Forlani and Silvia Pagani

Dipartimento di Scienze Molecolari Agroalimentari, Università degli Studi di Milano, via Celoria, 2, 20133, Milano, Italia @:william.remelli@unimi.it

Keywords: Rhodanese, oxidative stress

INTRODUCTION

Protein belonging to the "rhodanese-like" superfamily (Pfam Acc. N.:PF00581) are distributed and redundant in all evolutionary phyla. Their physiological functions are not completely understood, but recent studies have associated these proteins to the managing of redox homeostasis.
Azotobacter vinelandii possesses 11 ORFs coding for "rhodanese-like" proteins. The tandem domain "rhodanese-like" protein RhdA shows peculiar characteristic among the rhodaneses of *A. vinelandii*: the electropositive environment near the active site region helps the stabilization of the thiolate anion on the catalytic cysteine residue (Cys_{230}), the only one present in this protein (1).
Previous work correlated the expression of RhdA to the defense against stressful conditions (2). In particular the absence of RhdA lead *A. vinelandii* to the depletion of the total glutathione pool and the activation of the peroxide response system (3). In this work, in order to study the redox reactivity of Cys_{230} in relation to the *in vivo* function of the *A. vinelandii* "rhodanese-like" protein RhdA, we treated the RhdA Cys_{230} residue with different sulfur metabolites (thiosulfate and reduced glutathione) and tested its proficiency to be oxidized by the superoxide generator phenazine methosulfate (PMS).

RESULTS

Fluorescence and rhodanese activity assays showed that RhdA in both thiolic ($RhdA\text{-}S^-$) and persulfurated ($RhdA\text{-}S\text{-}S^-$) RhdA forms was very susceptible to PMS oxidation. Persulfurated RhdA underwent to oxidation that can be mostly reverted by a reducing treatment, whereas the PMS-oxidized $RhdA\text{-}S^-$ cannot. Furthermore, RhdA interacts with glutathione, and gluthatione-complexed RhdA (RhdA-S-SG) is unaffected by PMS treatment. This evidence suggest that in both, $RhdA\text{-}S\text{-}S^-$ and RhdA-S-SG forms Cys_{230} residue is not accessible to the oxidizing agent. These data allow us to hypothesize that "rhodanese-like" protein RhdA could be directly involved in the oxidative stress response system. In particular, reversible oxidation of persulfurated RhdA, together with the RhdA ability to interact with thioredoxin (3), is in line with other oxidative stress protection mechanisms proposed for "rhodanese-like" proteins (4).

REFERENCES

(1) Bordo, D., *et al.* (2000) *J. Mol. Biol. 298*, 691-704
(2) Cereda, A., *et al.* (2009) *Biochem. J.* 418, 135-143
(3) Remelli, W., *et al.* (2010) *J. Biol. Chem.* 391, in press.
(4) Nagahara, N. *et al.* (2005) *J. Biol. Chem.* 280, 34569-34576

55th National congress SIB
Milano, Italy, September 14-17, 2010

The *Azotobacter vinelandii* rhodanese RhdA catalyze production of reduced gluthatione using gluthathione thyil radical as substrate

Remelli William[1], Papenbrock Jutta[2], Guerrieri Nicoletta[1], Forlani Fabio[1] and Pagani Silvia[1]

[1]DiSMA, Università degli Studi di Milano, Milano, Italia [2]Institut für Botanik, Liebniz Universität, Hannover, Germany

Protein belonging to the "rhodanese-like" superfamily are redundant in all evolutionary phyla. Their physiological functions are not completely understood, but recent studies have associated these proteins to the managing of redox homeostasis. The *Azotobacter vinelandii* tandem domain "rhodanese-like" protein RhdA has been biochemical characterized and shows peculiar characteristic: the electropositive environment near the active site helps the stabilization of complexes on the catalytic cysteine residue (Cys_{230}). The *in vitro* RhdA reaction is the sulfur transfer from thiosulfate to cyanide with the concomitant formation of thiocyanate but recent *in vivo* studies have evidenced equal levels of intracellular thiosulfate in both wild type and *rhdA* null mutant strains focusing the attention on other *in vivo* substrates. In this work we studied the ability of RhdA to restore reduced glutathione pool in oxidative stress conditions. In particular we have characterized the bind between RhdA and reduced glutathione together with the *in vivo* study on intracellular glutathione levels and the ability of RhdA to catalyze glutathione oxidation when this molecule is present as a thyil radical. Our data highlights an implication of RhdA in the managing of the intracellular glutathione pool recovering thyil radical glutathione form.

36th FEBS congress.

Torino, Italy, June 25-30, 2011

Involvement of the Azotobacter vinelandii rhodanese-like protein RhdA in the glutathione regeneration pathway.

William Remelli[1], Nicoletta Guerrieri[1], Jennifer Klodmann[2], Jutta Papenbrock[3], Hans-Peter Braun[2], Silvia Pagani[1] and Fabio Forlani[1]

[1]DiSMA, Università degli Studi di Milano, Milano, Italia

[2]Institut für Pflanzengenetik, Leibniz Universität, Hannover, Germany

[3]Institut für Botanik, Leibniz Universität, Hannover, Germany

@: william.remelli@unimi.it

Abstract

An increasing number of studies correlated the expression of rhodanese-like proteins to the management of cellular redox homeostasis. In *Azotobacter vinelandii*, the absence of the rhodanese-like protein RhdA results in an impaired redox condition and in the activation of the OxyR-regulon mediated response. Moreover, the finding that in the RhdA-null mutant the glutathione pool was depleted and glutathione precursors were accumulated suggested an impairment in the regeneration pathway of reduced glutathione (GSH). In the presence of hydroxyl radical (OH*), GSH is oxidized to glutathione thiyl radical (GS*) which needs an enzymatic pathway to be recovered as glutathione disulfide (GSSG), a GSH-generable form. Proteins with a low-pKa cysteine residue (like in the case of RhdA) are good candidates to stabilize an adduct with GS* for enzymatic GSSG dependent recovery. In the present study, we found that RhdA was able to specifically bind both GSH and GS* *in vitro* with high affinity (K_d = μM range) and that RhdA-Cys_{230} residue was mandatory for the adduct formation. The RhdA/glutathione adduct was stable enough to be used as a substrate to produce GSSG (kcat = 628 s^{-1}), despite MS analyses did not reveal the formation of a covalent bond. The RhdA scavenging activity of GS* was O_2^- dependent suggesting that O_2 might be the final acceptor of the radical. The GS*-scavenging activity of RhdA supports the phenotype observed on the RhdA-null mutant defined in our previous studies, highlighting RhdA's key role as ROS-level mediator by preserving glutathione from irreversible oxidations induced by OH*.

1th International conference on microbial diversity (MD 2011)

Milano, Italy, October 26-28, 2011

Adaptive responses of *Azotobacter vinelandii* biofilm to oxidative stress: functional role of the rhodanese-like protein RhdA

VILLA Federica (1), REMELLI William (2), GUERRIERI Nicoletta (2), FORLANI Fabio (2), GAMBINO Michela (1), CAPPITELLI Francesca (1)*

(1) Dipartimento di Scienze e Tecnologie Alimentari e Microbiologiche, Facoltà di Agraria, Università degli Studi di Milano, Milan, Italy. (2) Dipartimento di Scienze Molecolari Agroalimentari, Facoltà di Agraria, Università degli Studi di Milano, Milan, Italy. * francesca.cappitelli@unimi.it

In both managed and natural soil system bacteria experience environmental stressors such as xenobiotics, temperature shock, changes in pH and osmolarity, water and oxygen limitation, as well as competition for nutrients. Plant-associated bacteria also encounter oxidative stress in the rhizosphere. Plant roots produce reactive oxygen species (ROS) in response to many stimuli and several studies implicate ROS in root development and in interactions between roots and microorganisms (Colburn-Clifford *et al.*, 2010). The nitrogen-fixing plant growth-promoting rhizobacterium (PGPR) *Azotobacter vinelandii* plays a key role in supporting and increasing plant health and growth. Thus, *A. vinelandii* is of interest for application in agriculture either as biofertiliser as well as for phytoremediation applications (Kennedy *et al.*, 2004). Rhizosphere colonization is a prerequisite for a successful plant-bacteria interaction and the evolutionary prospective on life in biofilm enhances the ability of rhizobacteria to adapt to the selective pressures of this complex and competitive environment.

A. vinelandii has long served as a model for biochemical and functional studies of the rhodanese RhdA that in vitro catalyzes the transfer of a sulfur atom from thiosulfate to cyanide with concurrent formation of thiocyanate, and belongs to the family of rhodanese-like proteins. Considering the fairly tight connection between biofilm formation and cellular response to various stresses including oxidative damage (Landini, 2009), the functionality of RhdA as a redox switch in planktonic cells (Remelli *et al.*, 2010), the redundancy and ubiquitary distribution of rhodanese-like proteins, a possible involvement of RhdA in biofilm genesis was postulated.

Consistent with this hypothesis, the present study investigated the adaptive response of *A. vinelandii* biofilm to oxidative stress by using a mutant strain, in which the *rhdA* gene was disrupted by deletion. The MV474 biofilm growth curve revealed that the lack of the antioxidant protein RhdA enhanced the ability of *A. vinelandii* to develop biofilm while the intracellular level of ROS decreased over time reaching the lower values in mature and late-stage biofilm. Particularly noteworthy was the observation that MV474 sustained a surface-associated movement resulting in a faster and efficient colonization of the polycarbonate membrane. Indeed, cryosectioning combined with microscopy revealed that MV474 biofilm was significantly thinner than the film formed by UW136 and the mutant strain of *A. vinelandii* synthesized a polysaccharide-rich extracellular polymer matrix. Developed biofilms of the wild-type and the mutant strains of *A. vinelandii* showed different protein profiles. Finally, we demonstrated that MV474 biofilm was less susceptible to biocide activities than UW136 biofilm. Likely, the deletion of the *rhdA* gene exposes *A. vinelandii* mutant strain to stress condition, which triggers a more efficient bacterial oxidative stress response and the activation of alternative defensive mechanisms like the social behavior in the sessile lifestyle. Taken together, our results indicate an involvement of bacterial rhodanese-like proteins in physiological processes related to biofilm formation.

References:

Kennedy I.R. et al. (2004). Soil Biol Biochem 36: 1229-1244.

Landini P. (2009). Res Microbiol 160: 259-266.

Remelli W. et al. (2010). Biol Chem 391: 777-784.

Colburn-Clifford J.M. et al. (2010). Appl Environ Microbiol 76: 7392-7399.

The following papers are under final revision and will submitted to publications before April 2012:

Involvement of the *Azotobacter vinelandii* rhodanese-like protein RhdA in the glutathione regeneration pathway.

William Remelli[#], Nicoletta Guerrieri[#], Jennifer Klodmann[§], Jutta Papenbrock[*], Silvia Pagani[#] and Fabio Forlani[#1]

[#]Dipartimento di Scienze Molecolari Agroalimentari, Università degli Studi di Milano, Milano, Italia.
[§]Institut für Pflanzengenetik, Leibniz Universität, Hannover, Germany
[*]Institut für Botanik, Leibniz Universität, Hannover, Germany

The deficiency of the rhodanese-like protein RhdA promotes oxidative stress tolerance and biofilm formation in *Azotobacter vinelandii*

Federica Villa,[1] William Remelli,[2] Fabio Forlani,[2] Michela Gambino,[1] and Francesca Cappitelli[1],*

[1] Dipartimento di Scienze e Tecnologie Alimentari e Microbiologiche, Università degli Studi di Milano, via Celoria 2, 20133 Milano, Italy.
[2] Dipartimento di Scienze Molecolari Agroalimentari, Università degli Studi di Milano, via Celoria 2, 20133 Milano, Italy.
*Corresponding author: Francesca Cappitelli, Università degli Studi di Milano, via Celoria 2, 20133 Milano, Italy. Phone: +39-0250319121. Fax: +39-0250319238.
E-mail: francesca.cappitelli@unimi.it